STATIC, FREE VIBRATION AND DYNAMIC STABILTY ANALYSIS OF SANDWICH BEAM WITH FUNCTIONALLY GRADED MATERIAL CONSTRAINING LAYER IN HIGH TEMPERATURE ENVIRONMENT

A thesis submitted in partial fulfillment

of the requirements for the degree of

Master of Technology

in

Mechanical Engineering

(Specialization: Machine Design and Analysis)

Submitted by

ANUP KUMAR SAHOO

(Roll No: 212ME1279)

DEPARTMENT OF MECHANICAL ENGINEERING

NATIONAL INSTITUTE OF TECHNOLOGY

ROURKELA-769008, INDIA

MAY-2014

STATIC, FREE VIBRATION AND DYNAMIC STABILTY ANALYSIS OF SANDWICH BEAM WITH FUNCTIONALLY GRADED MATERIAL CONSTRAINING LAYER IN HIGH TEMPERATURE ENVIRONMENT

A thesis submitted in partial fulfillment

of the requirements for the degree of

Master of Technology

in

Mechanical Engineering

(Specialization: Machine Design and Analysis)

Submitted by

ANUP KUMAR SAHOO

(Roll No: 212ME1279)

Under the guidance of

Prof. S.C.MOHANTY

DEPARTMENT OF MECHANICAL ENGINEERING

NATIONAL INSTITUTE OF TECHNOLOGY

ROURKELA-769008, INDIA

MAY-2014

NATIONAL INSTITUTE OF TECHNOLOGY
ROURKELA

CERTIFICATE

This is to certify that the thesis entitled, **" STATIC, FREE VIBRATION AND DYNAMIC STABILTY ANALYSIS OF SANDWICH BEAM WITH FUNCTIONALLY GRADED MATERIAL CONSTRAINING LAYER IN HIGH TEMPERATURE ENVIRONMENT "** submitted by **Mr. Anup Kumar Sahoo bearing Roll no. 212ME1279** in partial fulfillment of the requirements for the award of **Master Of Technology** degree in **Mechanical Engineering** with specialization in **Machine Design and Analysis** at the National Institute of Technology, Rourkela (India) is an authentic work carried out by him under my supervision and guidance.

To the best of my knowledge, the matter embodied in the thesis has not been submitted to any other University / Institute for the award of any Degree or Diploma.

Date:

Dr. S. C. Mohanty
Assoc. Professor
Department of Mechanical Engineering
National Institute of Technology
Rourkela-769008.

ACKNOWLEDGEMENT

I avail this opportunity to express my hereby indebtedness , deep gratitude and sincere thanks to my guide, **Prof. S.C. Mohanty**, Associate Professor, Mechanical Engineering Department for his in depth supervision and guidance, constant encouragement and co-operative attitude for bringing out this thesis work.

I also would like to express my sincere thanks to **Prof. K.P.Maity,** Head of the department, Mechanical Engineering for providing valuable departmental facilities.

Finally, I would like to thank my fellow post graduate students and the people who have been involved directly or indirectly in my endeavor.

ANUP KUMAR SAHOO
Roll No. 212ME1279
Dept.of Mechanical Engg.
(Machine Design & Analysis)

CONTENTS

ABSTRACT

The main objective of present work is to study the static, free vibration and dynamic stability of a sandwich beam with functionally graded material as constraining layer in high thermal environment. The top layer is the FGM layer with ceramic on its top face and stainless steel on its bottom. The sandwich beam is subjected to axial dynamic loading. The top face of the FGM layer is subjected to high temperature. All the rest of the layers are at room temperature.

Two cases of temperature variation along the thickness are considered i.e. linear and non-linear. The material properties of FGM depend on the volume fraction distribution of constituent materials and on the subjected temperature. The material properties are assumed to follow the power law distribution along the thickness direction.

The sandwich beam is modeled using finite element method. The beam element has four degrees of freedom for each node. The degrees of freedom per node are two longitudinal displacement for the two outer layers, lateral displacement and rotation. Free vibration, static and dynamic load analyses are done by varying different system parameters such as core thickness parameter, power law index and temperature of top face of FGM layer. Boundaries for stable and unstable regions are found out using Saito and Otomi conditions.

It is found that the buckling load of the beam decreases with increase in core thickness parameter, power law index and temperature of top face of FGM layer. The frequency of the beam also decreases with increase in core thickness parameter, power law index and temperature of top face of FGM layer. Linear and non-linear temperature variation along the thickness has negligible effect on buckling load as well as on natural frequency. The probability of instability

of the beam increases with increase in core thickness parameter, power law index and temperature of top face of FGM layer.

Keywords: Functionally graded material, viscoelastic, sandwich beam, dynamic stability, constraining layer.

List of figures and tables

Nomenclature

A_k - Cross-sectional area of k^{th} elastic layer'.

A_v- Cross-sectional area of visco-elastic layer.

E_k- Young's modulus of k^{th} elastic layer.

g- Shear parameter.

G_v- Complex shear modulus of visco-elastic layer.

t_2- Thickness of visco-elastic layer.

I_k- Moment of inertia of k^{th} elastic layer.

$\hat{k}$ - Thermal conductivity of FGM along its thickness.

n- Power law index of FGM.

$[K^{(e)}]$- Stiffness matrix of beam element.

$[K_p{}^{(e)}]$- Stability matrix of beam element.

$[\overline{K}]$- $[\mathrm{K}] - P_s[K_p]$.

L- Length of the beam.

L_e- Length of beam element.

$[N_k]$- Shape function matrix of k^{th} elastic layer for axial displacement.

$[N]^T$- Transpose of shape function matrix.

$[N_v]$- Shape function for visco-elastic layer.

$[N_w]$- Shape function matrix for transverse displacement..

P_s- Static component of load.

P_d- Time-dependent component of load.

$P(t)$ - Axial periodic force.

P_{cr}- Critical buckling load of equivalent Euler beam.

$[T_k{}^{(e)}]$ - Kinetic energy of beam element.

$[T_v{}^{(e)}]$- Kinetic energy of visco-elastic layer.

u_k- Axial displacement of k^{th}elastic layer.

$U_k{}^{(e)}$- Potential energy of constraining layer.

$U_v{}^{(e)}$- Potential energy of visco-elastic layer.

w- Transverse displacement.

$W_p{}^{(e)}$- Work done on beam element.

x- Axial co-ordinate.

α - Static load factor.

β- Dynamic load factor.

ρ- Mass density of elastic layer.

ρ_v- Mass density of visco-elastic layer.

Ω- Disturbing frequency.

Φ- Rotational angle.

ξ- x/L_e

γ_v- Shear strain of visco-elastic layer.

$\{\Delta^e\}$- Nodal displacement matrix of beam element.

[Φ]- Normalized modal matrix.

{Γ}- New set of generalized co-ordinates.

‘ - $\frac{\partial}{\partial x}$

. - $\frac{\partial}{\partial t}$

.. - $\frac{\partial^2}{\partial t^2}$

CHAPTER 1

INTRODUCTION

Damping has a very high importance in structures and systems subjected to dynamic loading. Passive damping treatment is one of the methods to control the noise and vibration in structures. The airborne and structure borne noise and vibration occur more frequently in systems. The traditional passive control methods that include use of absorbers, barriers, mufflers, silencers, etc. are for airborne noise. For systems with constant excitation frequency, modification of system's stiffness or mass reduces the unwanted vibrations as these parameters alter the resonant frequencies. But in most cases, the isolation or dissipation of vibrations is done by using isolators or damping materials. Viscoelastic materials (damping material) exhibits both viscous fluid and elastic solid material characteristics. There are mainly two methods of treatment of viscoelastic material viz., constrained layer and unconstrained layer or free layer treatment. Depending on the functional requirements, sandwich structure utilizes the constrained layer treatment method to obtain the best properties out from all layers. In this case the viscoelastic material is sandwiched between the surface of structure and thin facings of metallic material.

The traditional sandwich construction includes a relative thick core of low density material, sandwiched between the top and bottom face sheets (face layers) of relatively thin in size.

MATERIALS & MATERIAL PROPERTIES OF SANDWICH STRUCTURE

Depending on the performing function in which the sandwich beam is going to be used, the choice of materials is vast. The introduction and advancement of composite materials and functionally graded materials grease the wheels of researchers in choice of selection of materials for different applications. The choice of material in sandwich structure relies upon the property of requirement (high strength, high temperature resistivity, surface finish etc.). The number of available cores has increased greatly in recent times due to the introduction of more competitive cellular plastics. Combination options of the face sheet materials with different core materials enable new ideas to be integrated in a wide range of applications.

It is the obligation of the designer to have reliable information about the strength and stiffness of the materials used in the design for efficient analysis and design of sandwich structures. The best practice is to do tests for obtaining adequate material properties. An ample number of material choices may appear. The elementary objective of the designer is to achieve an efficient design that will utilize each material component to perform the function with good efficiency.

CORE MATERIAL

The core's function is to support the thin skins so that they do not buckle (deform) inwardly or outwardly, and to keep them in relative position against each other. Key requirements for the core are normally the shear modulus, strength and compressive modulus. The basic objective of the designer in choice of core material is that it should not fail under the applied load. There should be no deformation of core, in thickness wise, thus requiring a high modulus of elasticity perpendicular to the faces. The core is exposed to shear so that global deformations and core

shear stresses are developed by the shear strains in the core. Also the weight of the core material should be such that least load is added to the total weight of the structure.

The core material and thickness of the core are two main parameters that decide most of the properties (thermal, acoustical, damping) of the sandwich structure. The following are some typical features of the core material-

- Low density
- Dampening of vibration and noise
- Shear modulus and shear strength
- Stiffness perpendicular to the faces
- Thermal insulation

A variety of materials find application as core in sandwich structures, which are as follows-

Polymeric foam cores: Foams are one of the most common forms of core material and may be either closed cell or open cell. A wide variety of polymeric foams are available with unique properties. Different types of Polymeric foam cores are as follows

1. Polyethylene terephthalate (PET): These foams are easily machined and thermoformed. The main characteristics are good compression strengths and moduli, fatigue resistance, creep characteristics and thermal stability up to 150ºC
2. Polymethacrylimide (PMI): Foams combine the highest overall strength and stiffness for foam cores of a given density with high dimensional stability, high fatigue life and can be used at elevated temperatures. The drawback is the high cost which has limited its use to high performance composite components: helicopter rotor blades, ailerons and stringer profiles in pressure bulk heads.

3. Polyvinylchloride (PVC): are commonly used as core materials for high performance sandwich structures. They are usually a hybrid of PVC and polyurethane rather than pure PVC. They offer a balance of static and dynamic properties with good resistance to water absorption.
4. Syntactic cores: Syntactic foam is a lightweight composite consisting of hollow spheres in a resin matrix. These hollow spheres are normally polymeric or glass
5. Wood cores: End Grain Balsa (EGB) is an ultra-light wood product with one of the highest strength to weight ratios for a core material.
6. Honeycomb and corrugated cores: Many different materials may be used for honeycomb cores with the most common being aluminum, paper or polymers. Honeycomb cores are made by selectively bonding layers of scored material and then expanding the stack to produce a regular cellular structure. Alternative routes for their manufacture include corrugation followed by bonding and extrusion of thermoplastics.

FACE MATERIAL

The top and bottom layers of conventional sandwich structure are called as face layers or face sheets (as layers are in sheet form). Face materials can be obtained from any structural material that can be available in the form of thin sheets. The faces carry the tensile and compressive stresses in the sandwich beam. The local flexural rigidity is often so small that it can be ignored. It is also acceptable and common to choose fiber glass-reinforced plastics as face materials because of its following excellent characteristics.

- High impact resistance
- High tensile and compressive strength

- Wear resistance
- Resistance to different conditions (chemical, heat, etc.)
- High stiffness giving high flexural rigidity
- Good surface finish

Various types of materials used as face materials are as follows-

Metals and alloys: Metals and their alloys possess almost all the required properties of face materials. Conventional materials and their alloys such as steel, stainless steel and aluminum are often used as face material. As the thickness of the face layers are relatively thin so one limitation for using metals is that they can be formed into sheets.

Composites: Most composites offer properties similar to or even higher than those of metals. They have been substantially used in construction of sandwich structures. Particularly fiber reinforced composites are suitable for sandwich structures even though the stiffness is often lower in magnitude. Thus with a light core, the composites produce high rigidity.

Functionally graded materials or we may say special type composites, are especially applicable for some conditions. Ceramic-metal FGMs are best example for high temperature environment conditions. Exclusive properties of FGMs make them more suitable for specific applications.

DESIGN CONSIDERATIONS

A sandwich structure is designed to make sure that it is capable of taking structural loads throughout its design life. In addition, it should maintain its structural integrity in the in-service environments. The structure should satisfy the following criteria-

- The face sheets should have sufficient stiffness to withstand the tensile, compressive, and shear stresses produced by applied loads.
- The core should have sufficient stiffness to withstand the shear stresses produced by applied loads.
- The core should have sufficient shear modulus to prevent overall buckling of the sandwich structure under loads.
- Stiffness of the core and compressive strength of the face sheets should be sufficient to prevent the wrinkling of the face sheets under applied loads.
- The core cells should be small enough to prevent inter-cell buckling of the face sheets under design loads.
- The core should have sufficient compressive strength to prevent crushing due to applied loads acting normal to the face sheets or by compressive stresses produced by flexure.
- The sandwich structure should have sufficient flexural and shear rigidities to prevent excessive deflections under applied loads.
- Sandwich materials (face sheet, core and adhesive) should maintain the structural integrity during in-service environments.

APPLICATION AREAS OF SANDWICH STRUCTURES-

- In damped structures for effective vibration damping
- Aerospace field
- Building Construction
- Naval ships
- Rail Industry
- Automotive Industry

FUNCTIONALLY GRADED MATERIAL (FGM)

Some components of space structures, fusion reactors, space plane structures and turbine engines are used as thermal barriers. There was a need to invent an advanced material which could be used as thermal barriers in order to sustain surface temperature as high as 1800^0 C and temperature gradient of about 1300^0 C. The concept of FGMs was first proposed by the Japanese Scientist Koizumi and his co-researchers in 1984, as a solution to prepare such materials.

Functionally Graded materials belong to family of composites.

Metal Ceramic Fiber

The FGMs properties vary from one surface to another smoothly or gradually based on the spatial position throughout the thickness. Most frequently FGMs are made up of ceramic and metal material components.

The main role of the metal constituent in the FGM is to provide the structural support, while the other constituent ceramic is to provide heat shielding or thermal barrier when subjected to high

temperature environments. The material property variation makes it possible to accommodate the function to appropriate the needs of different applications.

FGMs offer a wide range of applications where the operating conditions are more difficult. The concentrations of material components are different for various functions. High amount of ceramic material or pure ceramic is needed to arrange at the upper face to resist high temperature conditions, and corrosive environments. In the same way high amounts of metal are provided at locations where mechanical properties such as high strength, toughness etc. are needed.

The FGM concept is not entirely new. Keen observation of some natural things reveals the truth as nature has been using the FGM concept. Some examples are bamboo in which spatial variation of voids and pores concentration makes them rich in bending rigidity with minimum mass. Human skin and Bones are some more examples of natural FGMs.

APPLICATIONS-

The following are the various application areas of functionally graded materials-

- Aerospace-

Functionally graded materials can be used under high temperature conditions with one of its constituents having low thermal conductivity. They can resist high thermal gradients; this makes functionally graded materials appropriate for structures in aerospace such as space plane body, rocket engine components etc.

- Medicine-

Living tissues like bones and teeth are described as natural functionally graded materials. A suitable material is required as substitute to these living tissues, if the original one not serving

purpose. The ideal one for this application is functionally graded material. FGM has find wide range of application in dental and orthopedic applications for teeth and bone replacement.

- Defence-

In defence application, such as armour plates and bullet-proof vests, penetration resistant materials are needed. One of the most important characteristics of functionally graded material is the ability to inhibit crack propagation, this makes functionally graded materials suitable for defence applications.

- Energy-

FGM are used in energy conversion devices. They also provide thermal barrier and are used as protective coating on turbine blades in gas turbine engine.

- Optoelectronics-

FGM also finds its application in optoelectronics as graded refractive index materials and in audio-video discs magnetic storage media.

Other areas of application are: cutting tool insert coating, automobile engine components, nuclear reactor components, turbine blade, heat exchanger, Tribology, sensors, fire retardant doors, etc. The list is endless and more application is springing up as the processing technology, cost of production and properties of FMG improve.

LIMITATIONS-

Today various methods are available for manufacturing of functionally graded materials with almost any material combination. Regardless of all achievements there will be new challenges in future when applications for FGMs will enlarge.

1. Conversion of manufacturing processes to mass production.

2. Cost-effectiveness of production processes
3. Quality control.
4. Repeatability of production processes and reliability of the produced FGMs.

PRESENT CONSIDERATION-

In the present analysis, a sandwich structure is considered which consists of-

Upper layer (top face): Functionally graded material

Middle layer (core): Viscoelastic material

Lower layer (bottom face): Metallic

CHAPTER 2

LITERATURE REVIEW

Introduction

Michael Faraday [21] in 1831 was the first scientist to observe parametric resonance. He observed that when a fluid filled glass is vibrating vertically, the fluid surface is oscillating at half the frequency at which the container is oscillating. In 1859, Melde [41] worked on parametric oscillation for lateral vibration. He produced parametric oscillation by using a tuning fork in a string. He varied the tension of the string at double of its resonant frequency. Beliaev [10] was the first scientist who made a theoretical analysis on the parametric stability of prismatic beams.

Many researchers have presented articles by reviewing the work of other eminent researchers. Evan-Iwanowski [20] had presented a review article on parametric resonance of structure. Ibrahim and his co-workers [26]-[32] have presented a review article on linear and non-linear parametric vibration of deterministic and stochastic type. Nakra [46]-[48] has presented an article on vibration control in visco-elastic material. Bolotin [13], Schmidt [56], Nayfeh and Mook [49] have published a book on the basic theory of dynamic stability of parametric resonance systems.

Classification of parametric resonance-

A multi-degree of freedom system can exhibit simple resonance, sum type or difference type resonance depending upon the type of loading, support conditions and system parameters.

Mettler [42] gave classification for various types of resonance exhibited by linear periodic system. Saito and Otomi [54] stated that for axial loading in visco-elastic beams with visco-elastic support there is no combination resonance of difference type.

Methods of stability analysis of parametrically excited systems-

Bolotin's [13] method based on Floquet's theory gives good results for simple resonance only. Then Steven [60] modified this method using complex differential equations of motion. Hsu [24]-[25] developed an approximated method for system subjected to small parametric excitation. This method gives instability regions for all cases- main, difference and combination types. Later Saito and Otomi [54] made changes in Hsu's method so as to make it suitable for systems with complex differential equations of motion. Takahashi [61] stated a method which removed the limitation of assuming small parameters. This method gives instability regions for simple and combination type. Zazaczkowski and Lipinski [64] and Zazaczkwoski [65] using Bolotin's method formulated equations for instability regions and calculated the steady state response of the system. The response is in form of a set of linear differential equations having time dependent parameters which is expressed in a trigonometric series. Lau et al [39] stated a method of variable parameter increment. In this method there is no need of assuming small parameters. Using this method non-linear system can also be considered.

Most of recent works on dynamic stability of elastic systems have used finite element method. Brown et al. [15] studied dynamic stability of uniform bar using finite element method. Abbas

and Thomas [1] and Yokoyama [63] analyzed the effect of support condition on dynamic stability of Timoshenko beam using finite element technique. Briseghella et al. [14] worked on dynamic stability problems of beams and frames using finite element method. .

SANDWICH BEAM-

1. Resonant frequencies and loss factor prediction

Kerwin [38] was the first scientist to do a quantitative analysis of damping effectiveness of a constrained visco-elastic layer. In his work he has formulated an expression for loss factor. Ungar [62] has formulated general expressions for the loss factor of uniform linear composites in terms of properties of its constituent materials. Di Taranto [19] gave a theory for finding natural frequencies and loss factors for finite length sandwich beams. Asnani and Nakra [4] has worked on multi-layer simply supported sandwich beams and found out the loss factors and displacement response for beams of different numbers of layers. Chatterjee and Baumgarten [17] has worked on simply supported beams and found out the natural frequencies in damping and logarithmic decrement for fundamental mode of vibration. They have verified their results experimentally also. Nakra and Grootenhieus [45] did both theoretical and experimental study on the vibration characteristics of asymmetric dual core sandwich beams. Later Rao [57] did the same study including the rotary and longitudinal inertia terms. Asnani and Nakra [6] analyzed the effect of number of layers and thickness ratio of layers on loss factor of a multi-layer simply supported beam. Rao [51] studied the effect of free vibration of a short sandwich beam considering higher order effects such as inertia, extension and shear of all layers. He found out that if these higher terms are not considered, then there is an error in the values of loss factor and natural frequencies as high as 45%. Rao [51] in his other work formulated equations for calculating frequencies and

loss factor for sandwich beams under different end conditions. Johnson and his co-workers [34]-[35] calculated frequencies and loss factor for beams and plates with constrained visco-elastic layer using finite element technique. Imaino and Harrison [33] used modal strain energy technique and finite element technique to study the damping of first and second bending resonance of a sandwich beam with constrained damping layer. Bhimaraddi [12] in his model of a simply supported beam with a constraining damping layer has considered the continuity of displacements and transverse shear stresses across the interface of layers and found out the resonant frequencies and loss factors. Sakiyama et al [55] has worked on three layer continuous sandwich beam and studied the effect of shear parameter and core thickness on the resonant frequencies and loss factors. Fasana and Marchesiello [22] used Rayleigh-Ritz method and found out the frequencies, loss factors and mode shapes for sandwich beams. They used polynomials which satisfied the boundary conditions. Banerjee [8] used dynamic stiffness matrix and found out the mode shapes and natural frequencies of a three layer sandwich beam.

2. Static and dynamic analysis of sandwich beams

Mead and Markus [40] analyzed the forced vibration of a three layered sandwich beam with visco-elastic core by using the method of Di Taranto [19]. Asani and Nakra [5] worked on forced vibration of a sandwich beam with visco-elastic core for fixed-fixed and cantilever type end conditions. Qian and Demao [50] used finite element method to do modal analysis and calculate the response in time domain.Ha [23] developed an exact analysis method for bending and buckling analysis of sandwich beam.

3. Stability study of sandwich beams

Chonan [18] worked on the stability of two layered sandwich cantilever beam with imperfect loading. Kar and Hauger [37] analyzed the dynamic stability of a sandwich beam on which a direction-controlled non-conservative force was acting. Ray and Kar [54] have studied the dynamic stability of sandwich beams under different boundary conditions. They have used Hamilton's principle for deriving the equations of motion and converted those equations into a set of coupled Hill's equation in time domain by Galerkin's method. They have assumed approximate series solution which satisfies most of the boundary conditions.

Functionally graded material-

Bhangale and Ganeshan [11] have studied the thermo-elastic vibration and buckling behavior of a functionally graded sandwich beam with constrained visco-elastic layer. They concluded that materials having lower co-efficient of thermal expansion value have high thermal buckling temperature. Also the thermal buckling temperature increases with increase in power law index of FGM and ratio of core to stiff layer. Aydogu and Taskin [7] studied free vibration of functionally graded beams with end condition as simply supported. Kapuria et al. [36] using zigzag theory analyzed the static and dynamic response of FGM with constituent materials as Al/SiC and Ni/Al_2O_3 for various boundary conditions. Simsek [57]-[59] using higher order theories worked on dynamic study of functionally graded beams. Akhtar and Kadoli [2] analyzed the static behavior of different functionally graded beams. Ashorbagy et al. [3] worked on the dynamic aspect of a functionally graded Euler-Bernoulli beam using principle of virtual work. Chakraborty et al [16] have worked on thermo-elastic behavior of functionally graded beams using finite element technique. They have considered both exponential law and power law

variation of material properties. . Mohanty et al. [43]-[44] have worked on static and dynamic study of a functionally graded Timoshenko beams using finite element method.

CHAPTER 3

FGM IN THERMAL ENVIRONMENT

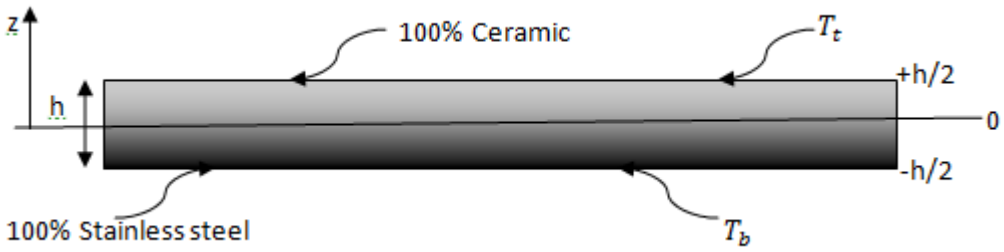

Figure 3.1 FGM beam in thermal environment

There can be two cases of temperature variation inside a FGM beam which are as follows-

1. Linear temperature variation

The T_t and T_b denotes the temperature at the top and bottom face of FGM beam respectively. The temperature variation inside FGM according to linear temperature variation in thickness 'z' - direction is expressed as

$$T(z) = T_b + \Delta T.\left(\frac{z}{h} + \frac{1}{2}\right)$$

where $\Delta T = T_t - T_b$ is the temperature gradient between the top and bottom face of FGM beam; T_b equals the initial temperature 300K. Here, the origin starts at the mid-point of the thickness of FGM beam as shown in figure (3.1).

2. Non-linear temperature variation

The non-linear temperature variation along the thickness direction of FGM beam is formulated by solving the one-dimensional heat conduction equation. The following equation denotes the equation for the temperature along the thickness 'z' direction-

$$-\frac{d}{dz}(\widehat{k}(z)\frac{dT}{dz}) = 0 \tag{3.1}$$

where $\widehat{k}(z)$ denotes the thermal conductivity of FGM along the thickness direction, $T = T_t$ at the top face of FGM beam ($z = +h/2$) and $T = T_b$ at the bottom face of FGM beam ($z = -h/2$). Here 'h' is the thickness of FGM beam, T_b is assumed to be the initial temperature 300 K. The analytical solution to Eq. (3.1) is

$$T(z) = T_t - (T_t - T_b)\frac{\int_{-h/2}^{z}\frac{1}{\widehat{k}(z)}dz}{\int_{-h/2}^{+h/2}\frac{1}{\widehat{k}(z)}dz} \tag{3.2}$$

The above equation does not consider the dependence of temperature on the material properties.

In the case of power law FGMs, the solution to Eq. (3.1) can also be expressed by means of polynomial series-

$$T(\xi) = T_b + \frac{T_t - T_b}{C_{tb}}\left[\begin{array}{l}\left(\frac{z}{2}+\frac{1}{2}\right) - \frac{\hat{k}_{tb}}{(n+1)\hat{k}_b}\left(\frac{z}{2}+\frac{1}{2}\right)^{n+1} + \frac{\hat{k}_{tb}^{\,2}}{(2n+1)\hat{k}_b^{\,2}}\left(\frac{z}{2}+\frac{1}{2}\right)^{2n+1} - \\ \frac{\hat{k}_{tb}^{\,3}}{(3n+1)\hat{k}_b^{\,3}}\left(\frac{z}{2}+\frac{1}{2}\right)^{3n+1} + \frac{\hat{k}_{tb}^{\,4}}{(4n+1)\hat{k}_b^{\,4}}\left(\frac{z}{2}+\frac{1}{2}\right)^{4n+1} - \frac{\hat{k}_{tb}^{\,5}}{(5n+1)\hat{k}_b^{\,5}}\left(\frac{z}{2}+\frac{1}{2}\right)^{5n+1}\end{array}\right]$$

with

$$C_{tb} = 1 - \frac{\hat{k}_{tb}}{(n+1)\hat{k}_b}\left(\frac{z}{2}+\frac{1}{2}\right)^{n+1} + \frac{\hat{k}_{tb}^{\,2}}{(2n+1)\hat{k}_b^{\,2}}\left(\frac{z}{2}+\frac{1}{2}\right)^{2n+1} - \frac{\hat{k}_{tb}^{\,3}}{(3n+1)\hat{k}_b^{\,3}}\left(\frac{z}{2}+\frac{1}{2}\right)^{3n+1} + \frac{\hat{k}_{tb}^{\,4}}{(4n+1)\hat{k}_b^{\,4}}\left(\frac{z}{2}+\frac{1}{2}\right)^{4n+1} - \frac{\hat{k}_{tb}^{\,5}}{(5n+1)\hat{k}_b^{\,5}}\left(\frac{z}{2}+\frac{1}{2}\right)^{5n+1}$$

where $\hat{k}_{tb} = \hat{k}_t - \hat{k}_b$, $\hat{k}_t$ and $\hat{k}_b$ denotes the thermal conductivity of the top and bottom face of the FGM beam respectively; n denotes the volume fraction index of power law FGMs, which is stated in Eq.(3.3).

Material properties

Generally, the properties of any FGM beam changes continuously due to gradual variation of the volume fraction of constituent materials, normally in thickness direction only. Power law function is usually used to show this variation of ceramic material volume fraction. This can be expressed as-

$$g(z) = .\left(\frac{z}{h}+\frac{1}{2}\right)^{n} \tag{3.3}$$

where $n\ (0 \le n \le +\infty)$, which shows the profile of material variation along the thickness direction of FGM beam.

The material properties- Young's modulus E, Poisson's ratio υ and Thermal co-efficient of expansion α – are the non-linear functions of temperature P (T). Their dependence on temperature can be expressed by the following equation-

$$P\,(T) \;=\; P_O^T \left(P_{-1}^T \frac{1}{T} + 1 + P_1^T T + P_2^T T^2 + P_3^T T^3 \right)$$

where $T = T_0 + \Delta T$, which denotes the environment's temperature, and T_0 is the temperature of free stress state i. e T_0 = 300K; P_0^T , P_{-1}^T, P_1^T, P_2^T and P_3^T are the constraints in the cubic equation stating the dependence of temperature by material property. According to the rule of mixture, the effective material properties can be expressed in following equation-

$$P_{eff}(z,T) = \; P_b(T) + [P_t(T) - \; P_b(T)]\; g(z)$$

where $P_{eff}(\xi, T)$ denotes the effective material properties of FGM at temperature T, $P_t(T)$ and $P_b(T)$ denotes the properties of the top and bottom face at temperature T respectively.

In this work, the effective Poisson's ratio υ, Young's modulus E and thermal co-efficient expansion α are assumed to be dependent on temperature, but the mass density ρ and thermal conductivity $\hat{k}$ are not dependent on temperature, i.e. -

$$E(z,T) = \; E_b(T) + [E_t(T) - \; E_b(T)]\; g(z)$$

$$\upsilon\,(z,T\,) = \; \upsilon_b(T) + \; [\,\upsilon_t(T) - \; \upsilon_b(T)]\; g(z)$$

$$\alpha\,(z,\,T\,) = \; \alpha_b(T) + [\alpha_t(T) - \alpha_b(T)]\; g(z)$$

$$\rho\,(z\,) = \rho_b + [\,\rho_t \; - \rho_b]\;\; g(z)$$

$$\hat{k}\,(z) = \hat{k}_{\,b} + [\,\hat{k}_{\,t} \; - \hat{k}_{\,b}]\;\; g(z)$$

CHAPTER 4

FORMULATION OF PROBLEM

Figure (4.1) shows a three layered symmetric sandwich beam of length L, consisting of top layer as constraining layer made up of Functionally Graded Material, middle layer made up of visco-elastic material and bottom layer made up of pure isotropic material subjected to a pulsating axial force

$P\ (t) = P_s + P_d\ cos\Omega t$ acting along its undeformed axis at one end, where P_s denotes the static component of load and P_d denotes the time-dependent component of load.

The following points have been assumed in developing the finite element model-

1. For all three layers, the transverse displacement w is same.
2. The shear deformation and rotary inertia in constrained layer are negligible.
3. Elastic and visco-elastic linear theories are used.
4. Between the layers there is no slip and at the interfaces there is perfect continuity.
5. As compared to Young's modulus of elastic material, Young's modulus of visco-elastic material is negligible.

As shown in the figure (4.2), the element model comprises of two nodes. Each node has four degrees of freedom. Nodal displacements can be expressed as follows-

$$\{\Delta^e\} = \{\ u_{1i}\ u_{3i}\ w_i\ \Phi_i\ u_{1j}\ u_{3j}\ w_j\ \Phi_j\ \} \tag{4.1}$$

where i and j are nodal numbers for the element. The displacement in axial direction of the constraining layer, the displacement in transverse direction and the rotational angle can be written in terms of nodal displacements and finite element shape functions.

$u_1 = [N_1]\{\Delta^e\}$, $u_3 = [N_3]\{\Delta^e\}$, $w = [N_w]\{\Delta^e\}$, $\Phi = [N_w]'\{\Delta^e\}$, (4.2)

where the prime means differentiation with respect to axial co-ordinate 'x' and the shape functions are written as

$[N_1] = [\ 1-\xi\ \ 0\ \ 0\ \ 0\ \ \xi\ \ 0\ \ 0\ \ 0\ ]$

$[N_3] = [\ 0\ \ 1-\xi\ \ 0\ \ 0\ \ 0\ \ \xi\ \ 0\ \ 0\ ]$

and

$[N_w] = [\ 0\ \ 0\ \ (1-3\xi^2+2\xi^3)\ \ (\xi-2\xi^2+\xi^3)L_e\ \ 0\ \ 0\ \ 3\xi^2-2\xi^3\ \ (-\xi^2+\xi^3)L_e\ ]$ (4.3)

where $\xi = x/L_e$ and L_e is the length of the element.

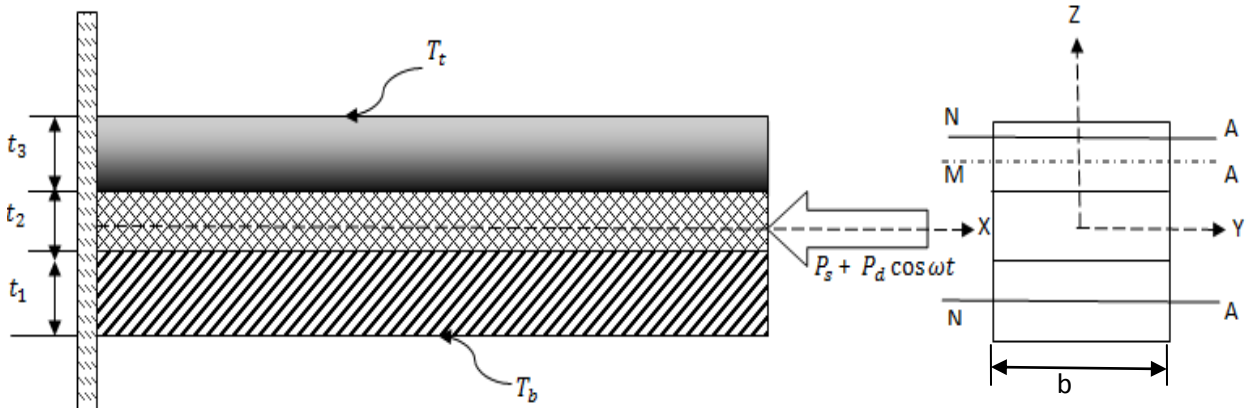

Figure 4.1 Three layered sandwich beam consisting top layer as FGM layer, middle layer as viscoelastic layer and bottom layer as pure metal, subjected to dynamic loading

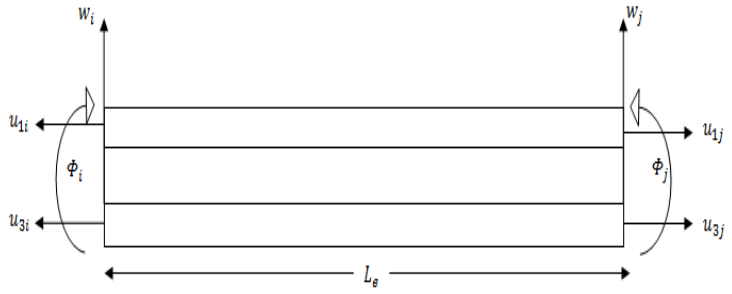

Figure 4.2 Sandwich beam element

Constraining Layer

The potential energy of this layer is expressed by the following equation-

$$U_k^{(e)} = \frac{1}{2}\int_0^{Le} E_k I_k \left(\frac{d^2 w_k}{dx^2}\right)^2 dx + \frac{1}{2}\int_0^{Le} E_k A_k \left(\frac{du_k}{dx}\right)^2 dx \qquad \text{k=1, 3} \qquad (4.4)$$

where E, A and I are the Young's modulus, cross-sectional area and moment of inertial respectively. The subscripts 1 and 3 denote the upper and lower constraining layer respectively.

The kinetic energy of this layer is expressed by the following equation-

$$T_k^{(e)} = \frac{1}{2}\int_0^{L_e L_e} \rho_k A_k \left(\frac{dw_k}{dt}\right)^2 dx + \frac{1}{2}\int_0^{L_e L_e} \rho_k A_k \left(\frac{du_k}{dt}\right)^2 dx \qquad \text{k=1, 3} \qquad (4.5)$$

where ρ is the mass density.

By putting Eq. (4.2) in Eq. (4.4) and Eq. (4.5), the elemental potential energy and the kinetic energy of this layer can be written as

$$U_k^{(e)} = \frac{1}{2}\{\Delta^{(e)}\}\left([K_{ku}^{(e)}] + [K_{kw}^{(e)}]\right)\{\Delta^{(e)}\} \qquad \text{k=1,3} \qquad (4.6)$$

and

$$T_k^{(e)} = \frac{1}{2} \{\dot{\Delta}^{(e)}\} ([M_{ku}{}^{(e)}] + [M_{kw}{}^{(e)}]) \{\dot{\Delta}^{(e)}\} \qquad k=1,3 \tag{4.7}$$

and the dot means differentiation with respect to time 't'.

where

$$[K_{ku}^{(e)}] = [K_{1u}^{(e)}] + [K_{3u}^{(e)}] = E_1 A_1 \int_0^{Le} [N_1]^{\mathrm{T}} [N_1]\, dx + E_3 A_3 \int_0^{Le} [N_3]^{\mathrm{T}} [N_3]\, dx$$

$$[K_{kw}^{(e)}] = [K_{1w}^{(e)}] + [K_{3w}^{(e)}] = E_1 I_1 \int_0^{Le} [N_w]^{\mathrm{T}} [N_w]\, dx + E_3 I_3 \int_0^{Le} [N_w]^{\mathrm{T}} [N_w]\, dx$$

$$[M_{ku}^{(e)}] = [M_{1u}^{(e)}] + [M_{3u}^{(e)}] = \rho_1 A_1 \int_0^{Le} [N_1]^{\mathrm{T}} [N_1] dx + \rho_3 A_3 \int_0^{Le} [N_3]^{\mathrm{T}} [N_3]\, dx$$

$$[M_{kw}^{(e)}] = [M_{1w}^{(e)}] + [M_{3w}^{(e)}] = \rho_1 A_1 \int_0^{Le} [N_w]^{\mathrm{T}} [N_w]\, dx + \rho_3 A_3 \int_0^{Le} [N_w]^{\mathrm{T}} [N_w]\, dx$$

Thermal load analysis-

Due to non-uniform thermal expansion in FGM, the thermal thrust developed R_{th} is written as-

$$R_{th} = \int_A E(z)\, \alpha(z)\, \Delta T\, dA \tag{4.8}$$

where E(z) denotes the Young's modulus of FGM layer, $\alpha(z)$ denotes the co-efficient of thermal expansion of FGM layer and ΔT denotes the steady temperature change.

Work done by thermal load W_{th} -

$$W_{th} = \frac{1}{2} \int_0^L R_{th} \left(\frac{\partial w}{\partial x}\right)^2 dx \tag{4.9}$$

Putting w from eqn. (4.2) in eqn. (4.9), we get

$$W_{th} = \frac{1}{2} \int_0^L R_{th} \,.\, ([N_w]\{\Delta^{(e)}\})'^2 \; dx \tag{4.10}$$

where the prime denotes differentiation w.r.t '*x*'.

On solving eqn. (4.10), we get

$$W_{th} = \frac{1}{2} \int_0^L R_{th} \,.\, [N'_w]\, [N'_w]^T \{\Delta^{(e)}\}\{\Delta^{(e)}\}^T \; dx \tag{4.11}$$

Also, strain energy stored in the beam element $W_{S.E}$ is as follows-

$$W_{S.E} = \frac{1}{2} [\, K^{(e)} \,]_{th} \{\Delta^{(e)}\}^2$$

$$\text{or} \quad W_{S.E} = \frac{1}{2} [K^{(e)}]_{th} \{\Delta^{(e)}\}\{\Delta^{(e)}\}^T \tag{4.12}$$

The work done by thermal thrust is equal to the strain energy stored in the beam. Hence,

$$W_{th} = W_{S.E}$$

Comparing eqn. (4.11) and eqn. (4.12), we get

$$[\, K^{(e)} \,]_{th} = \int_0^L R_{th} \,.\, [N'(x)]\, [N'(x)]^T \, dx$$

This is the thermal stiffness matrix of FGM layer.

Visco-elastic layer

The displacement u_v in axial direction and shear strain γ_v of this layer is found out by the kinematic relationships between the constraining layers as given by Mead and Markus [40]. They are written as-

$$u_v = \frac{u_1+u_3}{2} + \frac{(t_1-t_3\ )}{4}\frac{\partial w}{\partial x} \tag{4.13}$$

$$\Upsilon_v = \frac{u_1-u_3}{t_2} + \frac{(t_1+2t_2+t_3\ )}{2t_2}\frac{\partial w}{\partial x} \tag{4.14}$$

Putting Eq. (4.2) in Eq. (4.13) and Eq. (4.14), we get Υ_v and u_v in terms of nodal displacements and element shape functions:

$$u_v = (N_v)\{\Delta^e\}$$

$$\Upsilon_v = (N_\Upsilon)\{\Delta^e\}$$

where

$$(N_v) = \frac{1}{2}((N_1) + (N_3)) - \frac{(t_1-t_3)}{4}(N_w)$$

$$(N_\Upsilon) = \frac{1}{2}\frac{((N_1)-(N_3))}{t_2} + \frac{(t_1+2t_2+t_3)}{t_2}(N_w)$$

Due to shear deformation, the potential energy of this layer is written as-

$$U_v^{\{e\}} = \frac{1}{2}\int_0^{L_e} G_v A_v \Upsilon_v{}^2 \mathrm{dx} \tag{4.15}$$

where A_v denotes the cross-sectional area and G_v denotes the complex shear modulus of visco-elastic layer.

The kinetic energy of visco-elastic layer is expressed as follows-

$$T_v^{\{e\}} = \frac{1}{2}\int_0^{L_e} \rho_v A_v \left\{\left(\frac{dw}{dt}\right)^2 + \left(\frac{du_v}{dt}\right)^2\right\}\mathrm{dx} \tag{4.16}$$

where ρ_v denotes the mass density of visco-elastic material.

Putting Eq. (4.2) in Eq. (4.15) and Eq. (4.16), the potential energy and kinetic energy of visco-elastic material layer is written as-

$$U_v^{\{e\}} = \frac{1}{2}\{\Delta^{(e)}\}\ ([K_v^{(e)}])\ \{\Delta^e\} \tag{4.17}$$

where

$$T_v^{\{e\}} = \frac{1}{2}\ \{\dot{\Delta}^{(e)}\}\ ([M_v^{(e)}])\ \{\dot{\Delta}^{(e)}\} \tag{4.18}$$

where $[K_v^{\{e\}}] = G_v A_v \int_0^{L_e} [N_Y]^T [N_Y] dx$

$[M_v^{(e)}] = \rho_v A_v \int_0^{L_e} [N_v]^T [N_v]\ dx\ + \rho_v A_v \int_0^{L_e} [N_w]^T [N_w]\ dx$

and the dot means differentiation with respect to time 't'.

Work done by axial periodic force

Work done by axial periodic force P (t) is written as-

$$W_p^{(e)} = \frac{1}{2}\int_0^{L_e} P(t) \left(\frac{\partial w}{\partial x}\right)^2 dx \tag{4.19}$$

Putting Eq. (4.2) in Eq. (4.19), the work done by the axial periodic load can now be written as-

$$W_p^{(e)} = \frac{1}{2}\left\{\Delta^{(e)}\right\}^T P(t)\ K_p{}^{(e)} \{\Delta^{(e)}\} \tag{4.20}$$

where $\left[K_p{}^{(e)}\right] = \int_0^{L_e} [N_w]^T [N_w]\ dx$

The dynamic load P(t) = $P_s + P_d \cos \Omega t$, where Ω is the disturbing frequency, P_s the static and P_d the amplitude of time dependent component of the load, can be written as the fraction of the

fundamental static buckling load P_{cr} of a reference Euler beam, which is defined as an equivalent sandwich beam (similar geometrical dimensions) with pure stainless steel at the bottom layer and pure ceramic at the top layer beam with fixed-free end conditions. Hence, putting P (t) = $\alpha P_{cr} + \beta P_{cr} \cos \Omega t$ where α and β denotes the static and dynamic load factors respectively.

Equation of motion

The elemental equation of motion for a sandwich beam with constrained damping layer, on which an axial periodic load is acting, is found out using extended Hamilton's principle.

$$\delta \int_{t_1}^{t_2} (T^{(e)} - U^{(e)} + W_p^{(e)}) dt = 0 \quad (4.21)$$

Substituting Eq. (4.6), Eq. (4.7), Eq. (4.17), Eq. (4.18) and Eq. (4.20) into Eq. (4.21) the elemental equation of motion for the sandwich beam is obtained as follows:

$$[M^{(e)}]\{\ddot{\Delta}^{(e)}\} + [K^{(e)}]\{\Delta^{(e)}\} - P(t)[K_p{}^{(e)}]\{\Delta^{(e)}\} = 0 \quad (4.22)$$

where

$$[M^{(e)}] = [M_{1u}^{(e)}] + [M_{1w}^{(e)}] + [M_{3u}^{(e)}] + [M_{3w}^{(e)}] + [M_v^{(e)}]$$

$$[K^{(e)}] = [K_{1u}^{(e)}] + [K_{1w}^{(e)}] + [K_{3u}^{(e)}] + [K_{3w}^{(e)}] + [K_v^{(e)}]$$

Considering thermal stiffness matrix of beam element, effective stiffness matrix will decrease due to decrease of stiffness due to temperature rise ΔT, therefore-

$$[K^{(e)}]_{eff} = [K^{(e)}] - [K^{(e)}]_{th}$$

Assembling individual elements, the equations of motion of the global system can be written as

$$[M]\{\ddot{\Delta}\} + [K]\{\Delta\} - P(t)[K_p]\{\Delta\} = 0 \quad (4.23)$$

Substituting P (t), Eq. (4.23) becomes

$$[M]\{\ddot{\Delta}\} + [K]\{\Delta\} - (\alpha P_{cr} + \beta P_{cr}\cos\Omega t)[K_p]\{\Delta\} = 0 \quad (4.24)$$

$$[M]\{\ddot{\Delta}\} + ([K] - \alpha P_{cr}[K_p])\{\Delta\} - \beta P_{cr}\cos\Omega t\,[K_p]\{\Delta\} = 0 \quad (4.25)$$

$$[M]\{\ddot{\Delta}\} + [\bar{K}]\{\Delta\} - \beta P_{cr}\cos\Omega t\,[K_p]\{\Delta\} = 0 \quad (4.26)$$

where $[\bar{K}] = [K] - \alpha P_{cr}[K_p]$ (4.27)

It can be assumed that-

$$\{\Delta\} = [\Phi]\{\Gamma\} \quad (4.28)$$

where [Φ] denotes the normalized modal matrix corresponding to

$$[M\{\ddot{\Delta}\} + [\bar{K}]]\{\Delta\} = 0 \quad (4.29)$$

and { Γ} denotes a new set of generalized co-ordinates.

Substituting Eq. (4.28) in Eq. (4.26), Eq. (4.26) transforms to the following set of coupled Mathieu equations.

$$\ddot{\Gamma}_m + (\dot{\omega_m})^2\Gamma_m + \beta P_{cr}\cos\Omega t \sum_{n=1}^{N} b_{mn}\Gamma_{mn} = 0 \qquad m=1, 2 \ldots N \quad (4.30)$$

where $(\dot{\omega_m})^2$ are the distinct eigen values of $[M]^{-1}[\bar{K}]$ and b_{mn} are the elements of the complex matrix $[B] = -[\Phi]^{-1}[M]^{-1}[K_p][\Phi]$ and

$\omega_m = \omega_{m.R} + i\,\omega_{m.I.} \qquad b_{mn} = b_{mn.R} + i\,b_{mn.I}$

Unstable regions-

The boundaries of the unstable regions for simple and combination resonance are found out by applying the below stated conditions [56] in Eq. (4.30)

Simple Resonance

The boundaries of instability regions are given by

$$\left|\frac{\Omega}{2\omega_0} - \bar{\omega}_{\mu,R}\right| < \frac{1}{4}\left[\frac{\beta^2\,(b^2_{\mu\mu.R} + b^2_{\mu\mu.I})}{\bar{\omega}_{\mu,R}{}^2} - 16\bar{\omega}^2_{\mu.I}\right]^{\frac{1}{2}} \qquad \mu = 1, 2 \ldots N \qquad (4.31)$$

where ω_0 is the frequency of an equivalent sandwich beam with pure stainless steel at the bottom layer and pure ceramic at the top layer, $\bar{\omega}_{\mu,R} = \omega_{\mu.R}/\omega_0$ and $\bar{\omega}_{\mu,I} = \omega_{\mu.I}/\omega_0$

When damping is neglected, the regions of instability are given by

$$\left|\frac{\Omega}{2\omega_0} - \bar{\omega}_{\mu,R}\right| < \frac{1}{4}\left[\frac{\beta(b_{\mu\mu.R})}{\bar{\omega}_{\mu.R}}\right] \qquad \mu = 1, 2 \ldots N \qquad (4.32)$$

Combination resonance of sum type

The boundaries of the unstable regions of sum type are given by

$$\left|\frac{\Omega}{2\omega_0} - (\bar{\omega}_{\mu,R} + \bar{\omega}_{v,R})\right| < \frac{1}{8}\frac{(\bar{\omega}_{\mu,I} + \bar{\omega}_{v,I})}{(\bar{\omega}_{\mu,I}\bar{\omega}_{v,I})^{\frac{1}{2}}}\left[\frac{\beta^2\,(b_{\mu v.R}\,b_{v\mu.R} + b_{\mu v.I}\,b_{v\mu.I})}{\omega_{\mu.R}\;\omega_{v.R}} - 16\bar{\omega}_{\mu,I}\bar{\omega}_{v,I}\right]^{\frac{1}{2}} \qquad (4.33)$$

$\mu \neq v$, $\mu, v = 1, 2, \ldots\ldots\ldots N$

when damping is neglected, the regions of instability are given by

$$\left|\frac{\Omega}{2\omega_0} - \frac{1}{2}(\bar{\omega}_{\mu,R} + \bar{\omega}_{v,R})\right| < \frac{1}{4}\left[\frac{\beta^2\,(b_{\mu v.R}\; b_{v\mu.R})}{\omega_{\mu.R}\;\omega_{v.R}}\right]^{\frac{1}{2}} \tag{4.34}$$

$\mu \neq v$, $\mu,v=1,2,\ldots\ldots\ldots N$

Combination resonance of difference type

The boundaries of unstable regions of difference type are given by

$$\left|\frac{\Omega}{2\omega_0} - \frac{1}{2}(\bar{\omega}_{\mu,R} - \bar{\omega}_{v,R})\right| < \frac{1}{8}\frac{(\bar{\omega}_{\mu,I} + \bar{\omega}_{v,I})}{(\bar{\omega}_{\mu,I}\bar{\omega}_{v,I})^{\frac{1}{2}}}\left[\frac{\beta^2\,(b_{\mu v.R}b_{v\mu.R} + b_{\mu v.I}b_{v\mu.I})}{\omega_{\mu.R}\omega_{v.R}} - 16\bar{\omega}_{\mu,I}\bar{\omega}_{v,I}\right]^{\frac{1}{2}} \tag{4.35}$$

$v > \mu$, $\mu,v=1,2,\ldots\ldots\ldots N$

When damping is neglected, the regions of instability are given by

$$\left|\frac{\Omega}{2\omega_0} - \frac{1}{2}(\bar{\omega}_{\mu,R} - \bar{\omega}_{v,R})\right| < \frac{1}{4}\left[\frac{\beta^2\,(b_{\mu v.R}b_{v\mu.R})}{\omega_{\mu.R}\omega_{v.R}}\right]^{\frac{1}{2}} \tag{4.36}$$

$v > \mu$, $\mu,v = 1, 2 \ldots N$

CHAPTER 5

RESULTS AND DISCUSSION

A three layered sandwich beam is considered. The materials taken for each layer are as follows-

1. Top layer made up of FGM consisting of 100% ceramic Si_3N_4 on its top face and 100% stainless steel SUS304 on its bottom face.
2. Middle layer is visco-elastic.
3. Bottom layer made up of stainless steel SUS304.

Properties of ceramic and stainless are given in Table 1.

Table 1.

Material	$\mathbf{P_{-1}^T}$	$\mathbf{P_0^T}$	$\mathbf{P_1^T}$	$\mathbf{P_2^T}$	$\mathbf{P_3^T}$	**P (at 300K)**
SUS304						
E	0	201.04*10^9	3.079*10^4	-6.534*10^-7	0	207.7877*10^9
Y	0	0.3262	-0.0002002	3.797*10^-7	0	0.3178
A	0	12.330*10^-6	8.086*10^-4	0	0	1.5321*10^-5
P	0	8166	0	0	0	8166
$\widehat{k}$	0	12.04	0	0	0	12.04
Si_3N_4						
E	0	348.43*10^9	-0.000307	2.160*10^-7	-8.946*10^11	322.2715*10^9
υ	0	0.24	0	0	0	0.24
α	0	5.8723*10^7	9.095*10^-4	0	0	7.4746*10^-6
ρ	0	2370	0	0	0	2370
$\widehat{k}$	0	9.19	0	0	0	9.19

Table 1. shows the temperature dependent coefficients of Young's modulus E (Pa), Poisson's ratio υ, co-efficient of thermal expansion α (1/K), mass density ρ (kg/m^3) and co-efficient of thermal conductivity $\hat{k}$ (W/mK) of SUS304 and Si_3N_4.

Properties of viscoelastic core -

Complex shear modulus G_v = 344.8e06*(1+ 0.18i) Pa, Core loss factor (η_c) = 0.18

Mass density ρ_v= 1100 kg/m^3

Beam length is taken as 0.6m and breadth as 0.0254 m. The thickness for top and bottom layer is taken as 0.03m. The thickness of visco-elastic core layer is taken as 0.5 times the thickness of top FGM layer initially. The properties of top FGM layer are assumed to follow a power law. The maximum and minimum temperatures of the top face of FGM layer are taken as 450K and 300K respectively. All other surfaces are assumed to be at room temperature i.e. 300K.

The linear temperature variation along the thickness direction of FGM layer is plotted in figure (5.1).The temperature rise starts from bottom face of FGM layer at 300K and ends at top face at 450 K. The variation follows the same path for all power law indexes (n).

The non-linear temperature variation along the thickness direction of FGM layer for power law index (n) = 5.0, 10.0, 15.0, 20.0 is plotted in figure (5.2). It is found that there is a slight non-linearity only in the middle-section of FGM layer; otherwise it behaves linearly for rest of section. The non-linearity is found to be maximum for the lowest power law index i.e. for n=5.0 as indicated by the orange curve.

On superimposing both the figures for power law index=5.0 in figure (5.3), it is found that there is no significant deviation between the two curves.

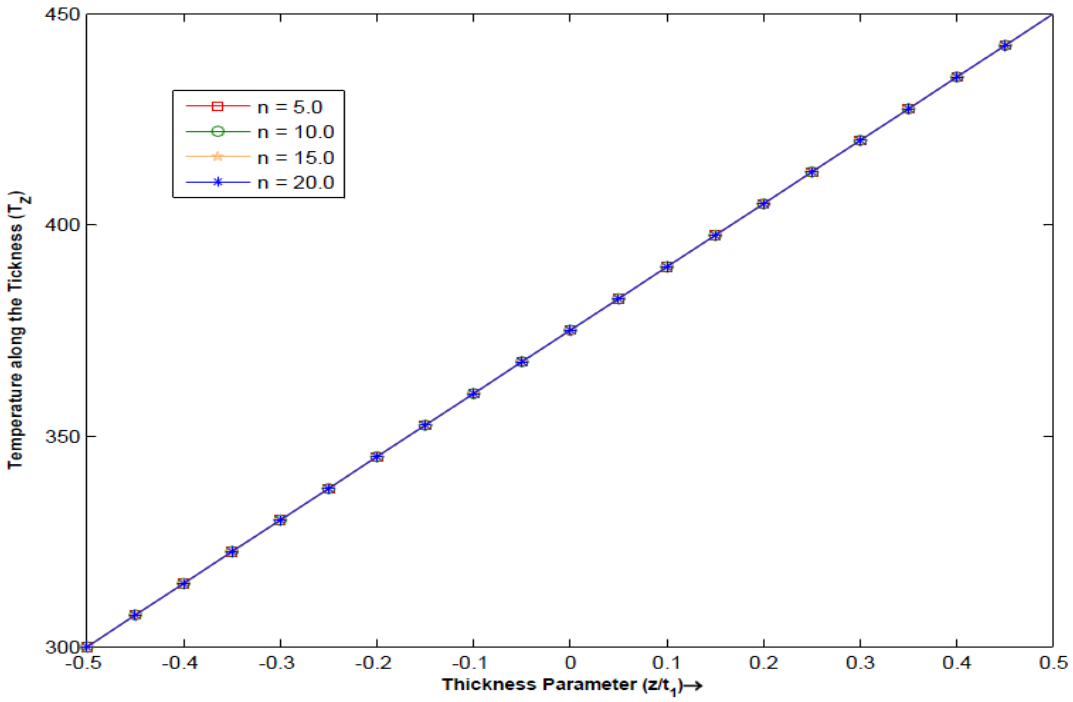

Figure (5.1) Linear temperature variation along the thickness direction of FGM layer for different power law indexes (n), $T_t = 450K$ and $T_b = 300K$.

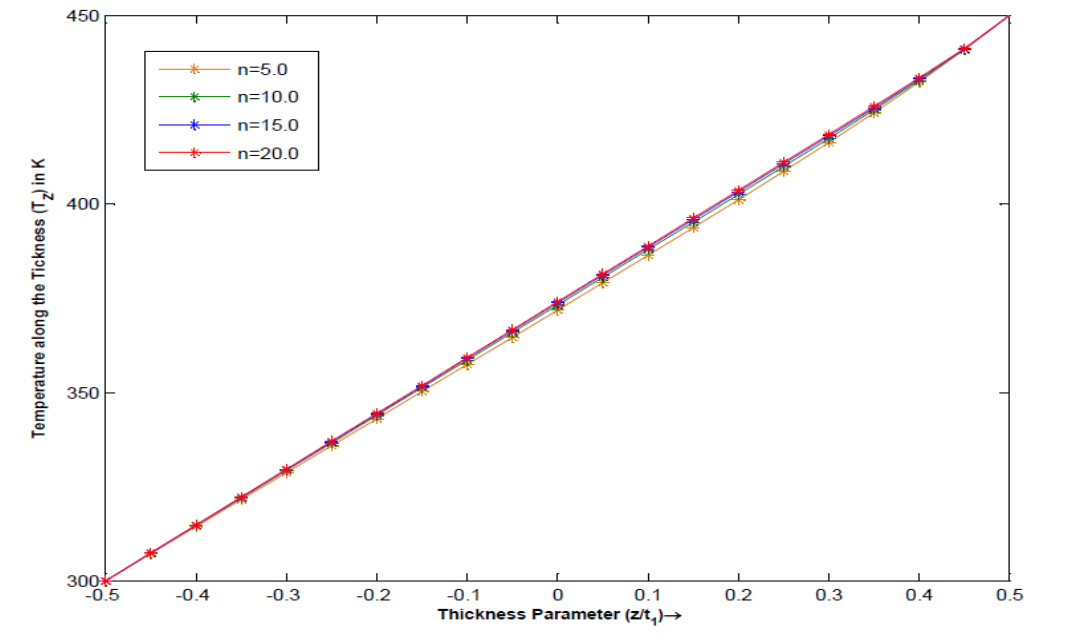

Figure (5.2) Non-linear temperature variation along the thickness direction of FGM layer for different power law indexes (n), $T_t = 450K$ and $T_b = 300K$.

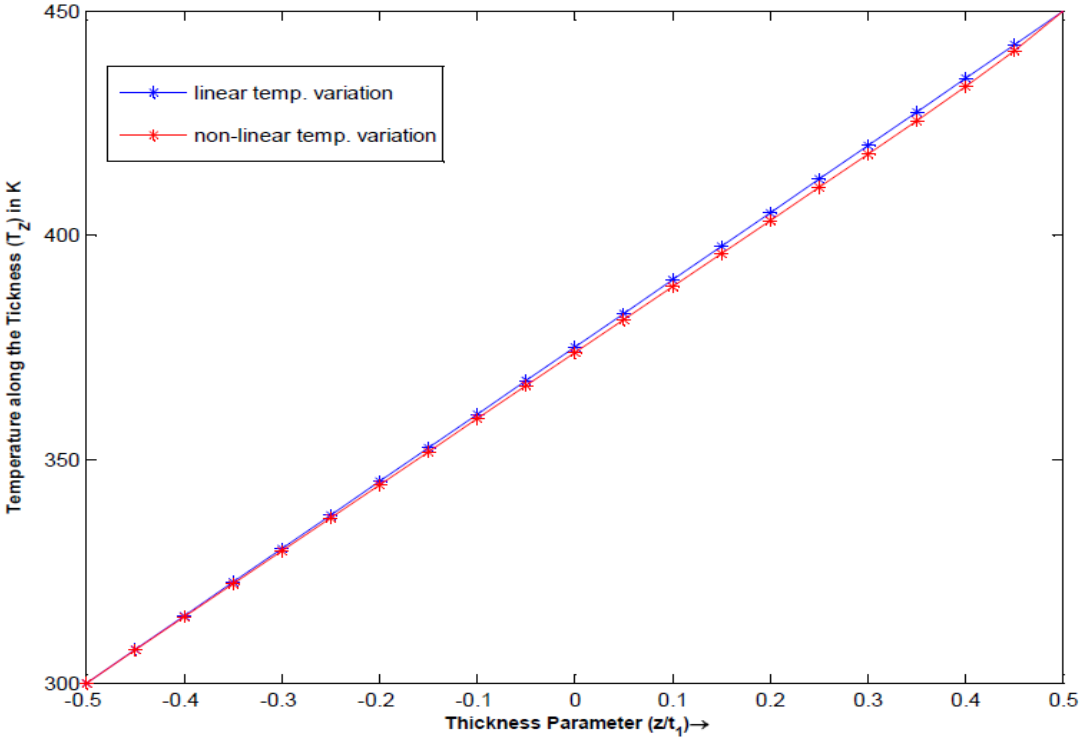

Figure (5.3) Superimposition of linear and non-linear temperature variation along the thickness direction of FGM layer for power law index (n) = 15.0, $T_t = 450K$ and $T_b = 300K$.

The figures (5.4)-(5.8) plotted show the variation of various mechanical properties along the thickness direction of top FGM layer for power law index (n) = 5.0, 10.0, 15.0, 20.0 in case of linear temperature variation. The variation starts from bottom stainless steel face to top ceramic face of FGM layer. Figure (5.4), Figure (5.5), Figure (5.6), Figure (5.7), Figure (5.8), represents the variation of Effective mass density, Effective Poisson's ratio, Effective thermal conductivity, Effective co-efficient of thermal expansion, Effective Young's modulus respectively.

All these variation follow the power law equation. It is quite interesting to find out that with increase in power law index the mechanical properties of the bottom face i.e. of stainless steel dominates for most of the thickness. All of the mechanical properties except Young's modulus of

stainless steel are higher than that of ceramic; therefore in figure (5.4)-(5.7), we get a decreasing slope on each curve. But the effective Young's modulus of ceramic is more than that of stainless steel. Hence, we get an increasing slope in figure (5.8).

Linear temperature variation-

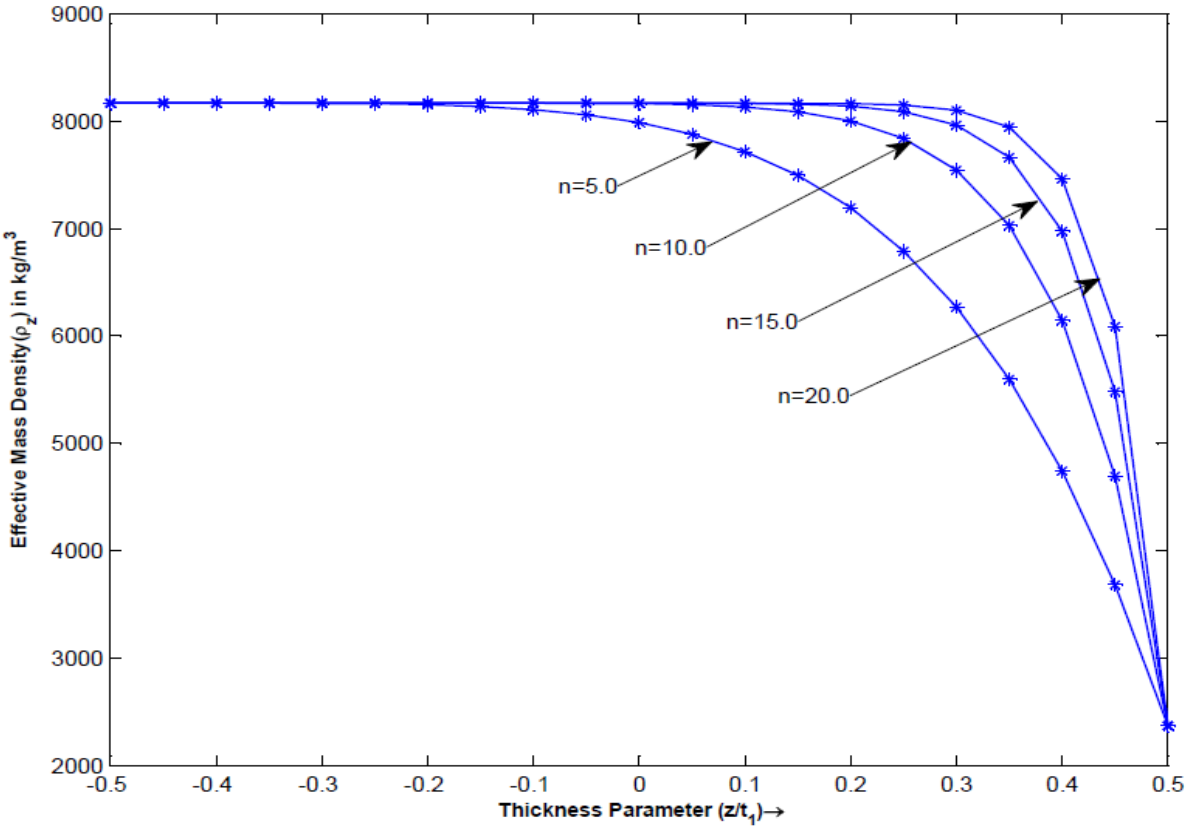

Figure (5.4) Variation of Effective Mass Density ratio along the thickness direction of FGM layer for different power law indexes for linear temperature variation, $T_t = 450K$ and $T_b = 300K$.

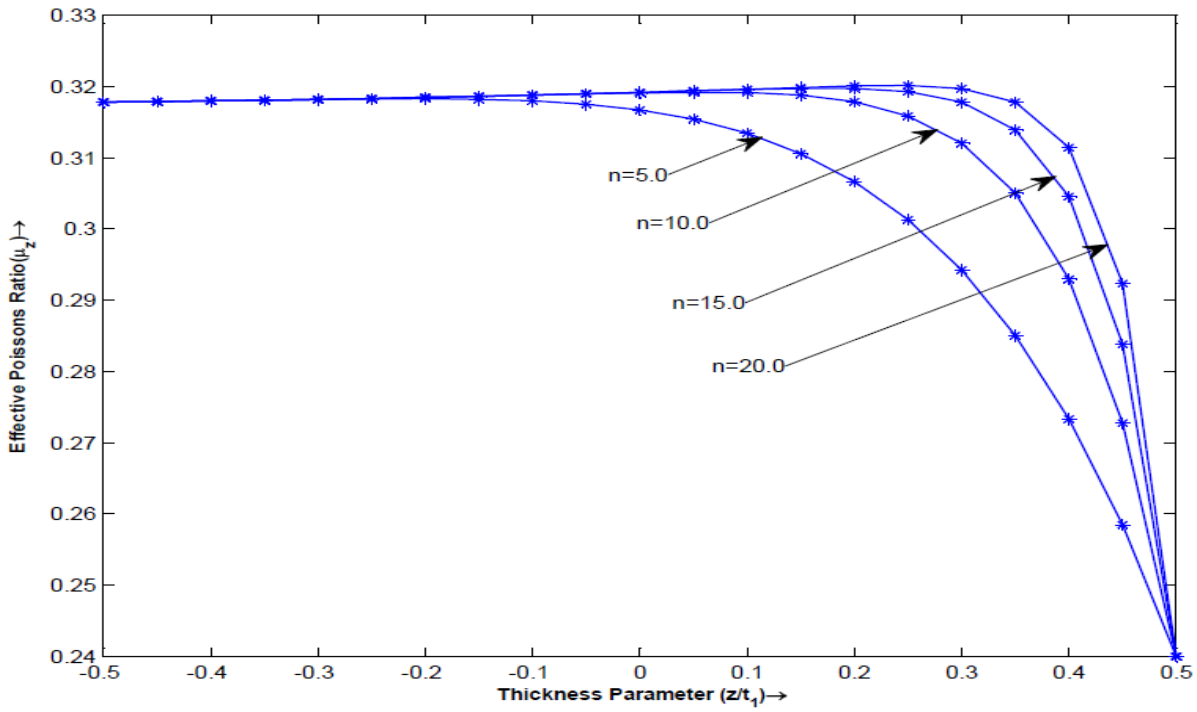

Figure (5.5) Variation of Effective Poisson's ratio along the thickness direction of FGM layer for different power law indexes for linear temperature variation, $T_t = 450K$ and $T_b = 300K$.

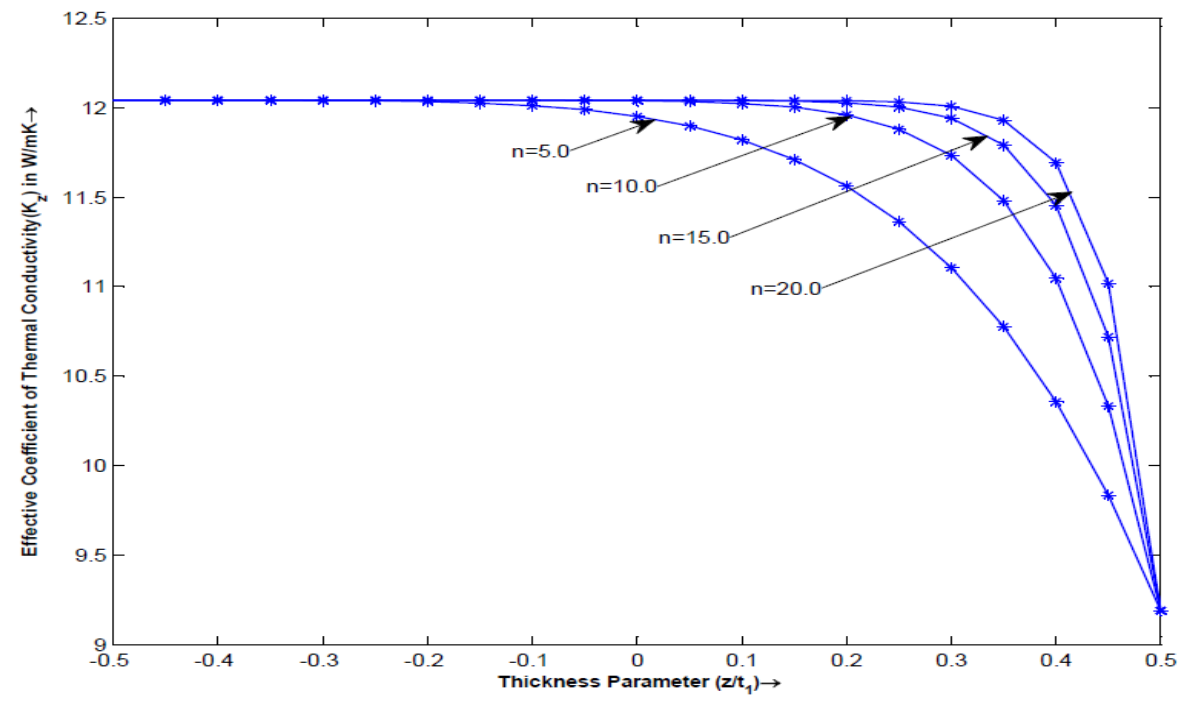

Figure (5.6) Variation of Co-efficient of thermal conductivity along the thickness direction of FGM layer for different power law indexes for linear temperature variation, $T_t = 450K$ and $T_b = 300K$.

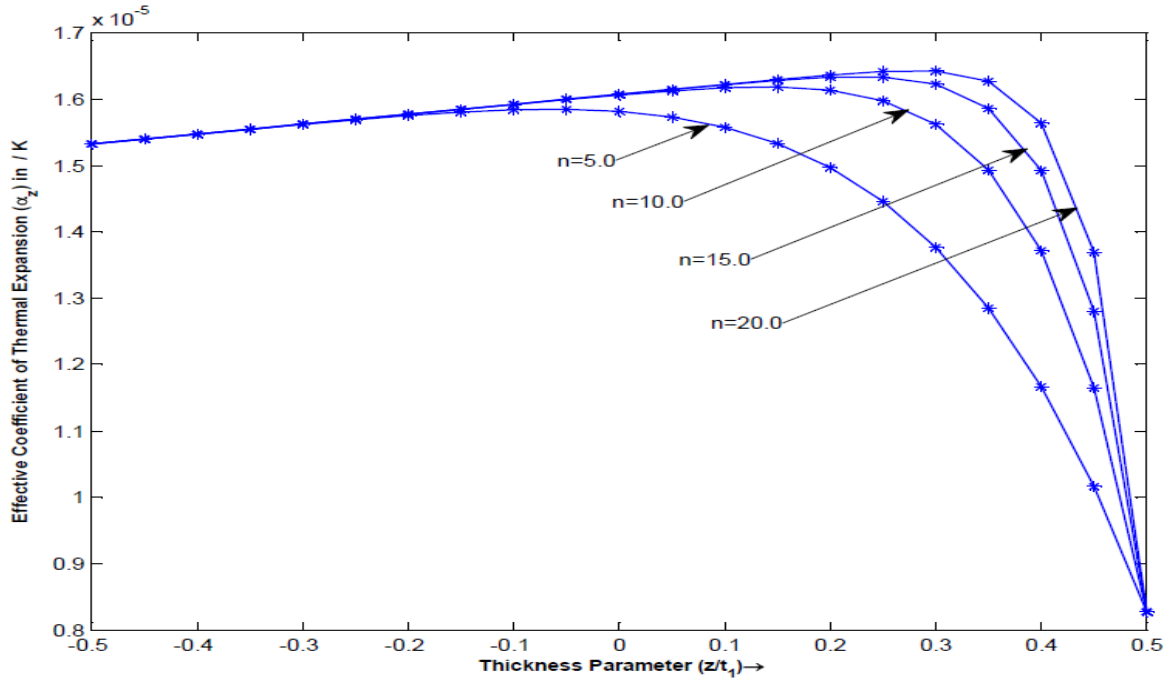

Figure (5.7) Variation of Effective Co-efficient of thermal expansion along the thickness direction of FGM layer for different power law indexes for linear temperature variation, $T_t = 450K$ and $T_b = 300K$.

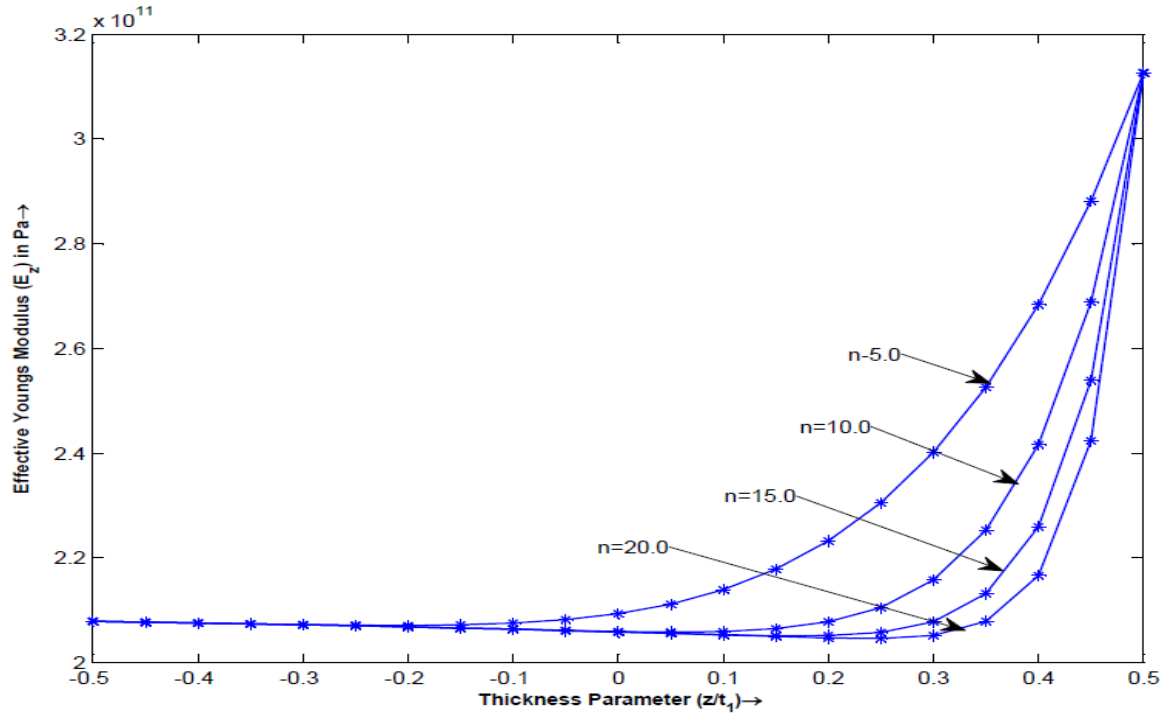

Figure (5.8) Variation of Effective Young's Modulus along the thickness direction of FGM layer for different power law indexes for linear temperature variation, $T_t = 450K$ and $T_b = 300K$.

Similarly, the figures (5.9)-(5.13) show the variation of mechanical properties for non-linear temperature variation under same working conditions as stated in linear temperature variation case. The curves obtained are very much identical to that of linear case because of the fact that there is no significant difference in variation of linear temperature and non-linear temperature, which has been discussed earlier. The superimposition of effective Young's modulus variation for both temperature variation cases is a proof to it, shown in figure (5.14). The two curves follow almost the same path.

Non-linear temperature variation-

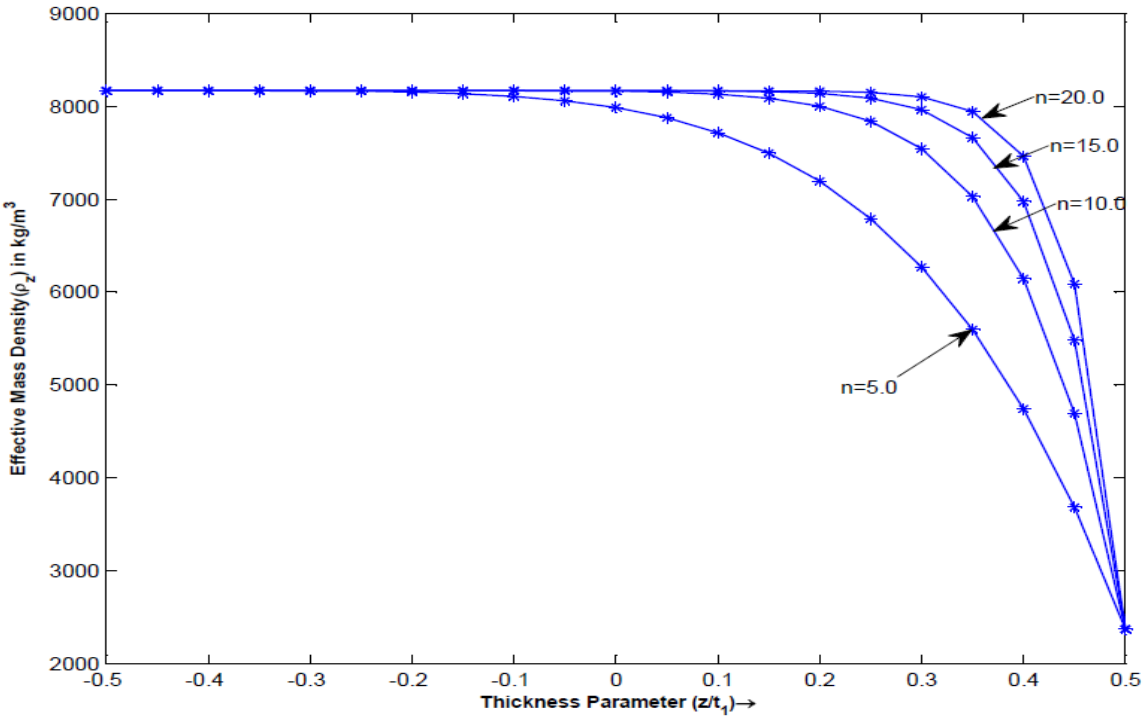

Figure (5.9) Variation of Effective Mass Density ratio along the thickness direction of FGM layer for different power law indexes for non-linear temperature variation, $T_t = 450K$ and $T_b = 300K$.

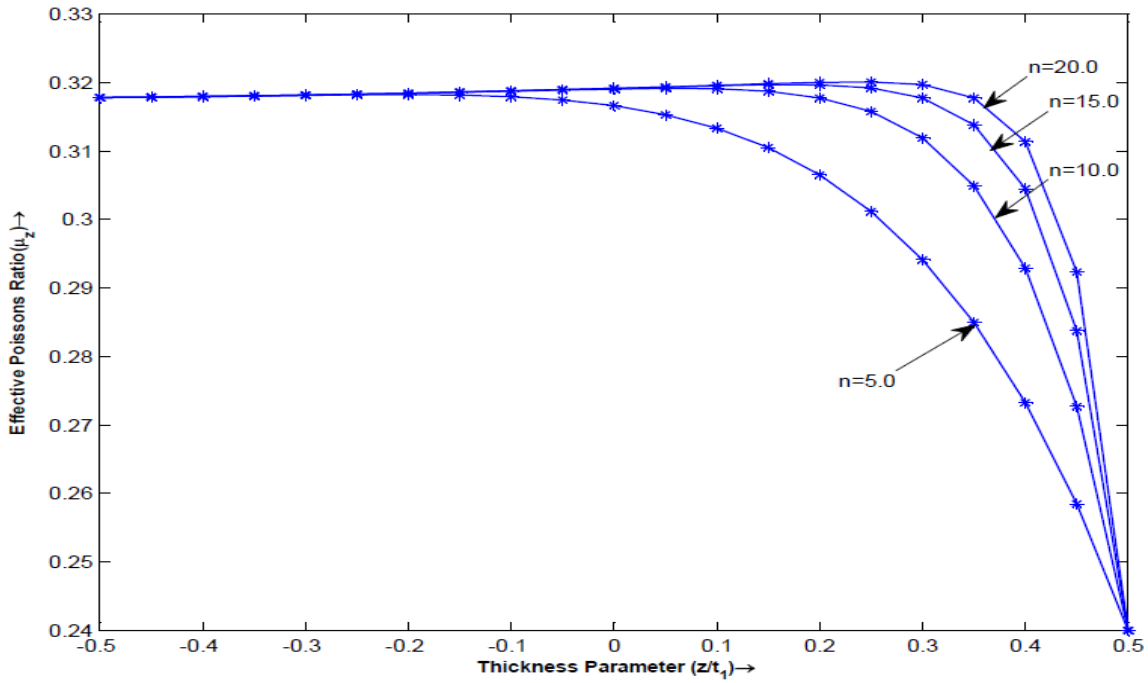

Figure (5.10) Variation of Effective Poisson's ratio along the thickness direction of FGM layer for different power law indexes for non-linear temperature variation, $T_t = 450K$ and $T_b = 300K$.

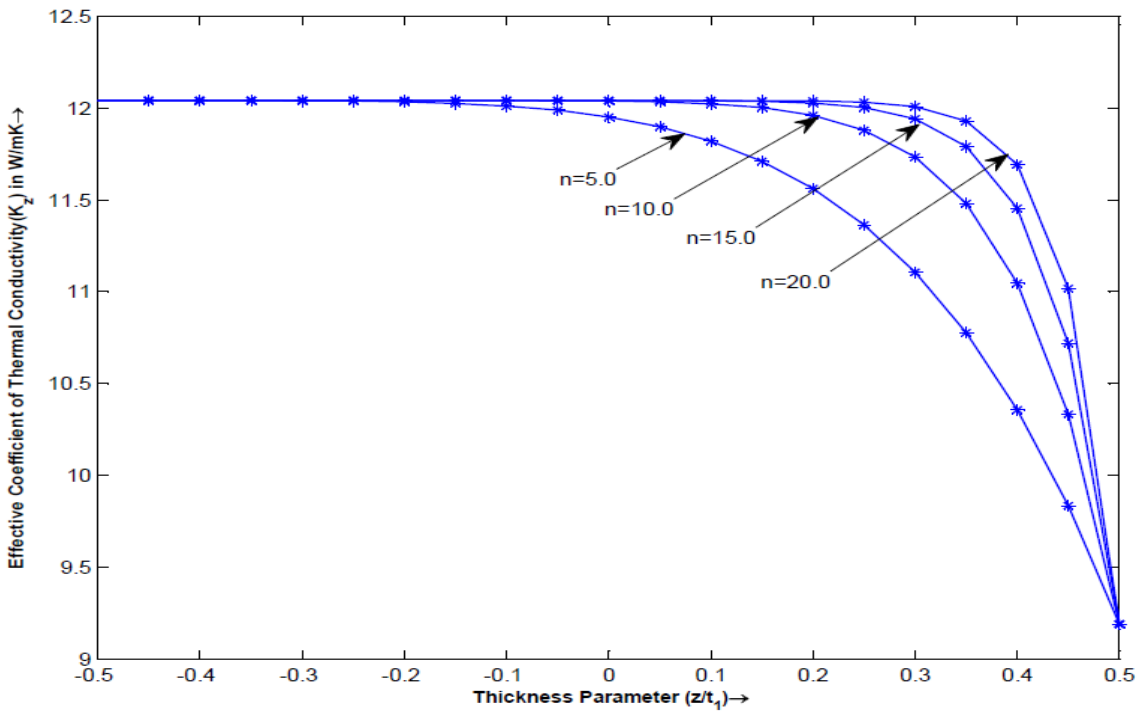

Figure (5.11) Variation of Effective Co-efficient of thermal conductivity along the thickness direction of FGM layer for different power law indexes for non-linear temperature variation, $T_t = 450K$ and $T_b = 300K$.

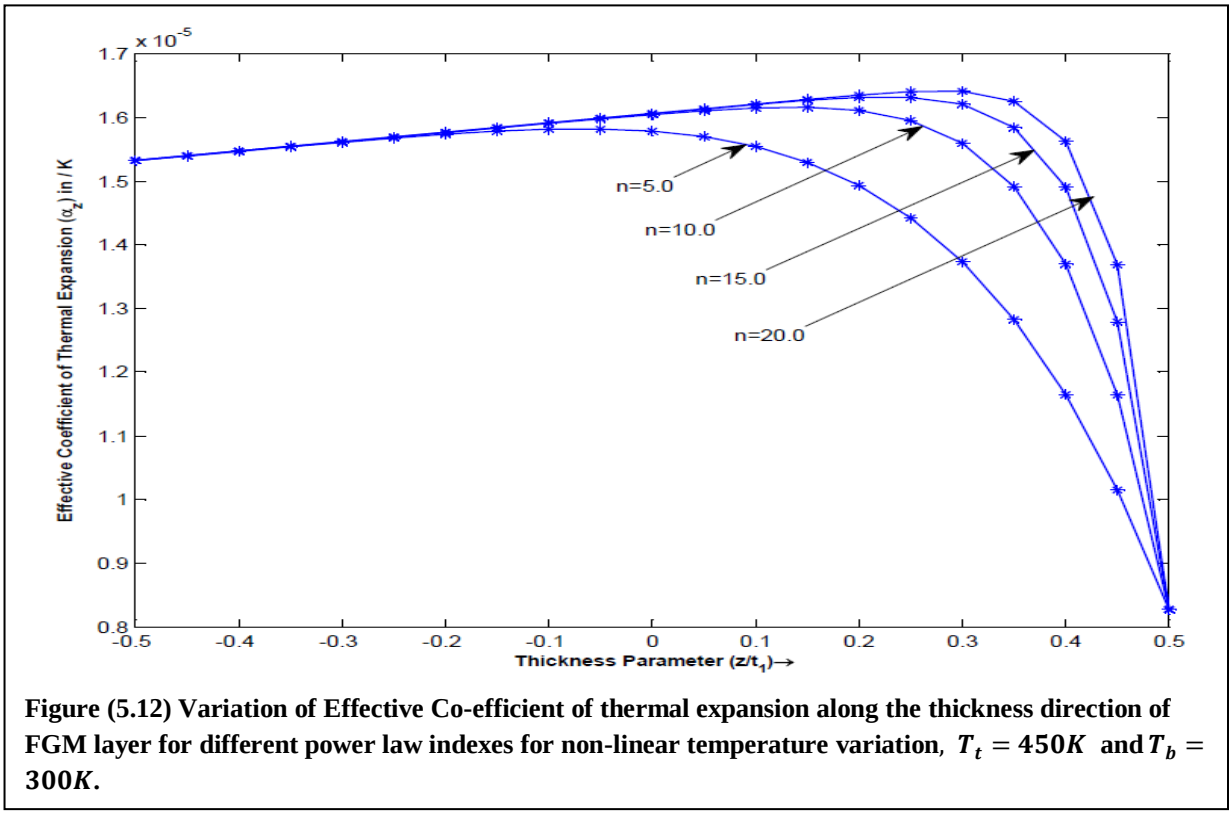

Figure (5.12) Variation of Effective Co-efficient of thermal expansion along the thickness direction of FGM layer for different power law indexes for non-linear temperature variation, $T_t = 450K$ and $T_b = 300K$.

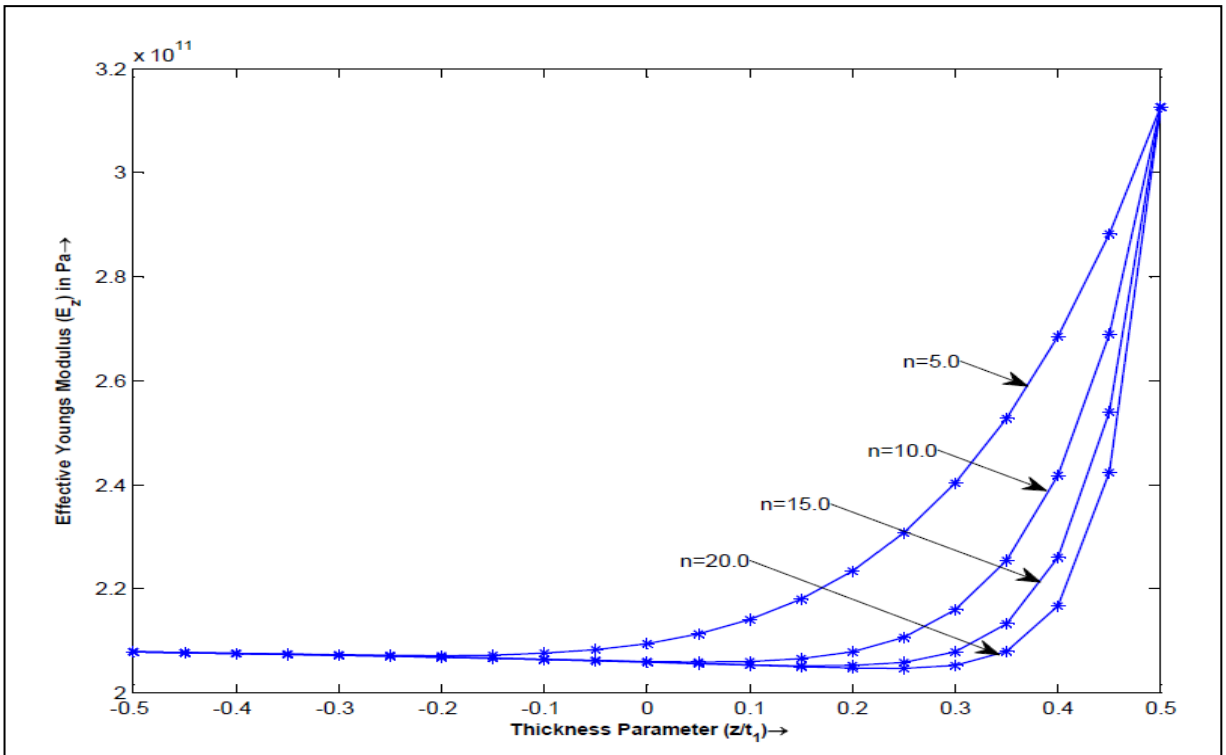

Figure (5.13) Variation of Effective Young's modulus along the thickness direction of FGM layer for different power law indexes for non-linear temperature variation, $T_t = 450K$ and $T_b = 300K$.

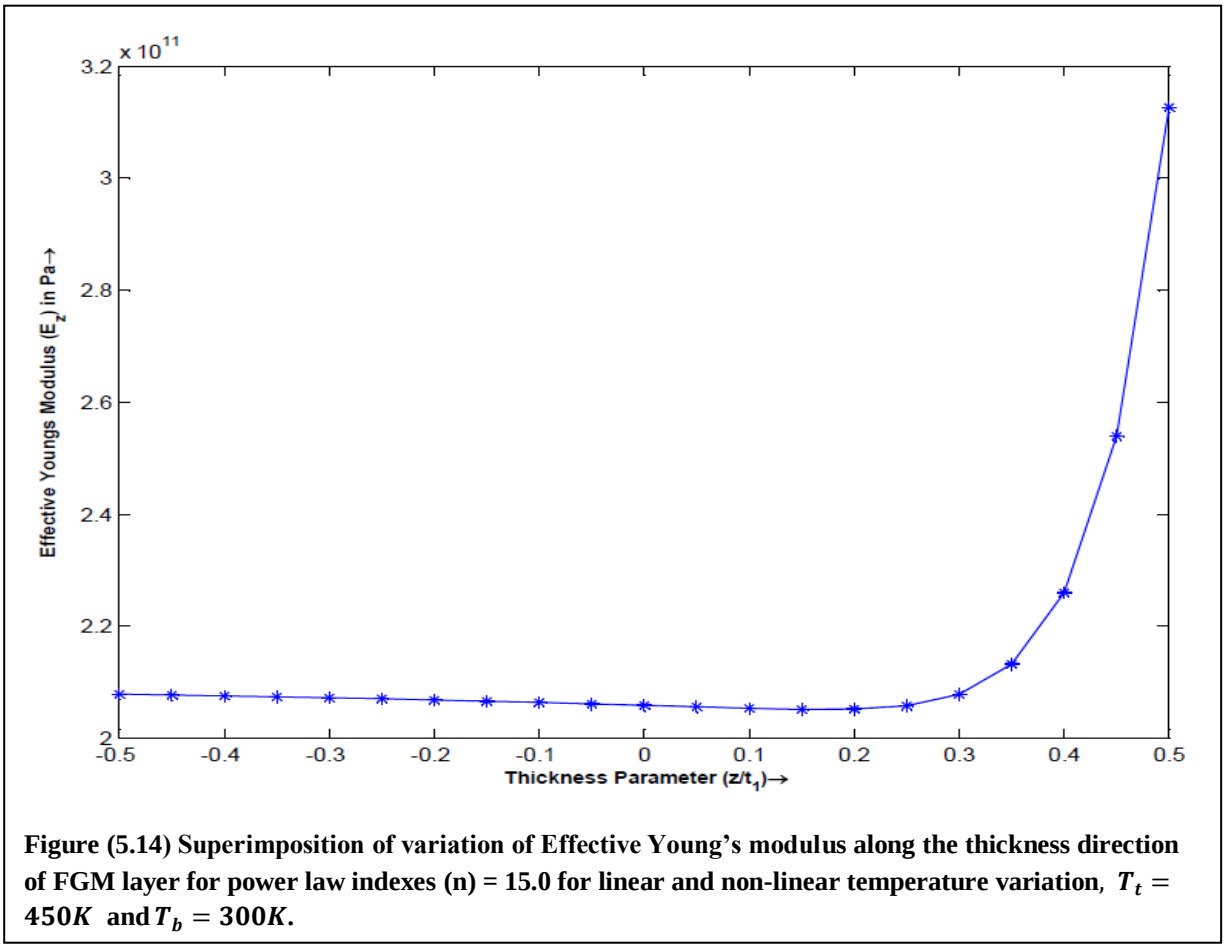

Figure (5.14) Superimposition of variation of Effective Young's modulus along the thickness direction of FGM layer for power law indexes (n) = 15.0 for linear and non-linear temperature variation, $T_t = 450K$ and $T_b = 300K$.

Free vibration analysis-

For free vibration analysis, Frequency parameter (f) is calculated. Frequency parameter (f) is defined as the ratio of frequency of the sandwich beam to the frequency of an equivalent sandwich beam with pure stainless steel at the bottom layer and pure ceramic at the top layer (for reference).

Linear temperature variation-

Figure (5.15) shows the variation of Frequency parameter (f) for the 1st three modes of vibration against core thickness parameter (t_2/t_1) for linear temperature variation. For power law index (n)

=15.0 and temperature of top face of FGM layer= 450K. The core thickness parameter starts at 0.1 and ends at 3.0 with increment of 0.1.

It is noted here that for 2nd and 3rd mode of vibration, the Frequency parameter (f) decreases with increase in core thickness parameter (t_2/t_1). But for 1st mode of vibration, the frequency parameter (f) first decreases up to the point at (t_2/t_1) = 1.5 and increases after that.

Linear temperature variation-

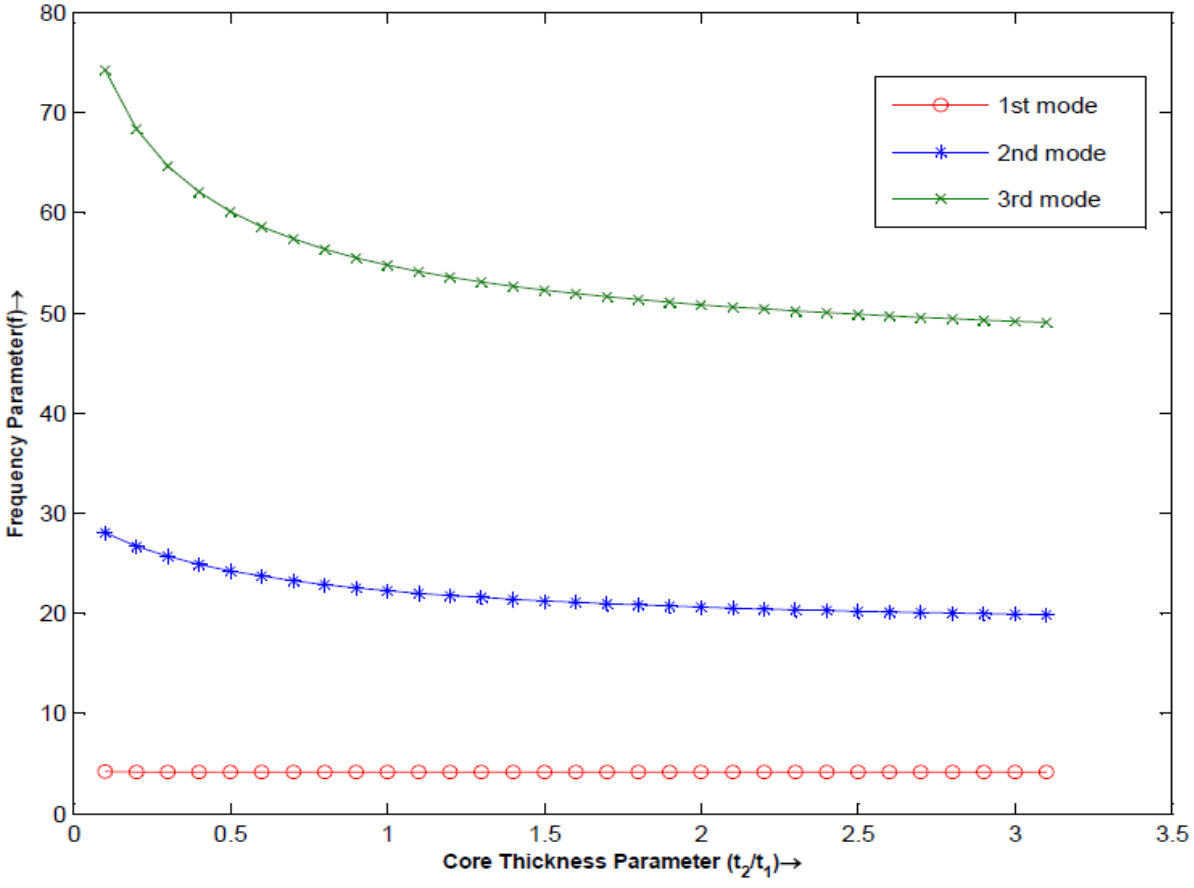

Figure (5.15) Effect of core thickness parameter (t_2/t_1) on Frequency Parameter (f) for power law index (n) =15.0, $\eta_c = 0.18$, $T_t = 450K$ and $T_b = 300K$ for linear temperature variation.

Figure (5.16) shows the variation of Frequency parameter (f) for the 1st three modes of vibration against power law index (n) for linear temperature variation for core thickness parameter = 0.5

and temperature of top surface of FGM layer= 450 K. The graph is plotted by taking result for power law index = 5.0, 10.0, 15.0 and 20.0.

It is noted here that the Frequency parameter (f) decreases with increase in power law index (n).

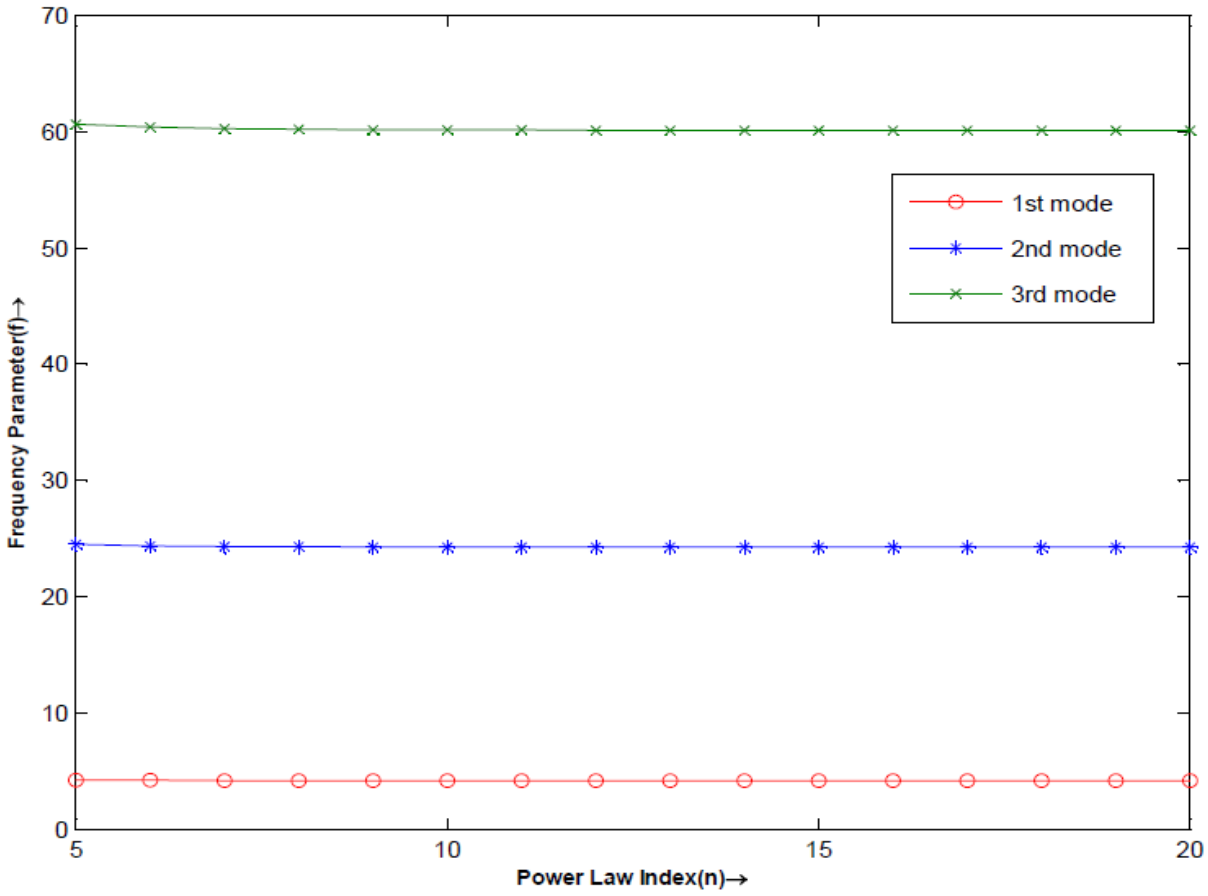

Figure (5.16) Effect of Power Law Index (n) on Frequency Parameter (f) for core thickness parameter (t_2/t_1) =0.5, $\eta_c = 0.18$, $T_t = 300K$ and $T_b = 450K$ for linear temperature variation.

Figure (5.17) shows the variation of Frequency parameter (f) for the 1st three modes of vibration against temperature of top face of FGM layer for linear temperature variation for core thickness

parameter = 0.5 and power law index=15.0. The minimum top face temperature is taken as room temperature i.e. 300K and maximum top face temperature as 450 K with increment of 50K.

It is noted here that the Frequency parameter (f) with increase in top face temperature of FGM layer. This is due to the fact that as the top surface temperature increases, the effective stiffness of the system decreases.

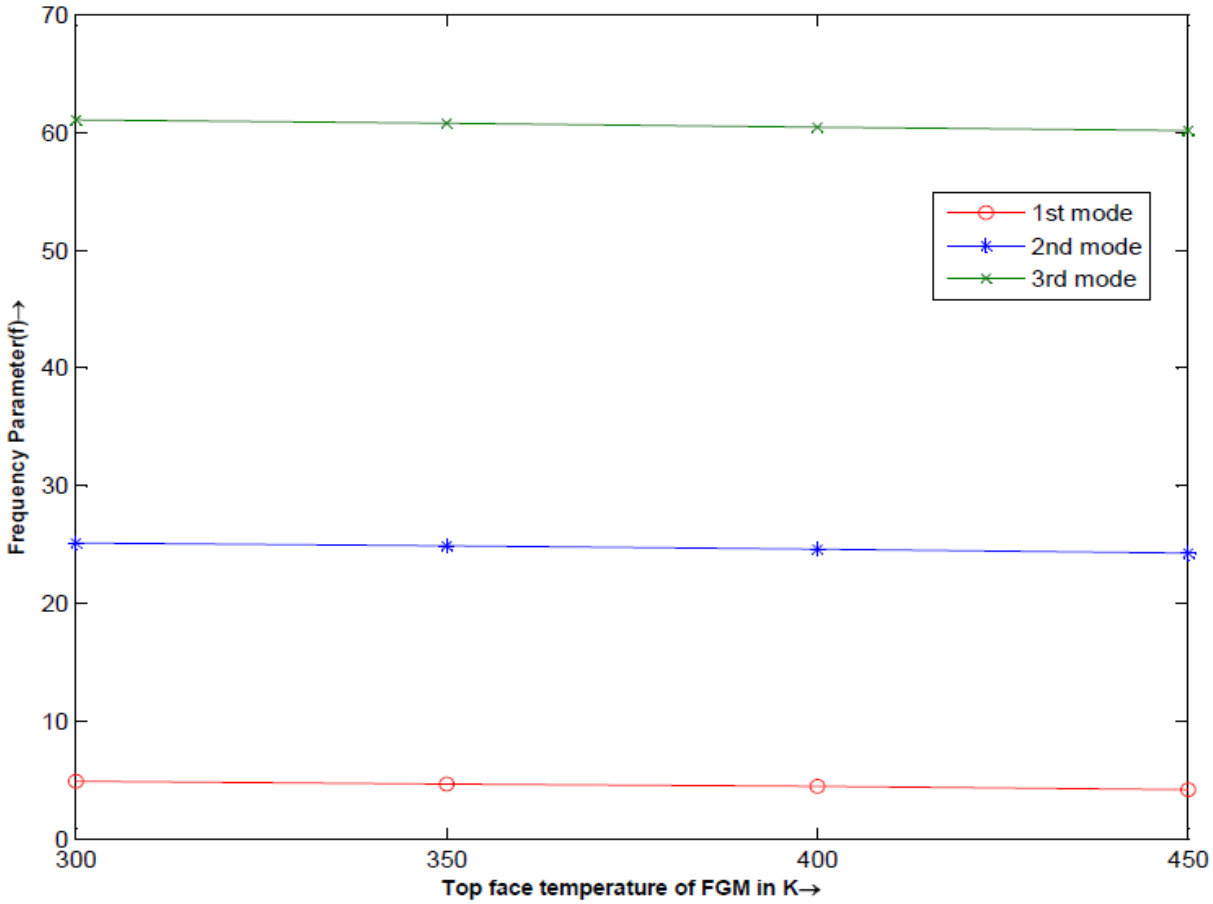

Figure (5.17) Effect of FGM layer top face temperature on Frequency Parameter (f) for core thickness parameter (t_2/t_1) = 0.5, $\eta_c = 0.18$, and power law index (n) =15.0, for linear temperature variation.

Figure (5.18) shows the variation of Loss Factor （η） for the 1st three modes of vibration against core thickness parameter (t_2/t_1) for linear temperature variation for power law index (n) =15.0 and temperature of top face of FGM layer= 450K. The core thickness parameter starts at 0.1 and

ends at 3.0 with increment of 0.1. Loss Factor is defined as the ratio of system loss factor to the core loss factor. It gives us an idea about the system damping capacity. Higher the Loss Factor, higher is the system damping capacity.

It is noted here that the Loss Factor (η) increases sharply for 1st mode of vibration with increase in core thickness parameter (t_2/t_1). For 2nd mode, the Loss factor increases gradually and for 3rd mode, the Loss factor decreases gradually. This shows that with increase in number of modes the Loss factor or the damping capacity of the system decreases with increase in core thickness parameter (t_2/t_1).

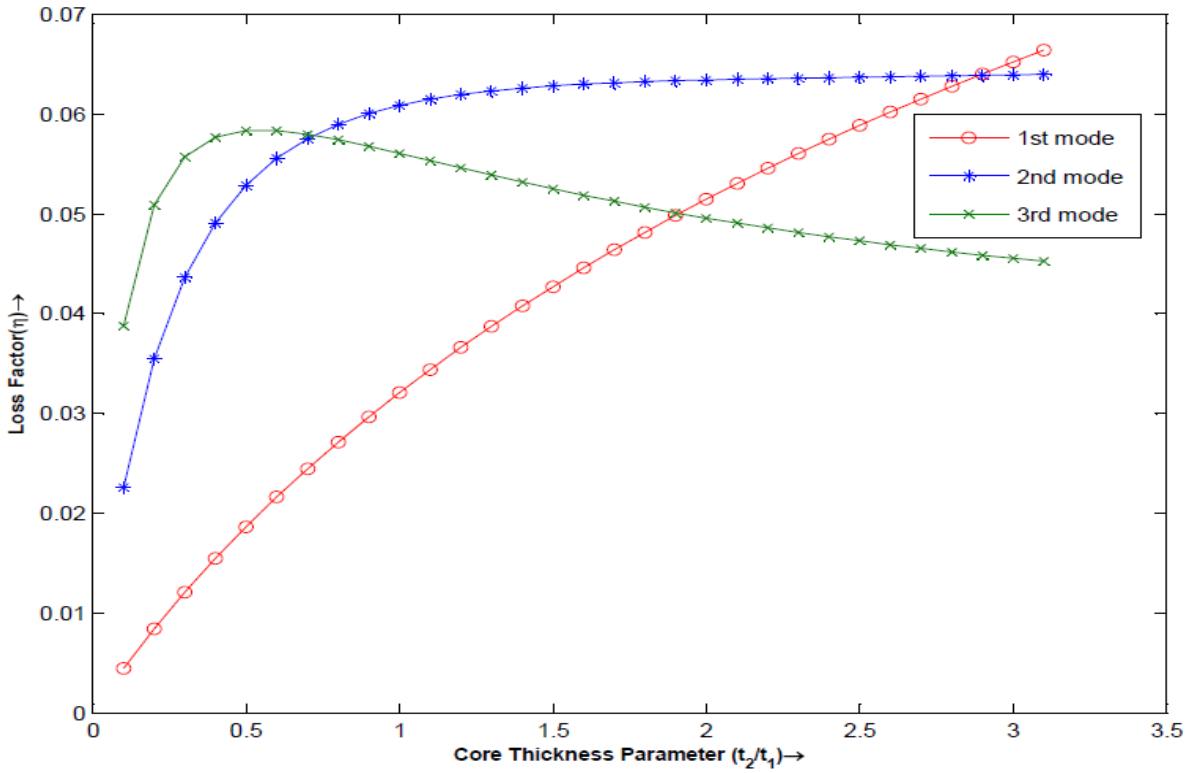

Figure (5.18) Effect of core thickness parameter (t_2/t_1) on Loss Factor (η) for power law index (n) =15.0, $\eta_c = 0.18$, $T_t = 450K$ and $T_b = 300K$ for linear temperature variation.

Figure (5.19) shows the variation of Loss Factor （η） for the 1st three modes of vibration against temperature of top surface of FGM layer for linear temperature variation for core thickness parameter (t_2/t_1) = 0.5 and power law index=15.0. The minimum top face temperature of FGM layer is taken as room temperature i.e. 300K and maximum top face temperature as 450 K.

The Loss Factor increases with increase in temperature of top surface of FGM layer.

The results of free vibration have been validated from the results obtained by Rao [53].

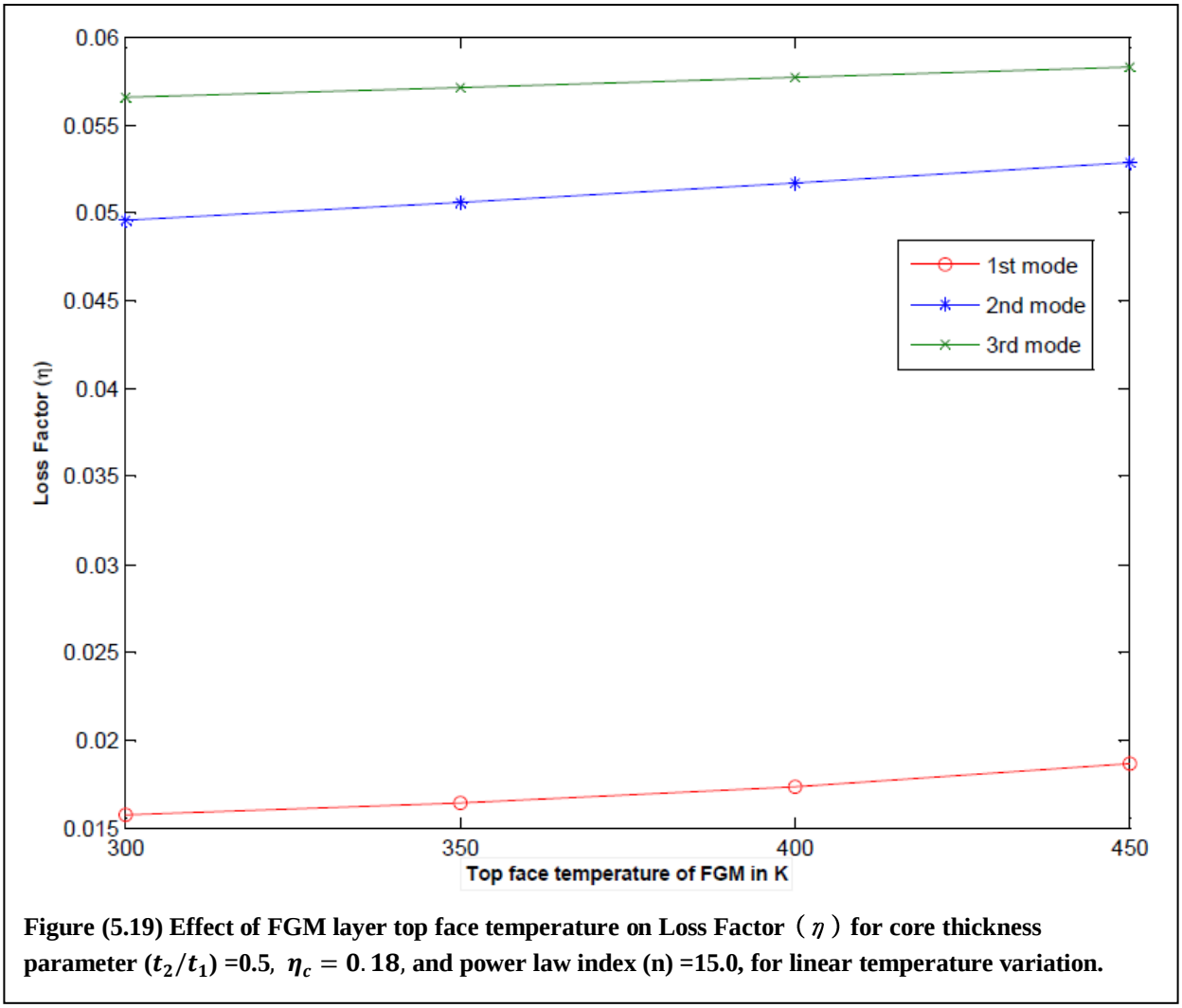

Figure (5.19) Effect of FGM layer top face temperature on Loss Factor （η） for core thickness parameter (t_2/t_1) =0.5, $\eta_c = 0.18$, and power law index (n) =15.0, for linear temperature variation.

Non-linear temperature variation-

Similarly, graphs are plotted for non-linear temperature variation under same conditions as stated in linear temperature variation case. Figures (20)-(24) shows the free vibration analysis for non-linear temperature vibration. The frequency parameter (f) varies in the same way as it did for linear temperature variation.

Non-linear temperature variation-

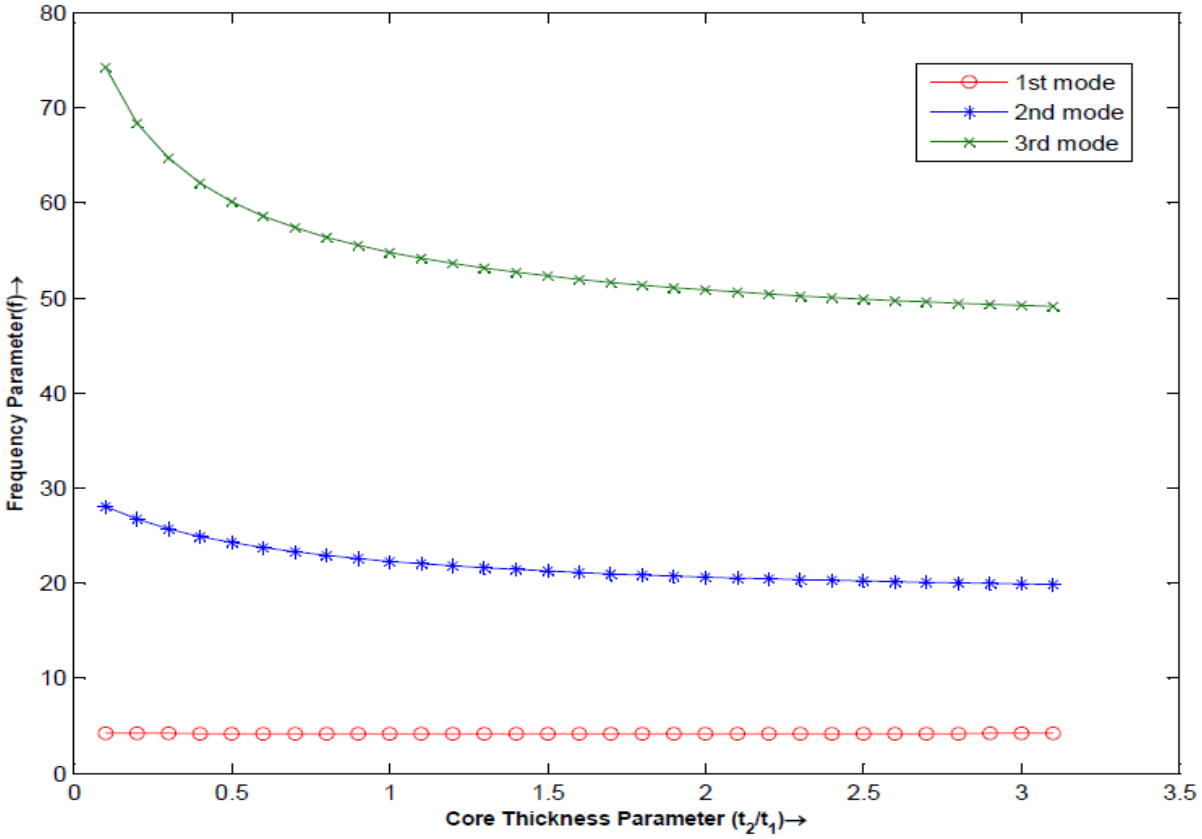

Figure (5.20) Effect of core thickness parameter (t_2/t_1) on Frequency Parameter (f) for power law index (n) =15.0, $\eta_c = 0.18$, $T_t = 450K$ and $T_b = 300K$ for non-linear temperature

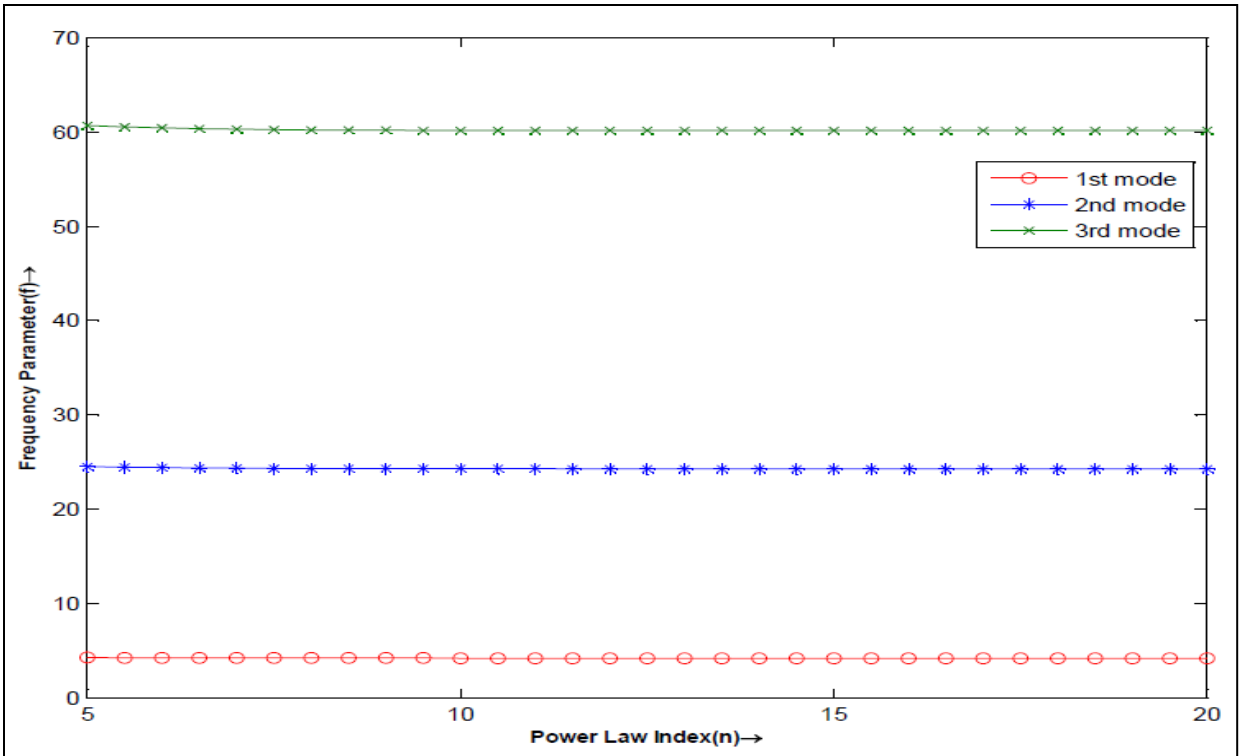

Figure (5.21) Effect of Power Law Index (n) on Frequency Parameter (f) for core thickness parameter (t_2/t_1) =0.5, $\eta_c = 0.18$, $T_t = 450K$ and $T_b = 300K$ for non-linear temperature variation.

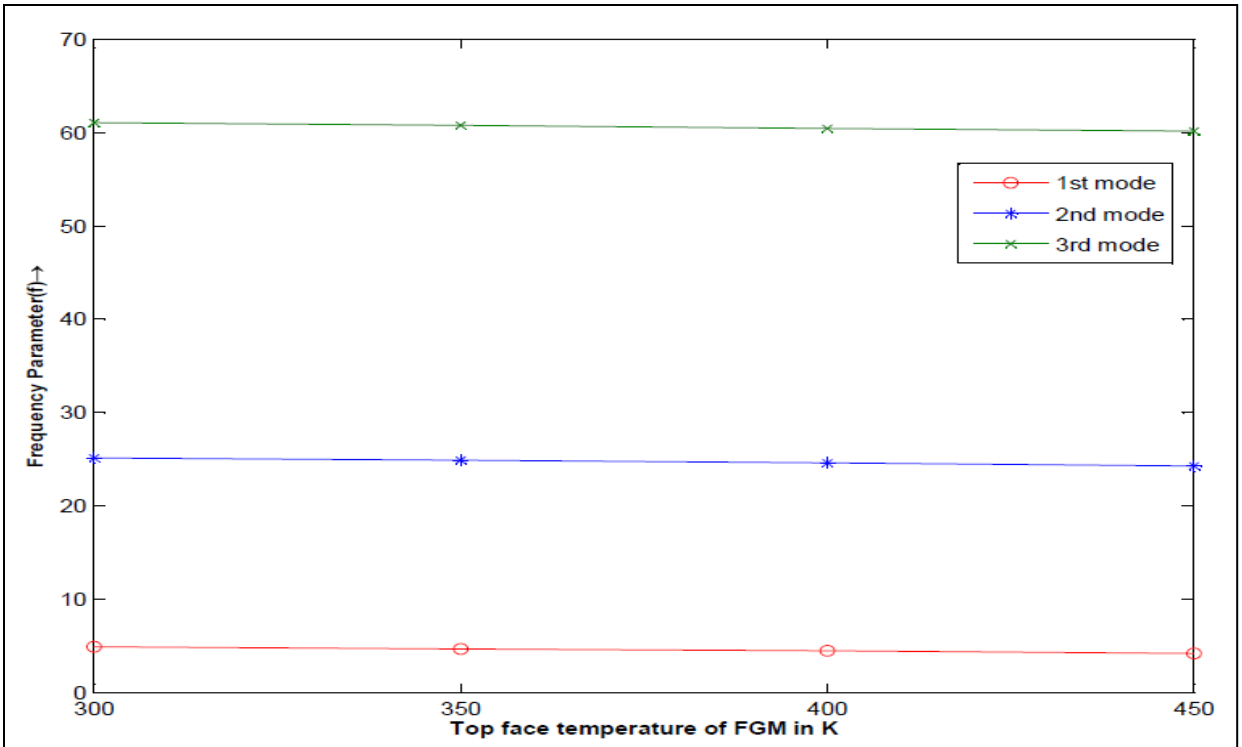

Figure (5.22) Effect of FGM layer top face temperature on Frequency Parameter (f) for core thickness parameter (t_2/t_1) = 0.5 and power law index (n) =15.0, $\eta_c = 0.18$, for non-linear temperature variation.

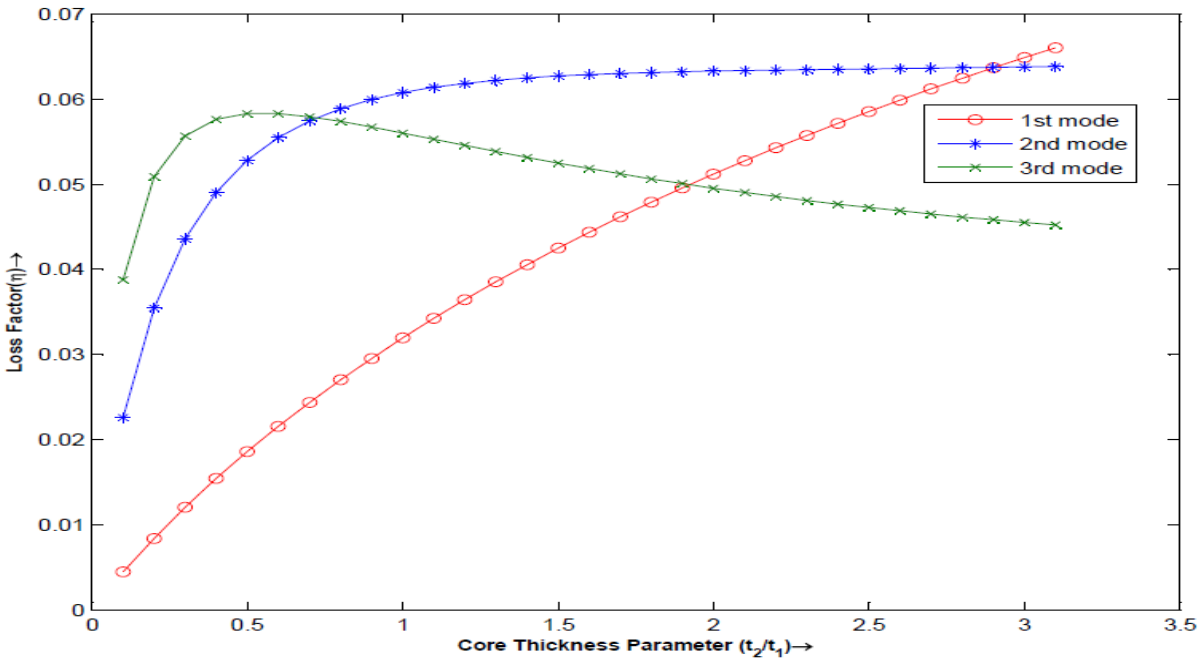

Figure (5.23) Effect of core thickness parameter (t_2/t_1) on Loss Factor (η) for power law index (n) =15.0 and FGM layer, $\eta_c = 0.18$, $T_t = 450K$ and $T_b = 300K$ for non-linear temperature variation.

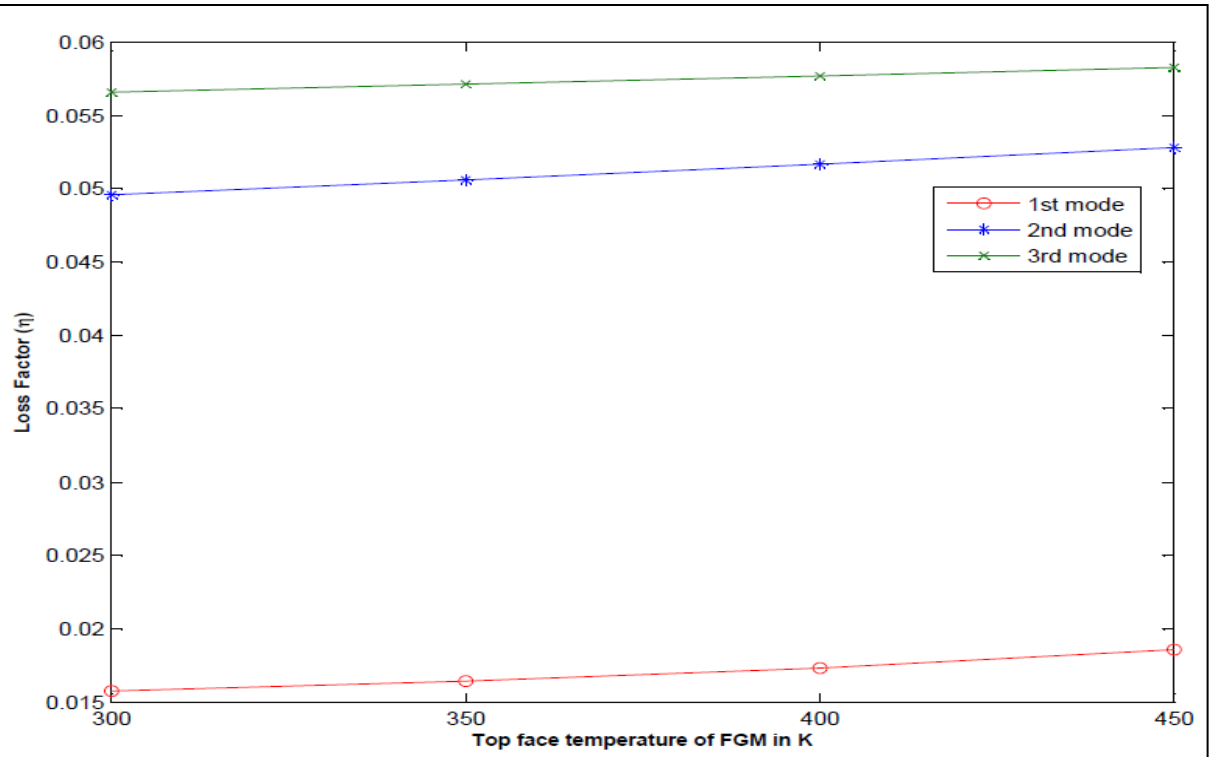

Figure (5.24) Effect of FGM layer top face temperature on Loss Factor (η) for core thickness parameter (t_2/t_1) =0.5, $\eta_c = 0.18$, and power law index (n) =15.0, for non-linear temperature variation.

Static load analysis-

For static loading analysis, Buckling load parameter (P_b) is calculated. Buckling load parameter (P_b) is defined as the ratio of buckling load that the sandwich beam can take to the buckling load that an equivalent sandwich beam with pure stainless steel at the bottom layer and pure ceramic at the top layer can take.

Linear temperature variation-

Figure (5.25) shows the variation of Buckling load parameter (P_b) for the 1st three modes of vibration against core thickness parameter (t_2/t_1) for linear temperature variation for power law index (n) =15.0 and temperature of top face of FGM layer= 450K. The core thickness parameter starts at 0.1 and ends at 3.0 with increment of 0.1.

It is noted here that for 2nd and 3rd mode of vibration, the Buckling load parameter (P_b) decreases with increase in core thickness parameter (t_2/t_1). But for 1st mode of vibration, the Buckling load parameter (P_b) increases with increase in core thickness parameter (t_2/t_1).

Linear temperature variation-

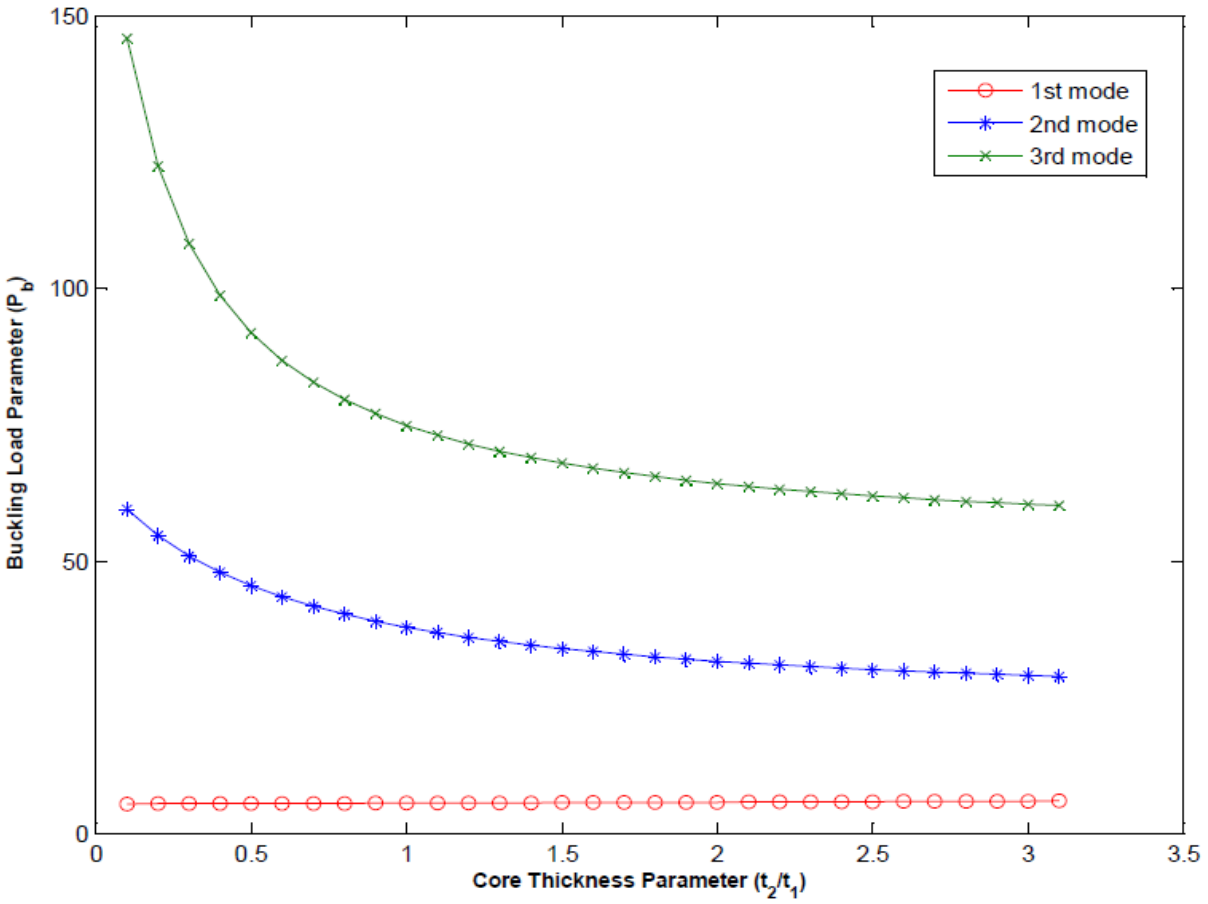

Figure (5.25) Effect of core thickness parameter (t_2/t_1) on Buckling Load Parameter (P_b) for power law index (n) =15.0, $\eta_c = 0.18$, $T_t = 450K$ and $T_b = 300K$ for linear temperature variation.

Figure (5.26) shows the variation of Buckling load parameter (P_b) for the 1st three modes of vibration against power law index (n) for linear temperature variation for core thickness parameter = 0.5 and temperature of top face of FGM layer= 350 K. The graph is plotted by taking result for power law index = 5.0, 10.0, 15.0 and 20.0.

It is noted here that the Buckling load parameter decreases with increase in power law index (n).

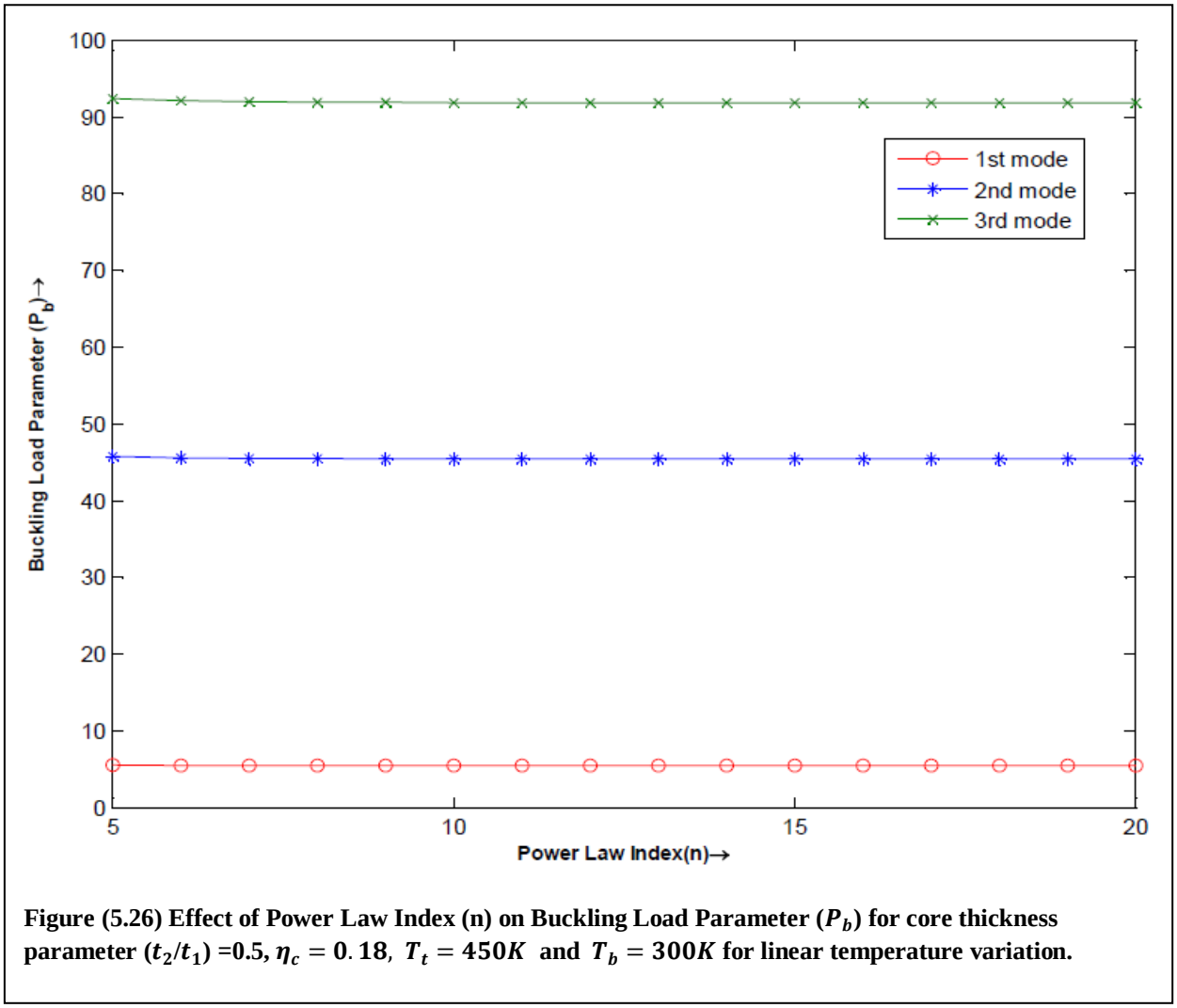

Figure (5.26) Effect of Power Law Index (n) on Buckling Load Parameter (P_b) for core thickness parameter (t_2/t_1) =0.5, $\eta_c = 0.18$, $T_t = 450K$ and $T_b = 300K$ for linear temperature variation.

Figure (5.27) shows the variation of Buckling load parameter (P_b) for the 1st three modes of vibration against temperature of top face of FGM layer for linear temperature variation for core thickness parameter = 0.5 and power law index=15.0. The minimum top face temperature of FGM layer is taken as room temperature i.e. 300K and maximum top face temperature as 450 K with increment of 50K.

It is noted here that the Buckling load parameter decreases with increase in top face temperature of FGM layer. This is because as the top surface temperature increases, the effective stiffness of the system decreases. Hence, it's buckling load carrying capacity decreases.

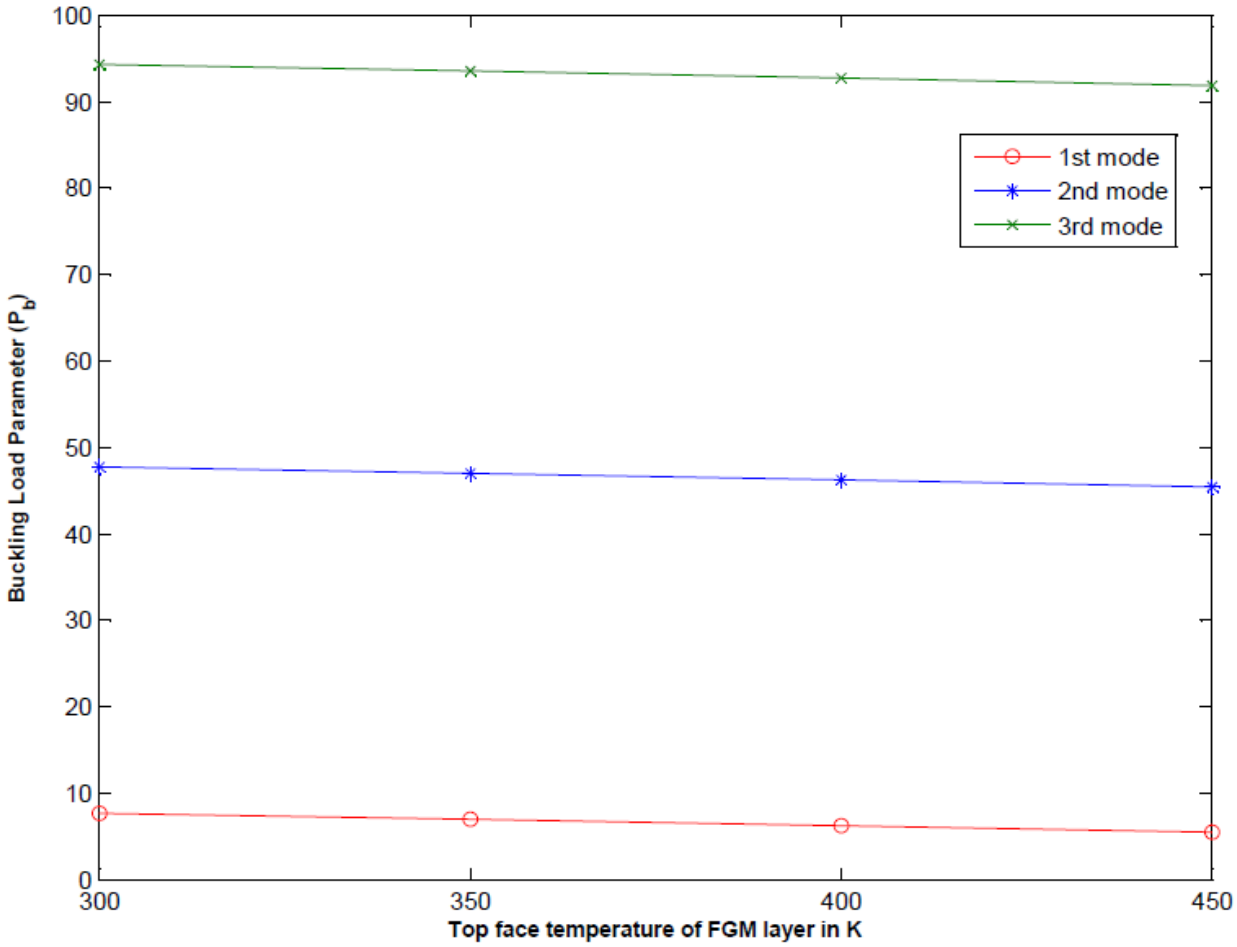

Figure (5.27) Effect of FGM layer top face temperature on Buckling Load Parameter (P_b) for core thickness parameter (t_2/t_1) = 0.5, $\eta_c = 0.18$ and power law index (n) =15.0, for linear temperature variation.

Non-linear temperature variation-

Similarly, graphs are plotted for non-linear temperature variation under same conditions as stated in linear temperature variation case. Figures (28) - (30) shows the static load analysis for non-linear temperature variation. The buckling load parameter (P_b) varies in the same way as it did for linear temperature variation.

Non-linear temperature variation-

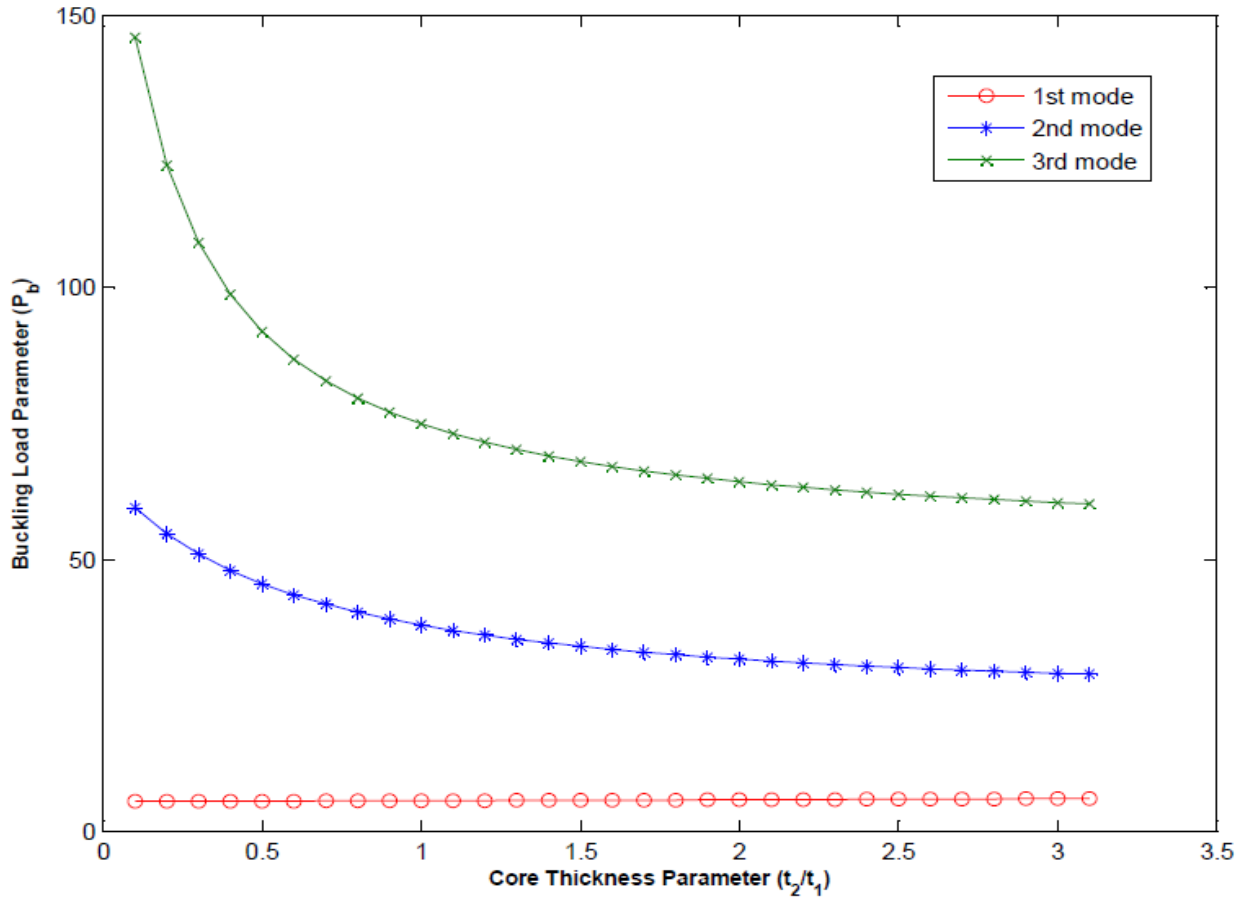

Figure (5.28) Effect of core thickness parameter (t_2/t_1) on Buckling Load Parameter (P_b) for power law index (n) =15.0, $\eta_c = 0.18$, $T_t = 450K$ and $T_b = 300K$ for non-linear temperature variation.

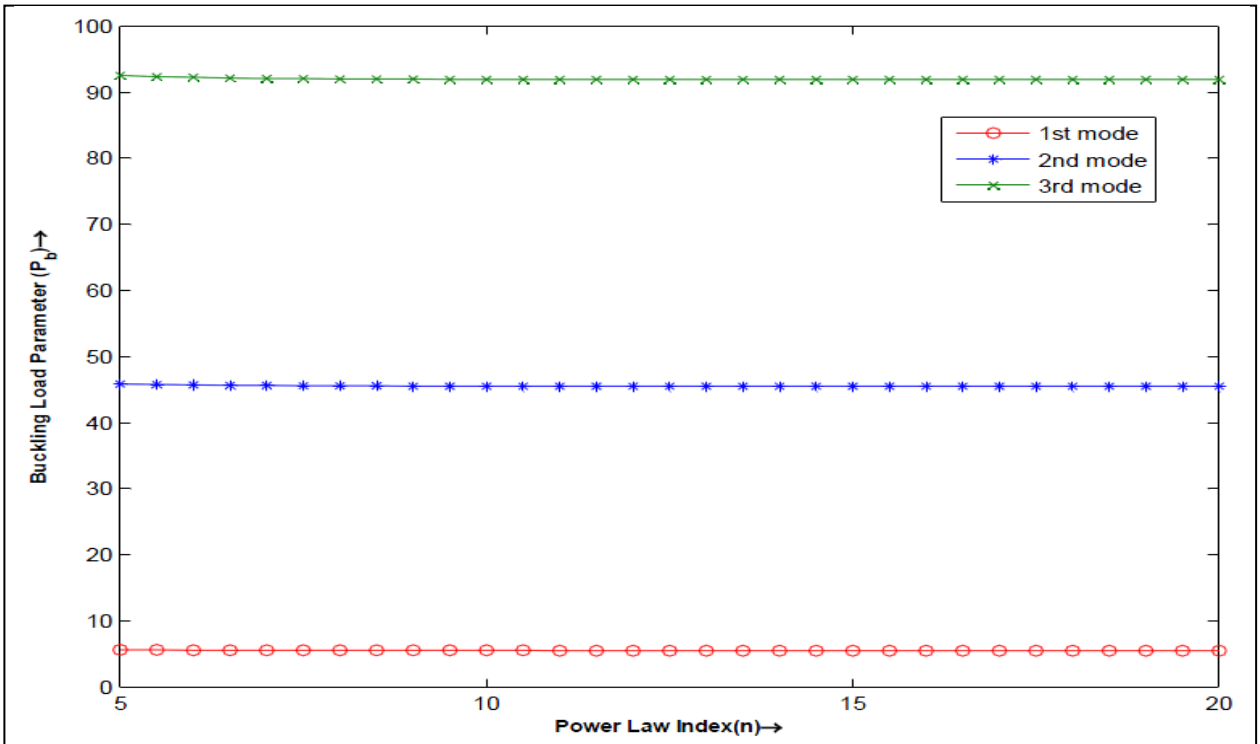

Figure (5.29) Effect of Power Law Index (n) on Buckling Load Parameter (P_b) for core thickness parameter (t_2/t_1) = 0.5, $\eta_c = 0.18$, $T_t = 450K$ and $T_b = 300K$ for non-linear temperature variation.

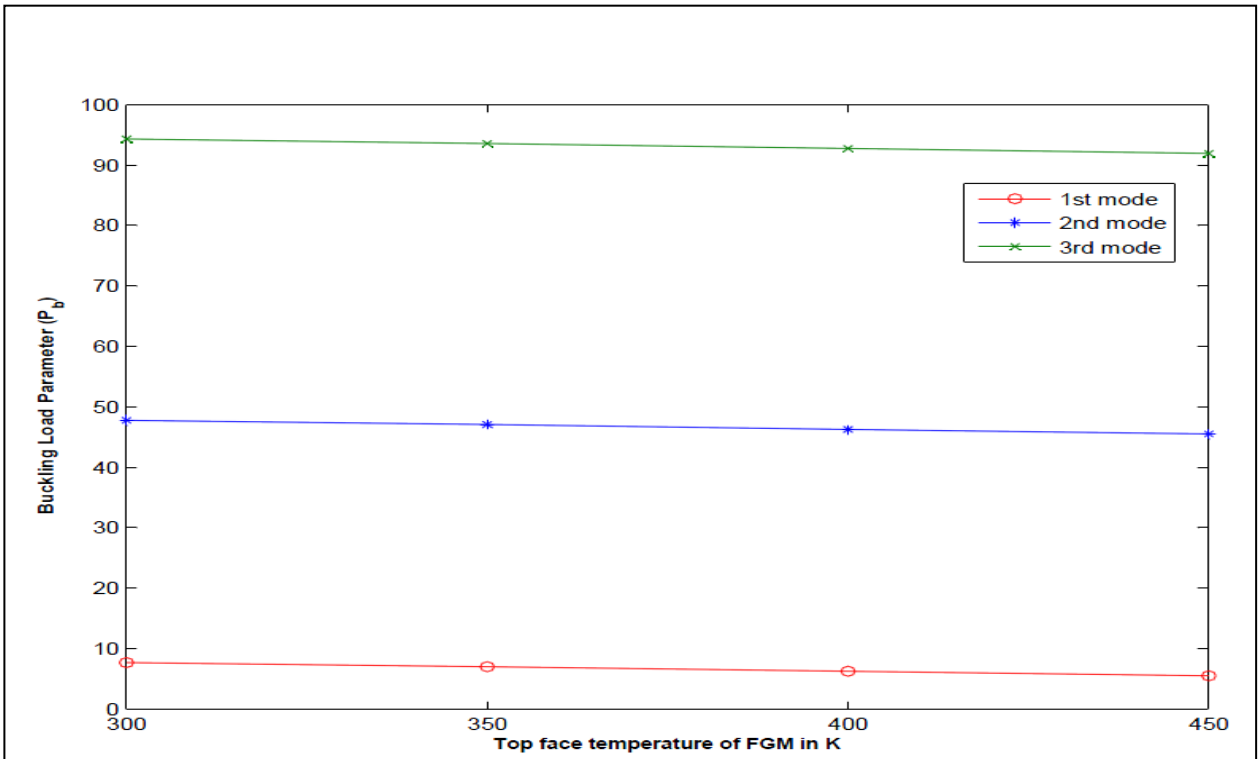

Figure (5.30) Effect of FGM layer top face temperature on Buckling Load Parameter (P_b) for core thickness parameter (t_2/t_1) = 0.5, $\eta_c = 0.18$, and power law index (n) =15.0, 3 modes for non-linear temperature variation.

On superimposing the response curves obtained in free vibration analysis and static load analysis for the two temperature variation cases, as shown in figures (31) –(38), it is found that the curves behaves identically for the two cases and there is no significant difference in variation between them.

Free vibration analysis-

Superimposition of linear and non-linear temperature variation-

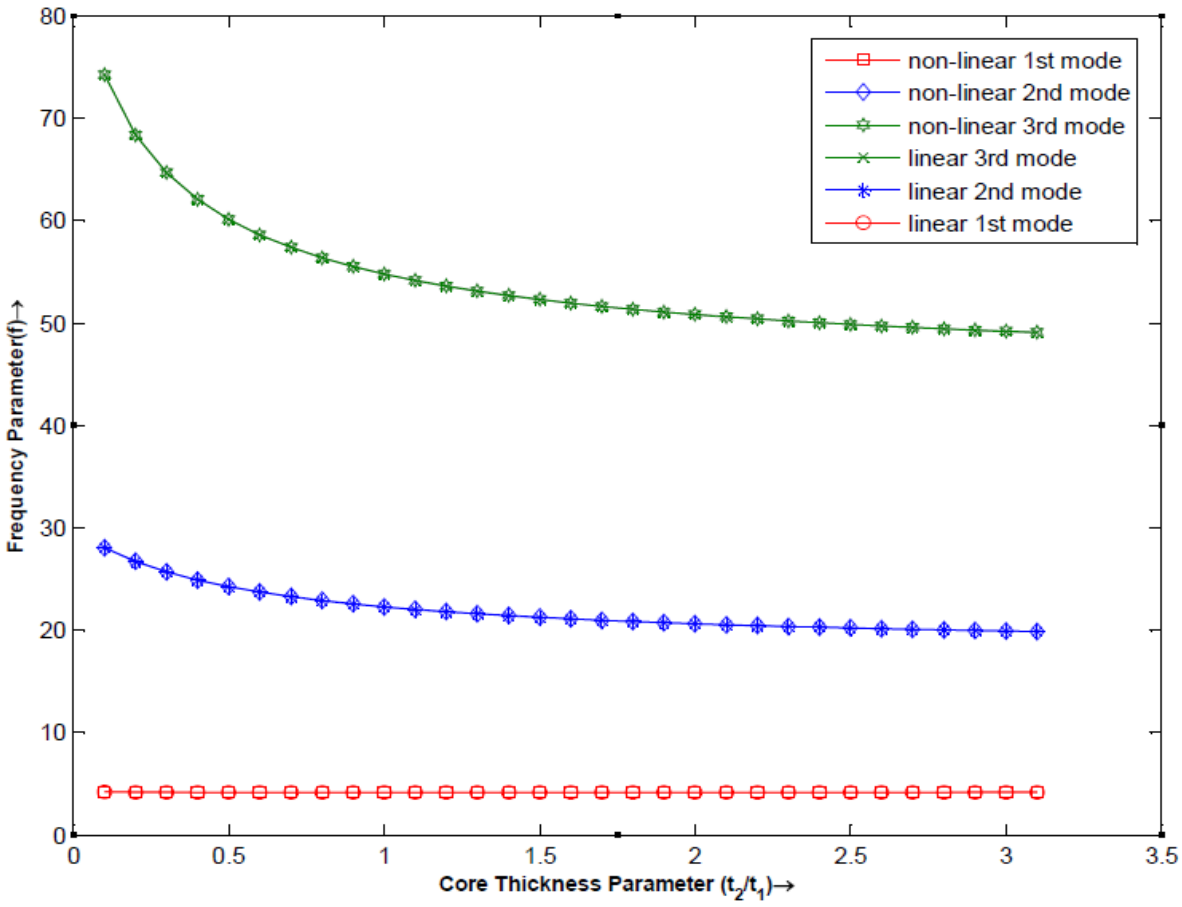

Figure (5.31) Effect of core thickness parameter (t_2/t_1) on Frequency Parameter (f) for power law index (n) =15.0, $\eta_c = 0.18$, $T_t = 450K$ and $T_b = 300K$ for linear and non-linear temperature variation.

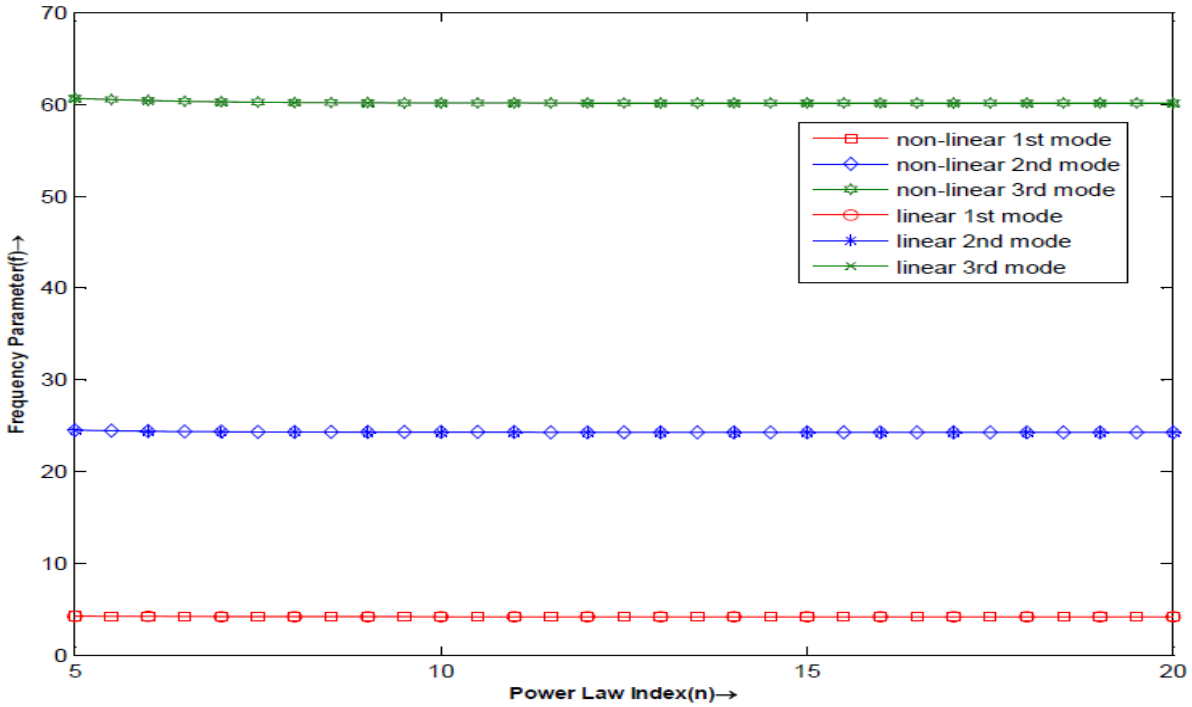

Figure (5.32) Effect of Power Law Index (n) on Frequency Parameter (f) for core thickness parameter (t_2/t_1) = 0.5, $\eta_c = 0.18$, $T_t = 450K$ and $T_b = 300K$ for linear and non-linear temperature variation.

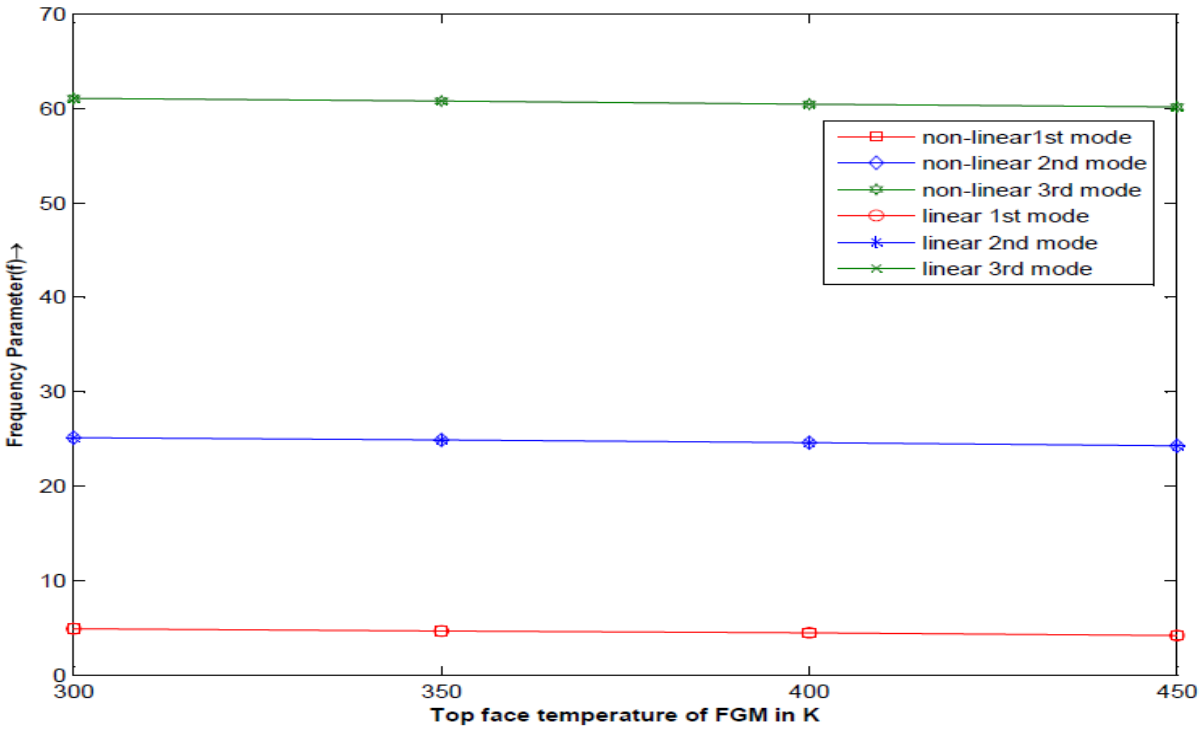

Figure (5.33) Effect of FGM layer top face temperature on Frequency Parameter (f) for core thickness parameter (t_2/t_1) = 0.5, $\eta_c = 0.18$, and power law index (n) = 15.0, for linear and non-linear temperature variation.

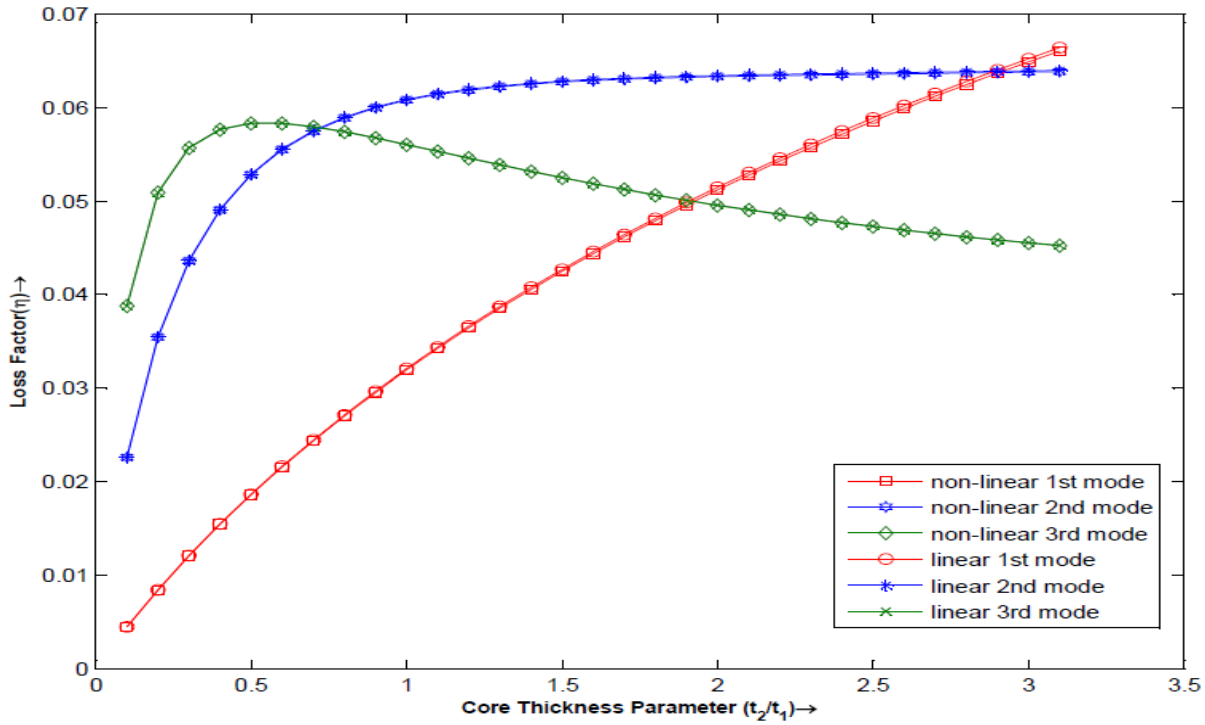

Figure (5.34) Effect of core thickness parameter (t_2/t_1) on Loss Factor （η）for power law index (n) =15.0, $\eta_c = 0.18$, $T_t = 450K$ and $T_b = 300K$ for linear and non-linear temperature variation.

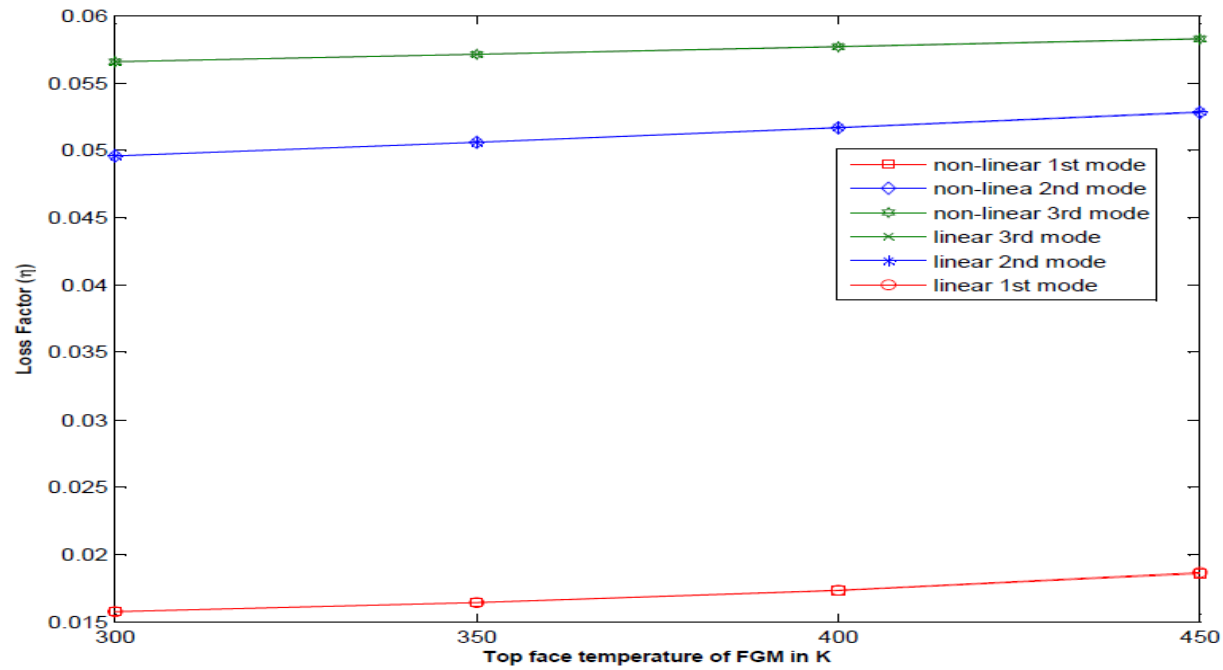

Figure (5.35) Effect of FGM layer top face temperature on Loss Factor （η）for core thickness parameter (t_2/t_1) = 0.5, $\eta_c = 0.18$, and power law index (n) =15.0 for linear and non-linear temperature variation.

Static load analysis

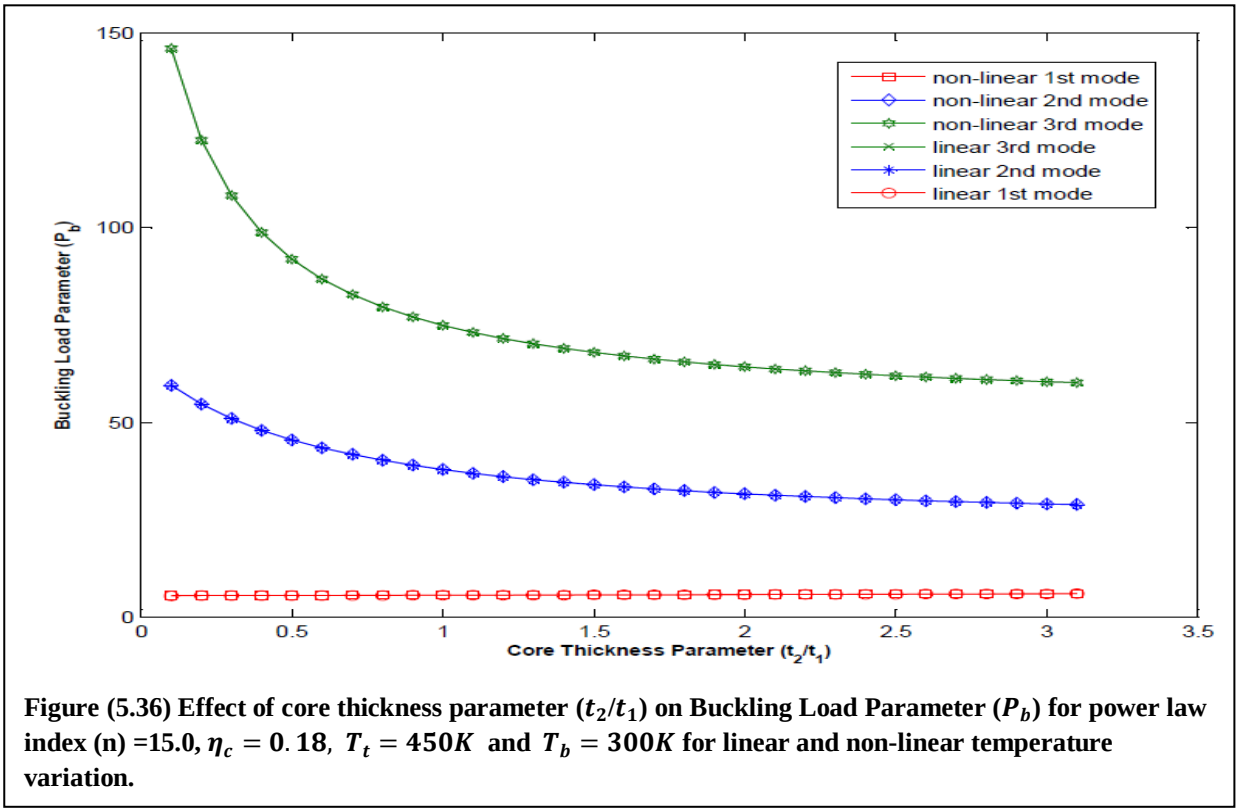

Figure (5.36) Effect of core thickness parameter (t_2/t_1) on Buckling Load Parameter (P_b) for power law index (n) =15.0, $\eta_c = 0.18$, $T_t = 450K$ and $T_b = 300K$ for linear and non-linear temperature variation.

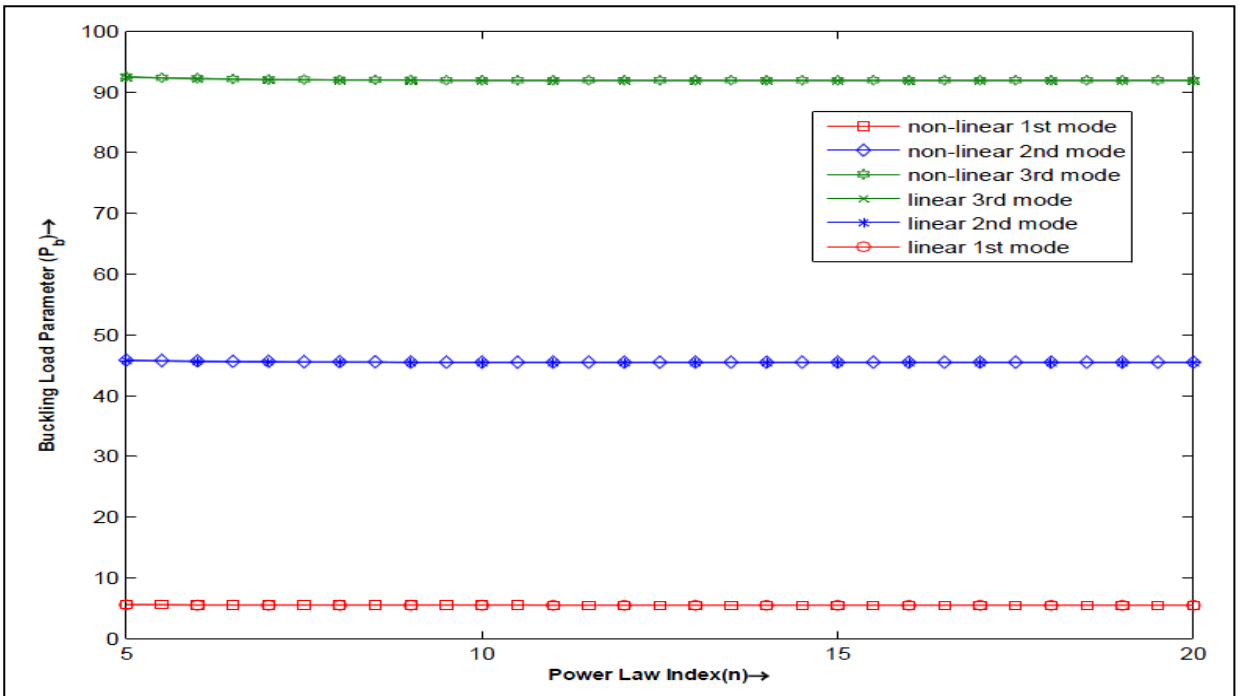

Figure (5.37) Effect of Power Law Index (n) on Buckling Load Parameter (P_b) for core thickness parameter (t_2/t_1) =0.5, $\eta_c = 0.18$, $T_t = 450K$ and $T_b = 300K$, for linear and non-linear temperature variation.

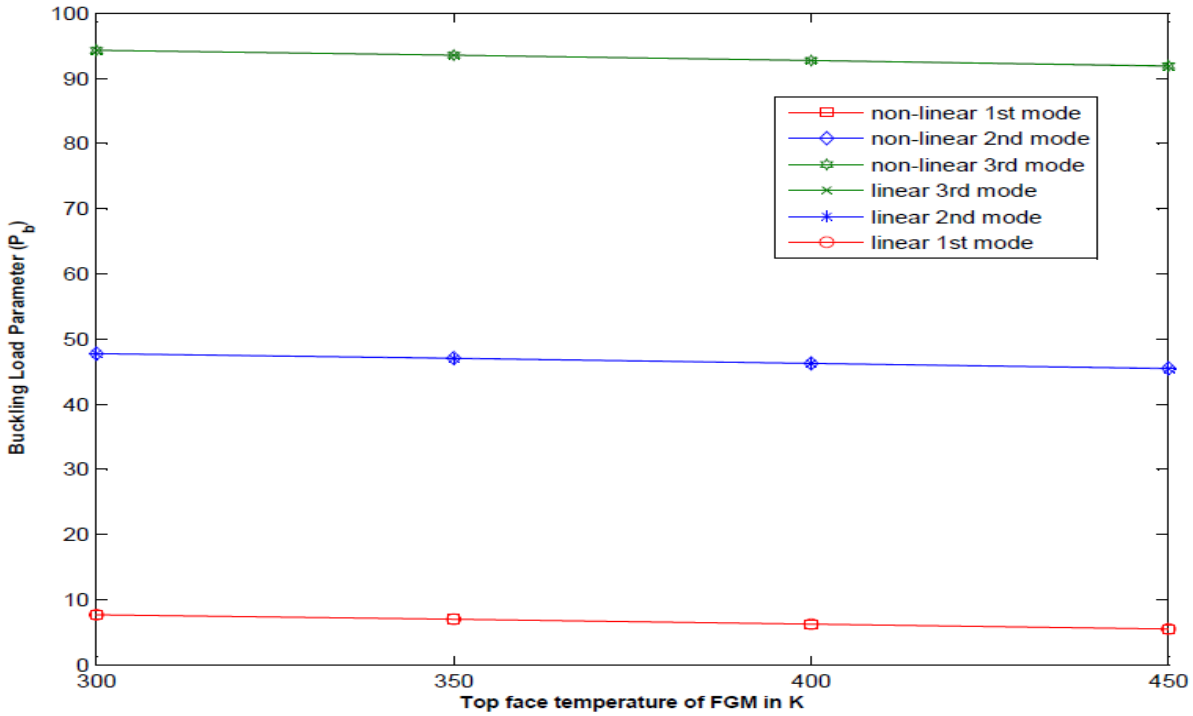

Figure (5.38) Effect of FGM layer top face temperature on Buckling Load Parameter (P_b) for core thickness parameter (t_2/t_1) = 0.5, $\eta_c = 0.18$ and power law index (n) =15.0, for linear and non-linear temperature variation.

Dynamic Stability Analysis

In Dynamic stability analysis, Dynamic Load Factor (β) is plotted against frequency ratio Ω/ω_0 to get the instability regions for simple resonance. Here Ω is the external applied frequency and ω_0 is the first natural frequency of the reference beam without temperature effect. The area inside the V-shape is the unstable region (U) and outside of it is stable region (S), as shown in figure (5.40). These instability regions are then compared by changing the values of system parameters (core thickness parameter (t_2/t_1), power law index (n) and temperature of top face of FGM layer) to understand the effect of system parameters on the instability of the system.

Figure (5.39) shows the effect of power law index (n) on the instability of the system for 1st mode of vibration. Instability regions for power law index (n) = 5.0 and 15.0 are compared for core thickness parameter (t_2/t_1) = 0.3, temperature of top face of FGM layer = 450K and temperature of bottom face of FGM layer = 300K.

It is found that with increase in power law index (n) from 5.0 to 15.0, the instability region shifts towards left i.e. it shifts towards lower frequency ratio or towards lower excitation frequency. This means that the probability of instability increases with increase in power law index (n).

Similarly, figures (5.40) and (5.41) are plotted for 2nd and 3rd mode of vibration respectively.

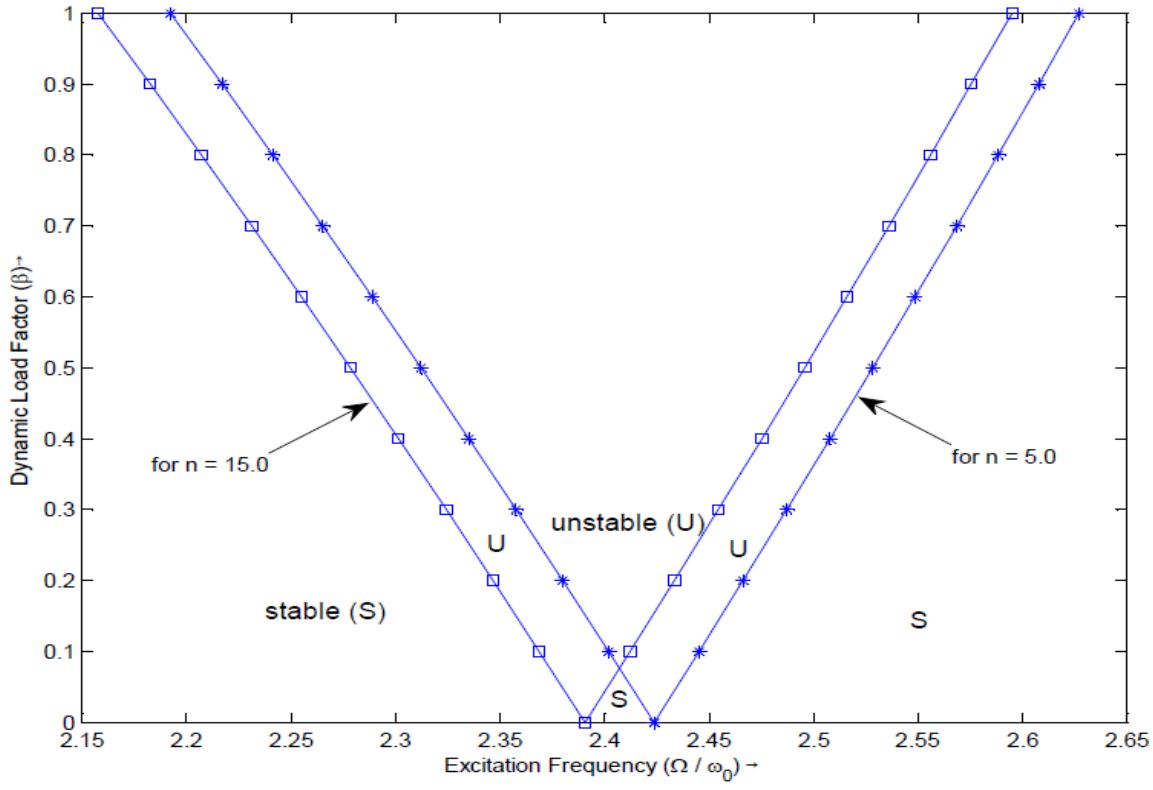

Figure (5.39) Effect of Power law index (n) on the instability regions of the system for core thickness parameter (t_2/t_1) = 0.5, $\eta_c = 0.18$, $T_t = 450K$ and $T_b = 300K$ for 1st mode of vibration, Simple Resonance.

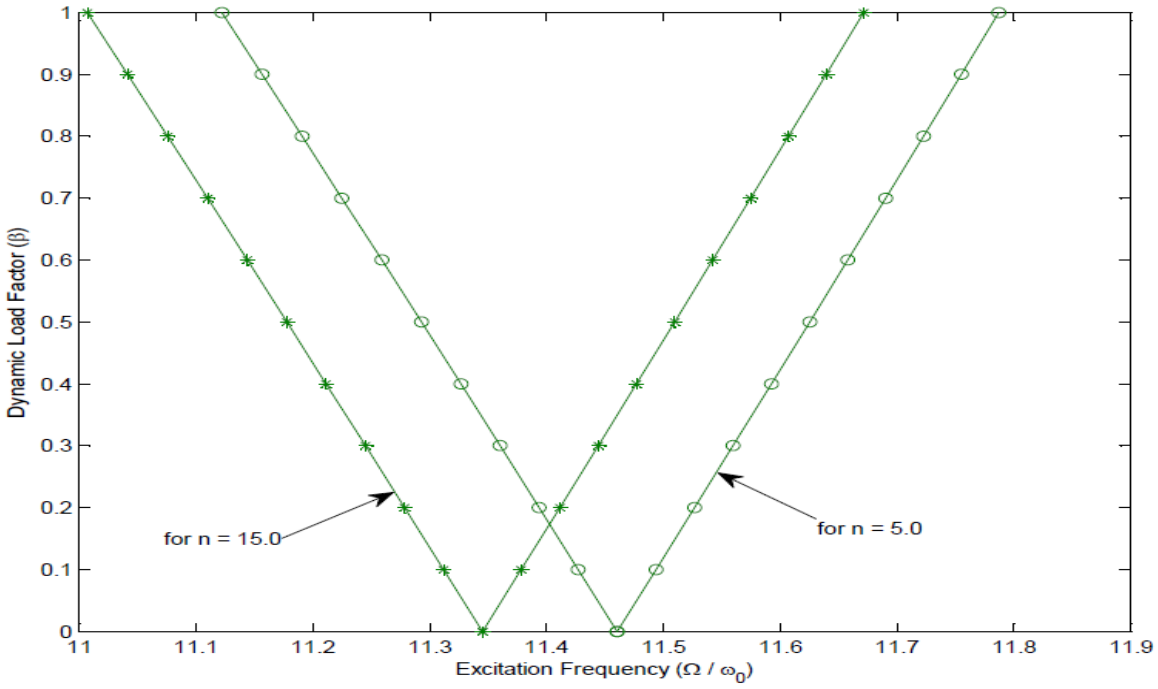

Figure (5.40) Effect of Power law index (n) on the instability regions of the system for core thickness parameter (t_2/t_1) = 0.5, $\eta_c = 0.18$, $T_t = 450K$ and $T_b = 300K$ for 2nd mode of vibration, Simple Resonance.

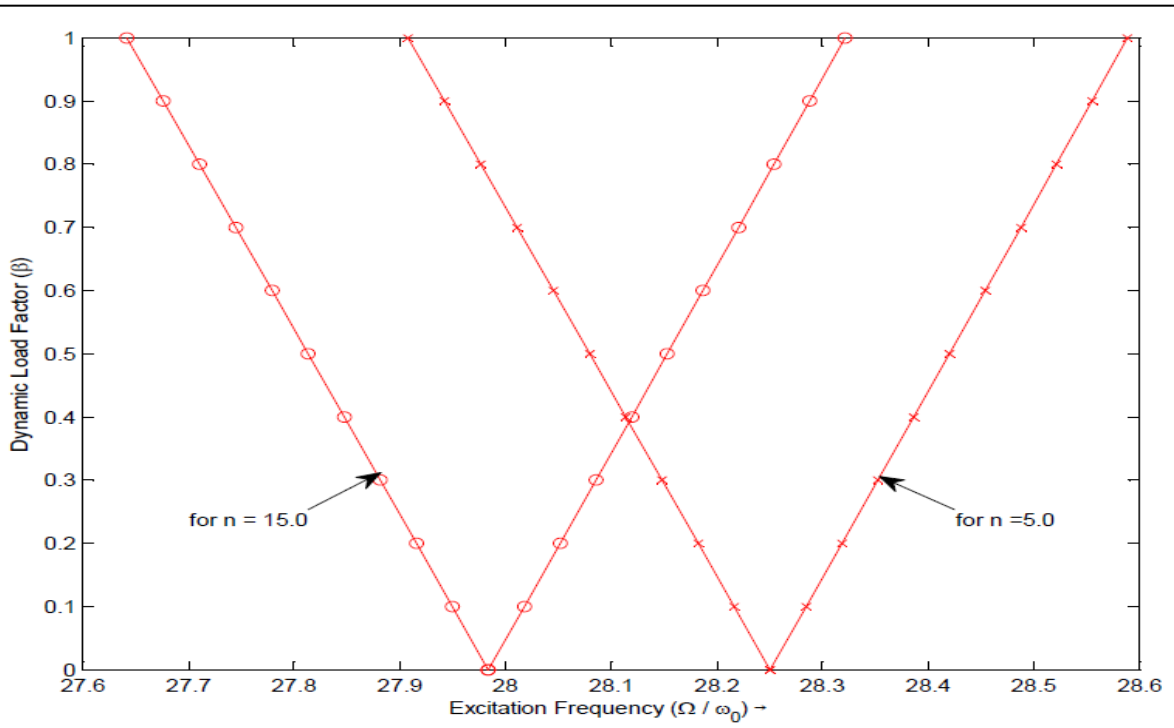

Figure (5.41) Effect of Power law index (n) on the instability regions of the system for core thickness parameter (t_2/t_1) = 0.5, $\eta_c = 0.18$, $T_t = 450K$ and $T_b = 300K$ for 3rd mode of vibration, Simple Resonance.

Figure (5.42)-(5.44) shows the effect of core thickness parameter (t_2/t_1) on instability of the system for the1st three modes of vibration. Instability regions for core thickness parameter (t_2/t_1) = 0.3, 0.6 and 3.0 are compared for power law index (n) = 5.0, temperature of top face of FGM layer = 450K and temperature of bottom face of FGM layer = 300K.

It is found that for 2nd and 3rd mode of vibration, with increase in core thickness parameter (t_2/t_1) from 0.3 to 3.0, the instability region shifts towards left i.e. it shifts towards lower frequency ratio or towards lower excitation frequency. This means that the probability of instability increases with increase in core thickness parameter (t_2/t_1). But for 1st mode of vibration the instability region shifts towards left for (t_2/t_1) = 0.6 but shifts towards right for (t_2/t_1) = 3.0. This is due to the increase in Frequency parameter (f) after the point at (t_2/t_1) = 1.5 for 1st mode of vibration, as discussed earlier. Hence, the probability of instability should be maximum at (t_2/t_1) = 1.5.

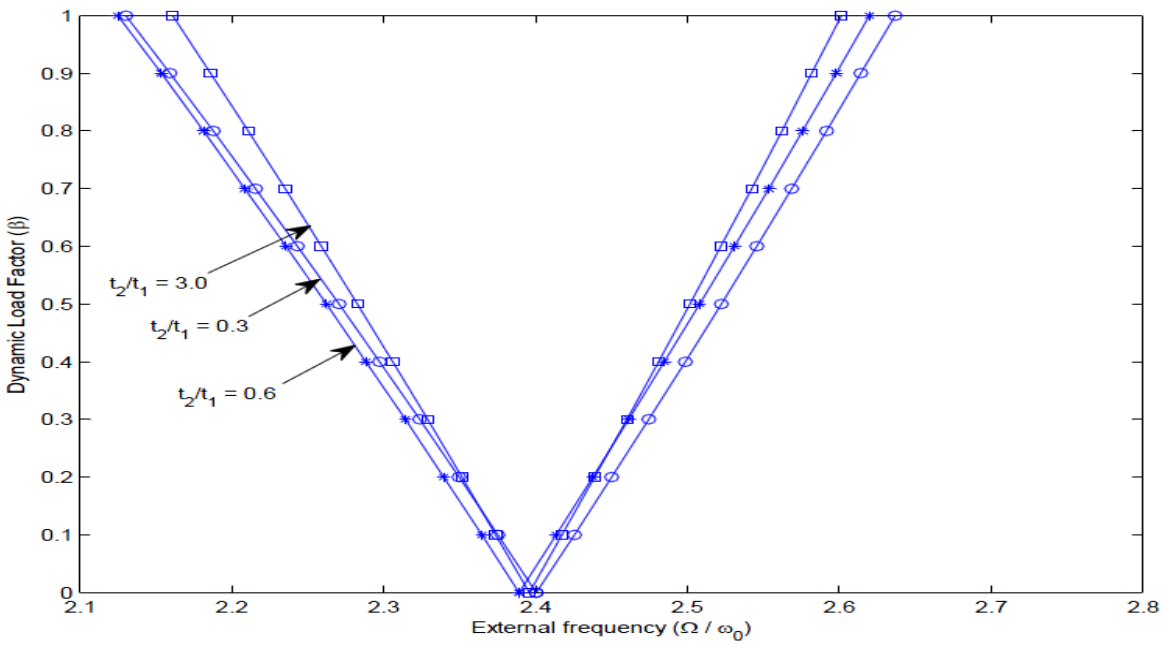

Figure (5.42) Effect of core thickness parameter (t_2/t_1) on the instability regions of the system for power law index (n) = 5.0, $\eta_c = 0.18$, $T_t = 450K$ and $T_b = 300K$ for 1st mode of vibration, Simple Resonance.

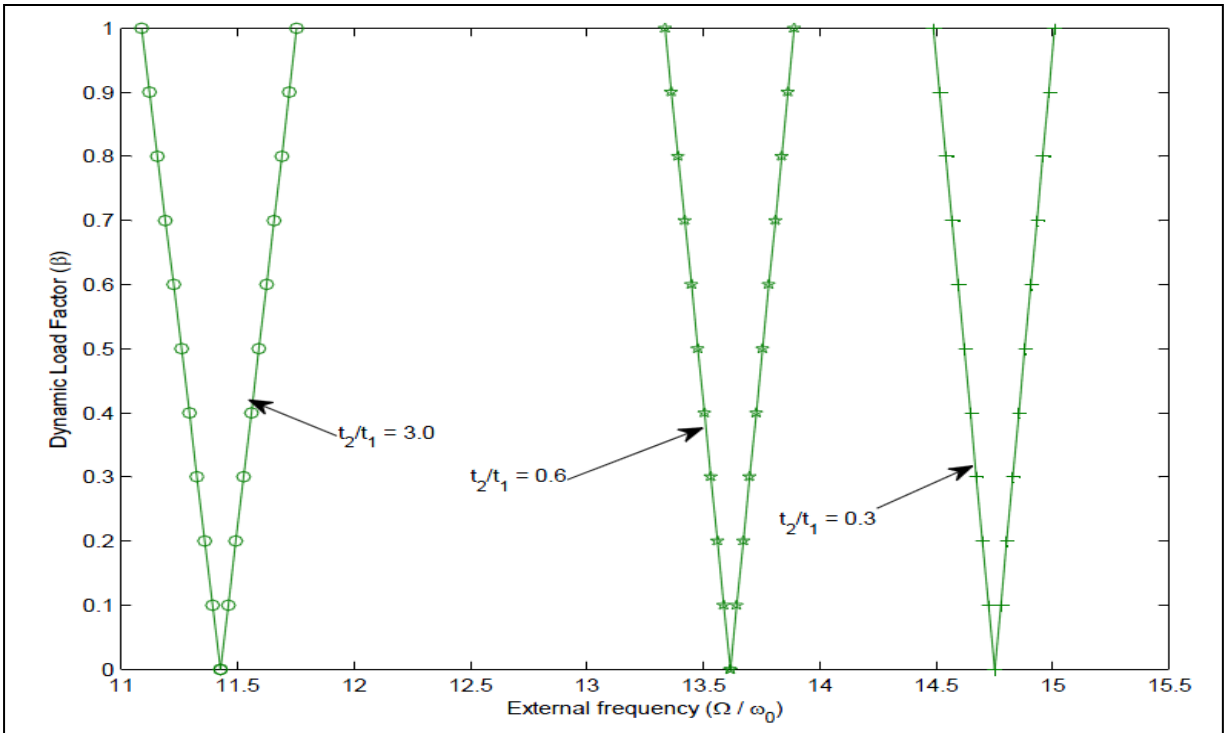

Figure (5.43) Effect of core thickness parameter (t_2/t_1) on the instability regions of the system for power law index (n) = 5.0, $\eta_c = 0.18$, $T_t = 450K$ and $T_b = 300K$ for 2nd mode of vibration, , Simple Resonance.

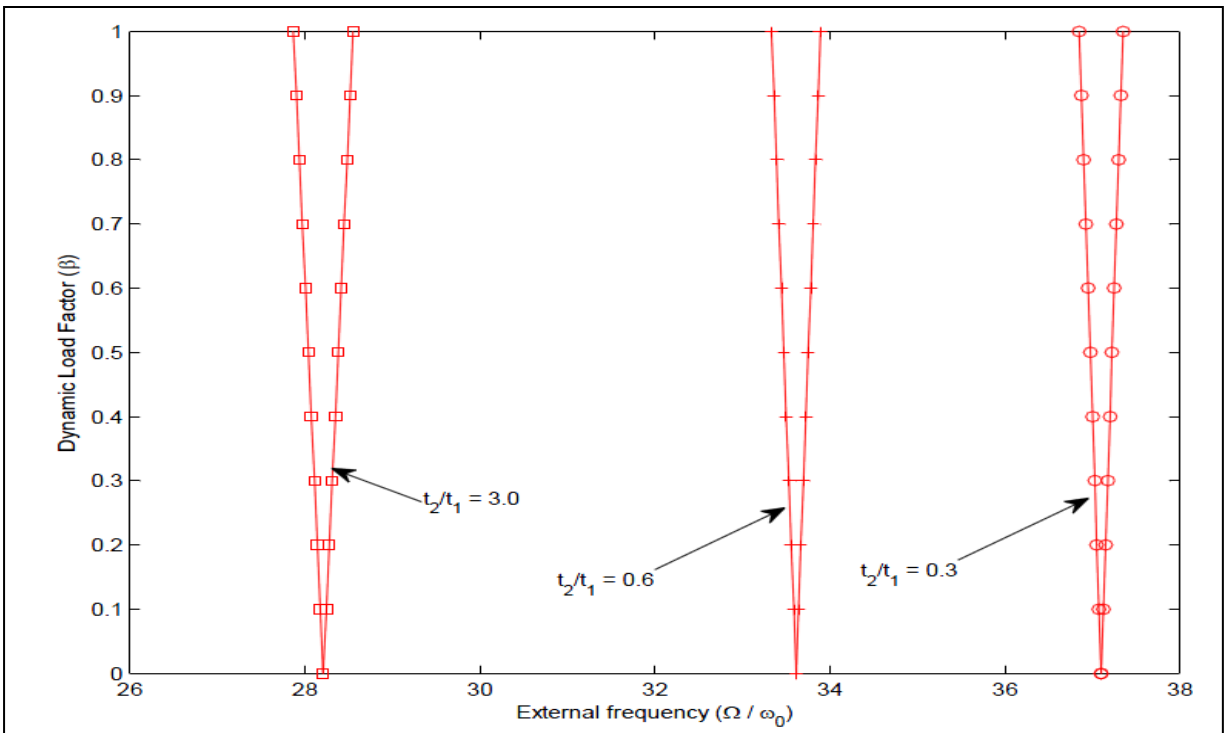

Figure (5.44) Effect of core thickness parameter (t_2/t_1) on the instability regions of the system for power law index (n) = 5.0, $\eta_c = 0.18$, $T_t = 450K$ and $T_b = 300K$ for 3rd mode of vibration, Simple Resonance.

Figure (5.45) shows the effect of temperature of top face of FGM layer on instability of the system for 1st mode of vibration. Instability regions for temperature of top face of FGM layer = 350K and 450K are compared for power law index (n) = 5.0, core thickness parameter (t_2/t_1) = 0.3 and temperature of bottom face of FGM layer = 300K.

It is found that with increase in temperature of top face of FGM layer from 350K to 450K, the instability region shifts towards left i.e. it shifts towards lower frequency ratio or towards lower excitation frequency. This means that the probability of instability increases with increase in temperature of top face of FGM layer

Similarly, figure (5.46) and (5.47) are plotted for 2nd and 3rd mode of vibration respectively.

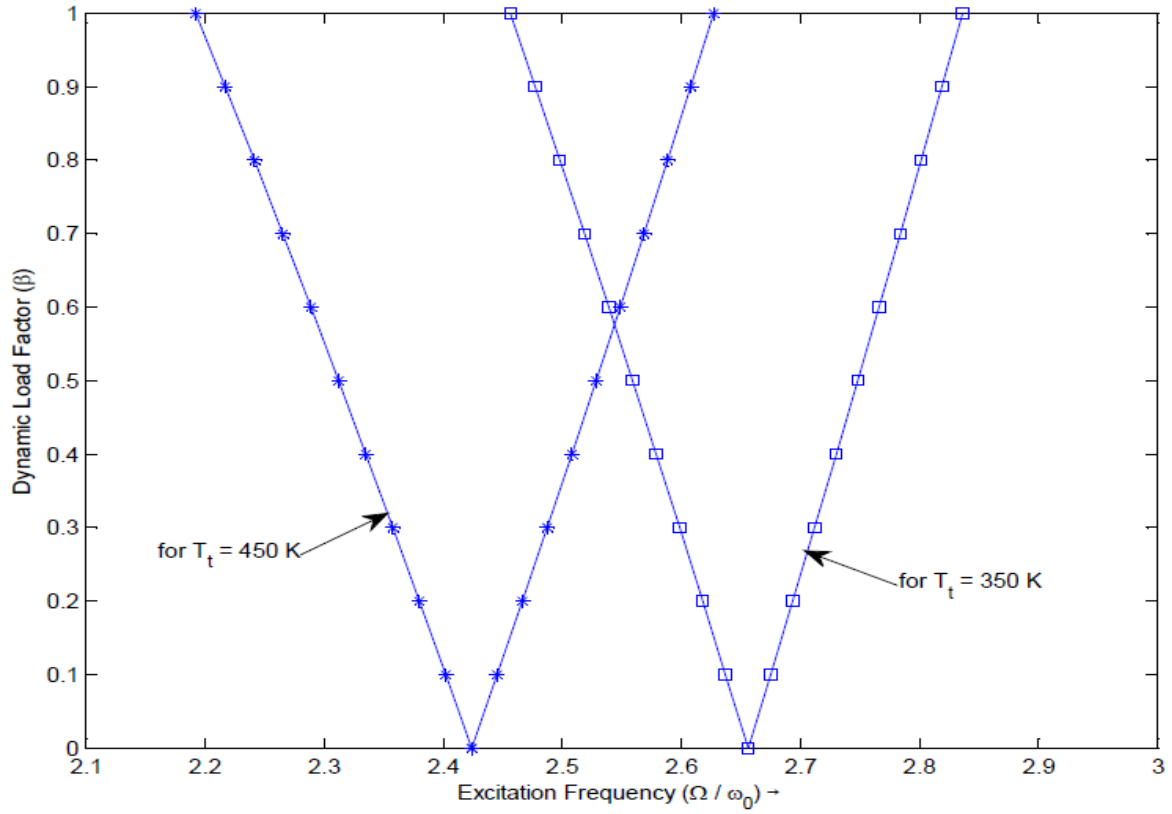

Figure (5.45) Effect of temperature of top face of FGM layer on the instability regions of the system for core thickness parameter (t_2/t_1) = 0.5, $\eta_c = 0.18$, Power law index (n) and $T_b = 300K$ for 1st mode of vibration, Simple Resonance.

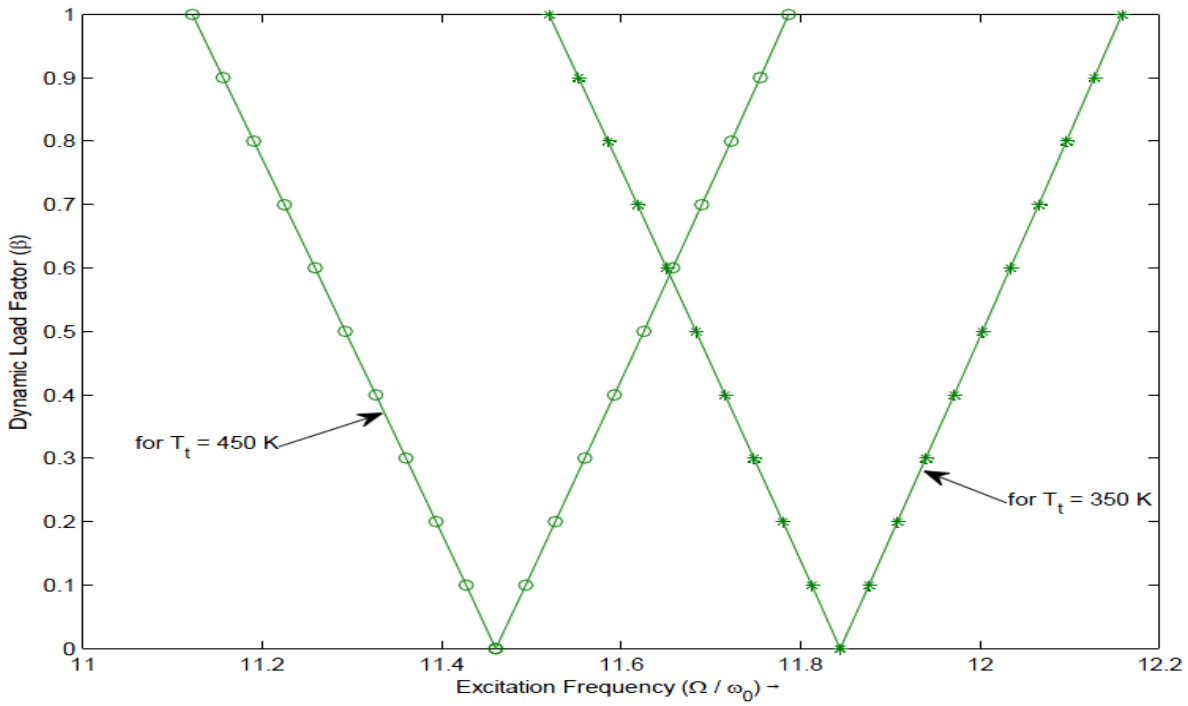

Figure (5.46) Effect of temperature of top face of FGM layer on the instability regions of the system for core thickness parameter (t_2/t_1) = 0.5, Power law index (n), $\eta_c = 0.18$, and $T_b = 300K$ for 2nd mode of vibration, Simple Resonance.

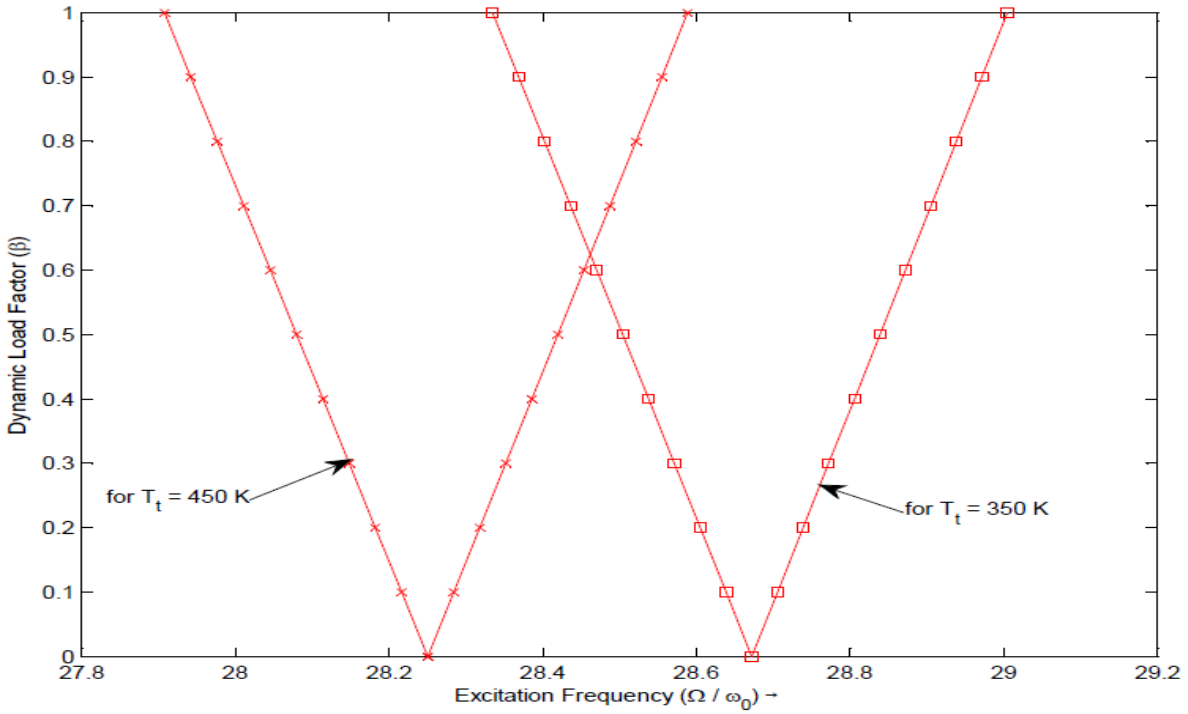

Figure (5.47) Effect of temperature of top face of FGM layer on the instability regions of the system for core thickness parameter (t_2/t_1) = 0.5, Power law index (n), $\eta_c = 0.18$, and $T_b = 300K$ for 3rd mode of vibration, Simple Resonance.

CHAPTER-6

CONCLUSION

1. The frequency of the beam decreases with increase in core thickness parameter (t_2/t_1) for 2nd and 3rd mode of vibration, keeping power law index (n) and top face temperature of FGM layer constant. For 1st mode, the frequency decreases up to the point at (t_2/t_1) = 1.5 and increases after that.
2. The frequency of the beam decreases with increase in power law index (n), keeping power law index (n) and top face temperature of FGM layer constant.
3. The frequency of the beam decreases with increase in top face temperature of FGM layer, keeping power law index (n) and core thickness parameter (t_2/t_1) constant..
4. The Loss Factor (η) decreases at higher modes with increase in core thickness parameter (t_2/t_1)**.**
5. The buckling load of the beam decreases with increase in core thickness parameter (t_2/t_1) for 2nd and 3rd mode of vibration, keeping power law index (n) and top face temperature of FGM layer constant. For 1st mode, the buckling load increases with increase in core thickness parameter (t_2/t_1).
6. The buckling load of the beam decreases with increase in power law index (n), keeping power law index (n) and top face temperature of FGM layer constant.
7. The buckling load of the beam decreases with increase in top face temperature of FGM layer, keeping power law index (n) and core thickness parameter (t_2/t_1) constant.

8. Comparing the cases of linear and non-linear temperature variation, it is found that the frequency and buckling load of the beam varies very close to each other. Hence, assumption of linear temperature distribution will also give satisfactory acceptable results and this would reduce a lot of complexities and time-consumption that occur in non-linear temperature variation computational process**.**

9. The instability of the system enhances with increase in power law index (n).
10. The instability of the system enhances with increase in core thickness parameter (t_2/t_1) for 2^{nd} and 3^{rd} mode of vibration but for 1st mode of vibration, the instability of the system increases up to the point at $(t_2/t_1) = 1.5$ and decreases after that.
11. The instability of the system enhances with increase in top face temperature of FGM layer,

Future Scope of work-

The present work can be extended to study the stability of structural elements like plates and shells.

CHAPTER-7

REFERENCES-

1. Abbas, B.A.H., dynamic stability of a rotating Timoshenko beam with a flexible root. Journal of sound and vibration, 108, 25-32, 1986.
2. Akhtar, K. and Kadoli, R., Stress analysis of SUS 304- ceramics functionally graded beams using third order shear deformation theory. IE(I) Journal-MC, 89, 31-37, 2008.
3. Alshorbagy, A. E, Eltaher, M. A. and Mahmoud, F. F., Free vibration characteristics of a functionally graded beam by finite element method. Applied mathematical modeling, 35, 412-425, 2011.
4. Asnani, N.T. and Nakra, B.C., Vibration analysis of multilayered beams with alternate elastic and visco-elastic layers. Journal of Institution of Engineers India, Mechanical Engineering Division, 50, 187-193, 1970.
5. Asnani, N.T. and Nakra, B.C., Vibration analysis of sandwich beams with visco-elastic core. Jr. Aeronautical Society of India, 24, 288-294, 1972.
6. Asnani, N.T. and Nakra, B.C., Forced Vibration damping characteristics of multilayered beam with constrained visco-elastic layers. J. Eng. (Indus), Trans. ASME, Series B. 98, 895-901, 1976.
7. Aydogdu, M. and Taskin, V., Free vibration analysis of functionally graded beams with simply supported edges.Materials & Design, 28(5), 1651-1656, 2007.
8. Banerjee, J.R., Free vibration of sandwich beams using the dynamic stiffness method. Computers and Structures, 81, 1915-1922, 2003.

9. Bauld, N. R. Jr., Dynamic stability of sandwich columns under pulsating axial loads. AIAA J., 5, 1514-1516, 1967.
10. Beliaev, N.M., Stability of prismatic rods subjected to variable longitudinal forces. Collection of papers: Eng. Construct, Struct. Mech., Put", Leningrad, 149-167, 1924.
11. Bhangale, R. K. and Ganeshan, N., Thermoelastic buckling and vibration behavior of a functionally graded sandwich beam with constrained visco-elastic core. Journal of Sound and Vibration, 295, 294-316, 2006.
12. Bhimaraddi, A., Sandwich beam theory and the analysis of constrained layer damping. Journal of sound and vibration, 179, 591-602, 1995.
13. Bolotin, V.V., The dynamic stability of elastic systems. Holden-Day, Inc., San Fransisco, 1964.
14. Briseghella, G., majorana, C.E., Pellegrino, C., Dybanic stability of elastic structures: a finite element approach. Computer and structures, 69, 11-25, 1998.
15. Brown, J.E., Hutt, J.M. and Salama, A.E., Finite elememt solution to dynamic stability of bars. AIAA J., 6, 1423-1425, 1968.
16. Chakrobarty, A., Gopalakrishnan, S. and Reddy, J. N., A new beam finite element for the analysis of functionally graded materials. International Journal of Mechanical Science, 45, 519-539, 2003.
17. Chaterjee, A. and Baumgarten, J.R., An analysis of visco-elastic damping characteristics of a simply supported sandwich beam. Journal of Engineering for industry, Trans of ASME, 93, 1239-1244, 1971.
18. Chonan, S. Vibration and stability of sandwich beams with elastic bending. Journal of sound and vibration, 85, 525-537, 1982.

19. Di Taranto, R. A., Theory of vibratory bending for elastic and visco-elastic layered finite length beams. Journal of Applied Mechanics, Trans of ASME, 87, 881-886, 1965.
20. Evan-Iwanowski, R. M.On the parametric response of structures. Applied Mechanics review, 18, 699-702, 1965.
21. Faraday,M.,On a peculiar class of acoustical figures and on certain forms assumed by a group of particles upon vibrating elastic surfaces, Phil. Trans., Roy. Soc., London, 299-318, 1831.
22. Fasana, A., and Marchesiello, S., Rayleigh-Ritz analysis of sandwich beams. Journal of sound and vibration, 241, 643-652, 2001.
23. Ha, K.H., Exact analysis of bending and overall buckling of sandwich beam systems. Computers and structures, 45, 31-40 1992.
24. Hsu, C. S., On the parametric excitation of a dynamic system having multiple degrees of freedom. J. Appl. Mech., Trans. ASME, 30, 367-372, 1963.
25. Hsu, C. S., Further results on parametric excitation of a dynamic system. J. Appl. Mech., Trans. ASME, 32, 373-377, 1965.
26. Ibrahim, R. A. and Barr, A. D. S., Paramteric vibration, part I: Mechanics of linear problems. Shock Vib. Dig., 10(1), 15-29, 1978.
27. Ibrahim, R. A. and Barr, A. D. S., Parametric vibration, part II: Mechanics of nonlinear problems. Shock Vib. Dig., 10(20), 9-24, 1978.
28. Ibrahim, R. A., Parametric vibration, Part III: Current problems (1). Shock vib.Dig., 10(3), 41-57, 1978.
29. Ibrahim, R. A., Parametric vibration, Part IV: Current problems (2). Shock Vib Dig., 10(4), 19-47, 1978.

30. Ibrahim, R. A., and Roberts, J. W., parametric vibration, Part V: Stochastic problems. Shock Vib. Dig., 10(5), 17-38, 1978.
31. Ibrahim, R.A. , Parametric vibration, Part VI: Stocjastic problems(2). Shock Vib. Dig., 13(9), 23-35, 1981.
32. Ibrahim, R. A., Parametric Random Vibration, Research studies Press Ltd., England, 1985.
33. Imaino, W. and Harrison, J. C., A comment on constrained layer damping structures with low visco-elastic modulus.Journal of sound and vibration, 149, 354-361, 1991.
34. Johnson. C. D., Kienholz, D.A., Rogers, L.C., Finite element prediction of damping in beams with constrained visco-elastic layers, Shock and vibration bulletin, 51(1), 71-81, 1981.
35. Johnson. C.D., Kienholz, D.A., Finite element prediction of damping in structures with constrained visco-elastic layers, AIAA Journal, 20(9), 1284-1290, 1982.
36. Jones. I.W., Salerno.N.L. and Savacchiop. A., An analytical and experimental evaluation of the damping capacity of sandwich beams with viscoelastic core. Journal of Engineering for Industry, Trans. Of ASME, 89, 438-445, 1967.
37. Kapuria, S., Bhattacharya, M. and Kumar. A. N., Bending and free vibration response of layered functionally graded beams: A theoretical model and its experimental validation. Composite Structures, 82, 392-402, 2008.
38. Kar, R.C. and Hauger, W., Stability of a sandwich beam subjected to a non-conservative force. Computers and structures, 46, 955-958, 1993.
39. Kerwin, E.M. Jr., Damping of flexural waves by a constrained visco-elastic layer. Journal of the Acoustical Society of America, 31, 952-962, 1959.

40. Lau, S.L. Cheung, Y.K. and Wu, S. Y., A variable parameter incrementation methods for dynamic instability if linear and nonlinear elastic systems. J. Appl. Mech., Trans. ASME, 49, 849-853, 1982.
41. Mead, D.J. and Markus, S., The forced vibration of three-layer, damped sandwich beams with arbitrary boundary conditions. Journal of sound and vibration, 10, 163-175. 1969.
42. Melde, F., ubererregungstehenderwelleneinesfadenformigenkorpers. ANN. Phys. Chem., 109, 193-215, 1859.
43. Mettler,E.,Allgemeine theorie der stabilitat erzwungener schwingung enelastischer koper. Ing. Arch, 17, 418-449, 1949.
44. Miyamoto. Y., Functionally Graded Materials: Design, Processing and Applications, Kluwer, Norwell, MA, 1999.
45. Mohanty , S. C., Dash, R.R. and Rout, T., Parametric instability of a functionally graded Timoshenko beam on a Winkler's elastic foundation. Nuclear Engineering and Design, 241, 2698-2715, 2011.
46. Mohanty, S.C., Dash, R. R. and Rout, T., Static and dynamic stability analysis of a functionally graded Timoshenko beam.International Journal of Structural Stability and Dynamics, 12(4), 2012.
47. Nakra, B.C. and Grootenhuis, P., Structural damping using a four layer sandwich.Journal of Engineering for industry, Trans.Of ASME, 74, 81-86, 1972.
48. Nakra, B.C., Vibration control with visco-elastic materials. The Shock and Vibration Digest, 8, 3-12, 1976.
49. Nakra, B. C., Vibration control with visco-elastic materials-II. The Shock and Vibration Digest, 13, 17-20, 1981.

50. Nakra, B. C.,Vibration control with visco-elastic materials-III. The Shock and Vibration Digest, 16, 17-22, 1984.
51. Nayfeh, A. H. and Mook, D. T., Nonlinear Oscillations. John Wiley & Sons, Inc., New York, 1979.
52. Qian. C. and demao, Z., Vibration analysis theory and application to elastic-visco-elastic composite structures. Computers and structures, 37, 585-592, 1990.
53. Rao, D.K., Frequency and loss factors of sandwich beams under various boundary conditions. J. Mech. Eng. Sci., 20, 271-282, 1978.
54. Rao, Y.V.K.S., Vibration of dual core sandwich beams. Journal of Sound and Vibration, 32, 175-187, 1974.
55. Ray, K. and Kar, R.C., Parametric instability of a sandwich beam under various boundary conditions. Computers and structure, 55, 857-870, 1995.
56. Saito, H. and Otomi, K., Parametric response of visco-elastically supported beams. Journal of Sound and Vibration, 63, 169-178, 1979.
57. Sakiyama, T., Matsuda, H. and Morita. C., Free vibration analysis of continuous sandwich beams with elastic or visco-elastic cores by applying the discrete Green function. Journal of sound and vibration, 198, 439-445, 1996.
58. Schimdt, G., ParametererregteSchwingungen. VEB Deutscherverlag der Wissenschaften, Berlin, 1975.
59. Simsek.M., Non-linear vibration analysis of a functionally graded Timoshenko beam under action of a moving harmonic load.Composite structures, 92(10), 2532-2546, 2010.
60. Simsek, M.,Vibration analysis of a functionally graded beam under a moving mass by using different beam theories. Composite Structures, 92(4), 904-917, 2010.

61. Simsek, M., Fundamental frequency analysis of functionally graded beams by using different higher-order beams theories. Nuclear Engineering and Design, 240, 697-705, 2010.
62. Stevens, K.K., On the parametric excitation of a visco-elastic column. AIAA journal, 4, 2111-2115, 1966.
63. Takahashi, K., An approach to investigate the instability of the multiple-degree-of-freedom parametric dynamic systems. Journal of Sound and Vibration, 78, 519-529, 1981.
64. Ungar. E.E., Loss factors of visco-elastically damped beam structures. Journal of the Acoustical Society of America, 34, 1082-1086, 1962.
65. Yokoyama, T., Parametric instabilioty of Timoshenko beams resting on an elastic foundation. Computer and structures.28, 207-216, 1988.
66. Zajaczkowski, J. and Lipinski, J. Vibrations of parametrically excited systems.Journal of Sound and Vibration, 63, 1-7, 1979.
67. Zajaczkowski, J., An approximate method of analysis of parametric vibration. Journal of Sound and Vibration, 79, 581-588, 1981.